Design and optimization of beam shaping assemblies for boron neutron capture therapy based on accelerators and DD/DT neutron generators

by

VAHAGN IVANYAN

Supervisor: Prof. dr. hab. Pawel Moskal
Auxiliary supervisor: Dr. Michal Silarski

Marian Smoluchowski Institute of Physics
Jagiellonian University in Cracow

Department of Experimental Particle Physics and Applications
Faculty of Physics Astronomy and Applied Computer Science

A thesis submitted for the degree of
Doctor of Philosophy (PhD)

Cracow 2022

Wydział Fizyki, Astronomii i Informatyki Stosowanej

Uniwersytet Jagielloński

Oświadczenie

Ja niżej podpisany Vahagn Ivanyan (nr indeksu: 1160081) doktorant Wydziału Fizyki, Astronomii i Informatyki Stosowanej Uniwersytetu Jagiellońskiego oświadczam, że przedłożona przeze mnie rozprawa doktorska pt. *„Design and optimization of beam shaping assemblies for boron neutron capture therapy based on accelerators and DD/DT neutron generators''* jest oryginalna i przedstawia wyniki badań wykonanych przeze mnie osobiście, pod kierunkiem Prof.dr hab. Pawła Moskała i Dr Michała Silarskiego. Pracę napisałem samodzielnie.

Oświadczam, że moja rozprawa doktorska została opracowana zgodnie z Ustawą o prawie autorskim i prawach pokrewnych z dnia 4 lutego 1994 r. (Dziennik Ustaw 1994 nr 24 poz. 83 wraz z późniejszymi zmianami).

Jestem świadom, że niezgodność niniejszego oświadczenia z prawdą ujawniona w dowolnym czasie, niezależnie od skutków prawnych wynikających z ww. ustawy, może spowodować unieważnienie stopnia nabytego na podstawie tej rozprawy.

Kraków, dnia 8.03.2022 r. ……

podpis doktoranta

Acknowledgments

I am grateful for the direct or indirect help for reaching this scientific level.

My grandfathers gave me the first hint and whole my family headed by my parents and brother were supporting me during my way and for the obtaining the academic knowledge. I was able to rely on myself with pieces of advice, lectures, share of the experience and skills, and at the same time learning from others mistakes. During my PhD studies I had a chance to meet with high-ranked scientists, Nobel laureates and surrounded by academicians, professors, wise teachers, colleagues and friends all the pressure and for a moment even imaginary problems were solvable. I do not want to mention someone and forget about the rest of them or underestimate the support given by one of them compared with other's advice, comment or remark as even small punctuation point which can be seen by auxiliary supervisor or a friend can change the whole meaning of the sentence, chapter and the PhD thesis. Jagiellonian University in Cracow will always stay in my mind and for the rest of my life it will follow me with all of its changes and influences on me, but I will do my best to stay the same first grade student of a school to learn something new and valuable for making the life of the humanity healthier, safer and easier.

List of Abbreviations

AANL……...…… A. Alikhanian National Laboratory

BNCT……...Boron Neutron Capture Therapy

BPA……..BoronPhenylAlanine

BSA……...Beam Shaping Assembly

BSH……...Borocaptate Sodium Hydrophilic

CNG…….…Compact Neutron Generator

C18/18……Cyclone 18/18

DD……...….. Deuterium-Deuterium

DNA…….DeoxyriboNucleic Acid

DT…….….. Deuterium-Tritium

FLUKA……...FLUktuierende KAskade (German: Fluctuating Cascade)

GEANT4……GEometry And Tracking 4 (4th version)

HUH……..…….……. Helsinki University Hospital

IAEA..…….……....International Atomic Energy Agency

IBA……...…… Ion Beam Applications

MC …….…….. Monte Carlo

MCNP…….……..Monte Carlo N Particle

NTI…….. Neutron Therapeutics Incorporation

RNA……..RiboNucleic Acid

SF……..Spontaneous Fission

Abstract

The aim of this thesis was to design and optimize neutron beam shaping assemblies (BSA) for adapting neutron beams produced by Deuterium-Deuterium (DD) and Deuterium-Tritium (DT) neutron generators as well as by Cyclotron C18/18 for application in boron neutron capture therapy (BNCT). A series of GEANT4 simulations were performed in order to find a BSA design enabling formation of neutron flux meeting recommendations of the International Atomic Energy Agency (IAEA) for BNCT. Energies of neutrons produced by generators and by protons from cyclotrons are too high, and the neutron flux is too much diffused for the direct applications in BNCT. Therefore, the thermalization, as well as focusing processes need to be performed before the treatment. The design of BSA included optimization of shapes and materials for multipliers, moderators, reflectors and shielding purposes for DT and DD neutron generator were performed using computer simulations applying GEANT4 programming package. The main optimization criterion for BSA design was the maximization of the epithermal neutron flux with respect to the flux of thermal and fast neutrons and with respect to the radiation dose from gamma quanta. The simulations were performed by taking into account 2.5 MeV initial energy and 10^{11} n/s to 10^{13} n/s neutron yield of DD compact neutron generators, as well as 14.1 MeV and up to 10^{14} n/s neutron yield of DT neutron generators. Also, separately cyclotron C18/18 based BSA design and optimization was simulated, by selecting exact thickness and material type for the proton beam of the C18/18 cyclotron installed at A. Alikhanian National Laboratory of Armenia. For the above-mentioned purposes, nat-U, nat-W, and its ^{182}W, ^{184}W, ^{186}W isotopes were discussed as first part of the moderator. It is known, that materials mixed with fluorine, such as AlF_3, MgF_3, AlF_3 mixtures with nat-Al and other materials, can be useful to increase the number of neutrons in the epithermal energetic region from 1 eV to 10 keV and may be placed next to the first part of moderator as the second layer of the thermalization system. Before collimating the flux, filters like hydrogen borate (boric acid), cadmium, lead and other materials were placed in as filters to lower the amount of thermal neutrons. The best established version of the DD based BSA includes moderator consisting of 8 cm thick ^{186}W, 45 cm thick mixture of 5% Fe and 95 % AlF_3, 1.25 cm thick LiF, 0.5 mm Bi and 1 mm thick lead, and the 20 cm thick back and 15 cm thick side Pb reflectors with 15 cm thick lead collimator. As for DT neutron generator based BSA the best design consisted from 27 cm thick Bi, 53 cm thick $FeAlF_3$, 3 cm thick Al, and 1 cm thick LiF moderator with 25 cm thick back and side lead reflectors and 10 cm thick lead collimator. The achieved epithermal over thermal neutron ratio was larger than 100 and comparably lower fast neutrons flux was registered from 10^6 initially simulated neutrons/projectiles. Thermal/epithermal neutron flux of C18/18 based BSA for BNCT as result of the GEANT4 simulation study is ~ $5 \cdot 10^8$ n/ (s·cm^2), where the majority of particles are epithermal neutrons in energy range from 1 eV to 10 keV, while DD based BNCT yet needs to be revised as the highest yield of neutrons was less than needed >10^{13} n/s. The system resulting

in epithermal neutron current over the epithermal neutron flux which should be > 0.7 is under development.

Table of Content

Introduction.....7

Author contribution.....10

1. Basics of BNCT

1.1. Base Definitions and requirements by IAEA for BNCT.....11

1.2. Applications of neutrons.....13

1.3. Neutron sources.....15

1.4. Boron neutron capture therapy.....20

1.5. Modern Beam Shaping Assemblies for BNCT.....22

2. State of the art of the BSA for CNG

2.1. BSA for BNCT based on DD Compact Neutron Generators.....26

2.2. BSA for BNCT based on DT Compact Neutron Generators.....36

2.3. Selection of a source and a BSA.....42

2.4. Estimation of absorbed dose.....43

2.5. BNCT for brain tumor.....44

3. Materials and Methods

3.1. Monte Carlo Codes.....47

3.2. GEANT4 Monte-Carlo Code…….....48

3.3. Neutron sources based on Cyclone 18/18 cyclotrons and DD/DT CNG.....49

4. GEANT4 study of the optimal BSA for BNCT

4.1. Design and optimization of the BSA for BNCT based on C18/18 cyclotron.....52

4.2. Design and optimization of the BSA for BNCT based on DD CNGs.....57

4.3. Design and optimization of the BSA for BNCT based on DT CNGs.....63

4.4. Irradiation of soft tissue by wide range energetic neutrons.....68

5. Summary and Conclusions.....75

Appendix.....78

Bibliography.....105

Introduction

In 1932 the discovery of an uncharged particle by James Chadwick (J. Chadwick 1932), which later was called neutron, initiated new fields of study in both, fundamental and applied physics. Four years later Gordon Locher published an article describing the concept of a novel method of a cancer treatment called boron-neutron capture therapy (BNCT) (G. Locher 1936). BNCT is a binary method including the delivery of boron ^{10}B isotope into the malignant tumor cells and irradiation by epithermal neutrons leading to nuclear capture reaction resulting in intermediated ^{11}B nucleus with following recoiled ^{7}Li nucleus and a high-linear energy transfer α particle (^{4}He). The two main processes of neutron capture in boron ^{10}B are as follows:

$$^{10}B + n_{th} \rightarrow [^{11}B] \rightarrow {}^{4}He + {}^{7}Li + 2.79 \text{ MeV } (6\%),$$
$$^{10}B + n_{th} \rightarrow [^{11}B] \rightarrow {}^{4}He + {}^{7}Li + \boldsymbol{\gamma} \text{ (0.48 MeV) } + 2.31 \text{ MeV } (94\%).$$

The absorption cross section of the 0.025 eV thermal neutrons is equal to 3840 b and in Figure 1 the energy dependences of the total and absorption cross sections on ^{10}B are presented. As one can see the capture reactions are dominant up to the energy of about 10 keV.

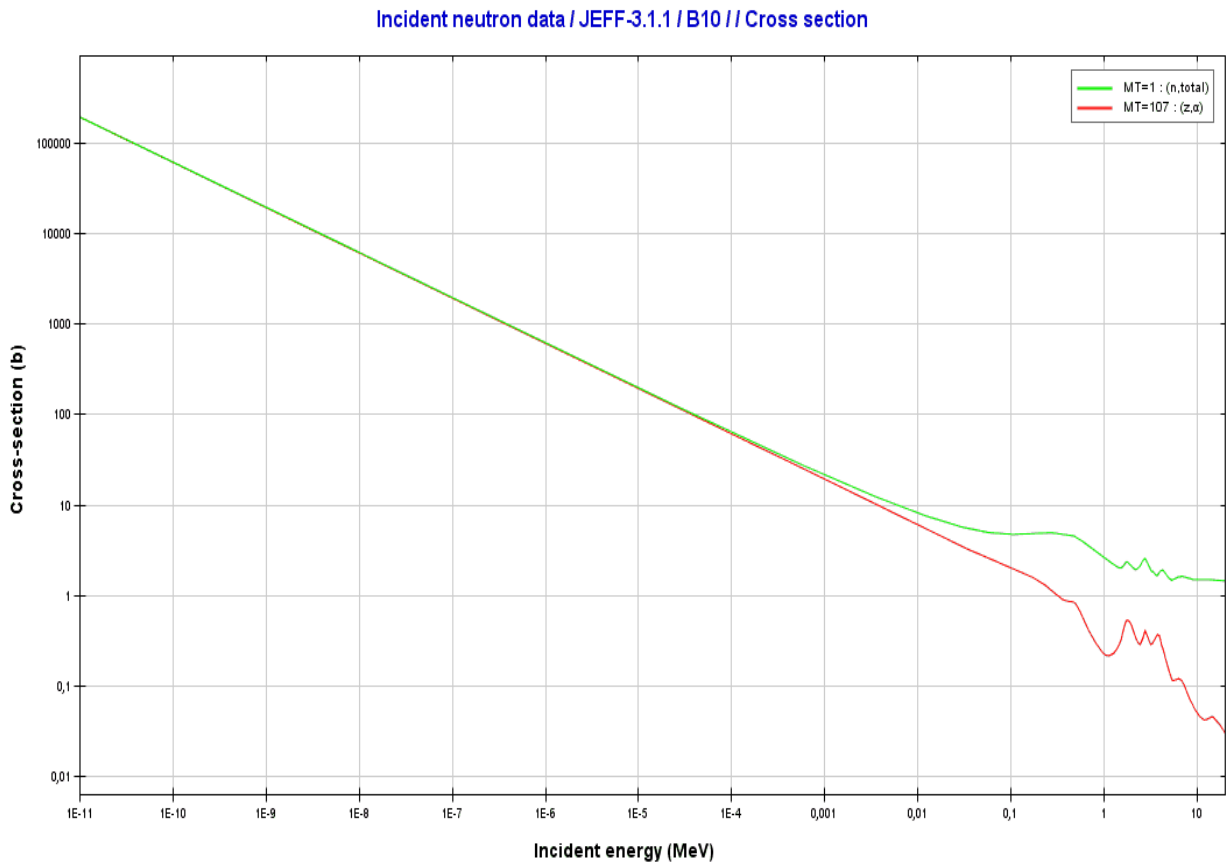

Figure 1. *Comparison of the total cross-section (green curve) and cross-section for neutron capture reactions (n, alpha) (red curve) on ^{10}B (calculated by JANIS code).*

Due to the short path length of alpha particles in the tissue (4-9 μm), the adjacent healthy cells are not damaged as the size of eukaryotic cells in human and animal bodies is bigger (M. Ginzberg et al. 2015, R. Kumar 2021, E. B. Wilson 1923). Thus the whole process results mostly in killing of the cancer cell containing boron.

It should be admitted that BNCT is a treatment method applied in case when other treatment methods were not effective. It is considered as an optimal treatment for head and neck cancer, especially for the glioblastoma multiform brain tumor (Chadha et al. 1998, Henriksson 2008, Malouff 2021). Glioblastoma multiform is an hyperactive and one of the most rapidly growing types of malignant tumors (J. Kunikowska 2020), with the average lifetime of patients amounting to six months after the diagnosis even with standard treatments (IAEA TECDOC 2001). The successful treatment depends mainly on the boron-10 carrier and neutron flux with correspondingly small contamination of thermal and fast components, as well as the secondary gamma rays.

The development of BNCT requires progress mainly in improvement of boron delivery agents (D. Kaniowski et al 2017, D. Novopashina et al 2021) and of the neutron beams. The best carrier should be nontoxic for cells from biological and clinical point of view with a high accumulation in tumor with respect to healthy cells (ratio greater than 3:1). The typical concentration of the boron carrier in the cancer cells amounts to ~20 – 50 μg ^{10}B/g (IAEA TECDOC 2001). Currently, the BNCT therapy employs mostly two boron carriers (S. Kawabata et al 2009): sodium borocaptate (BSH) and boronophenylalanine (BPA), with their limitations regarding their transportation inside cells, and yet there is still a need for better options to deliver boron more effectively. For that purpose the boron delivery system development has taken two directions of boron carriers and conveyors, where boron carriers include carboranes, amino acids and monoclonal antibodies or growth factors (R. Barth et al. 2018, H. Nakamura et al. 2012, W. Sauerwein et al. 2012). As regards conveyors to transfer boron into cells, liposomes are quite promising alternatives (M. Szczepanek 2020). Due to their structure, hydrophilic and hydrophobic molecules such as proteins, RNA, DNA, enzymes, vaccines and imaging agents can be carried by them.

Currently, several types of neutron sources are used for BNCT. First, they were based only on nuclear reactors, where radioactive decay of uranium was followed by fission processes (S. Altieri and N. Protti 2018). Progress in the development of a more comfortable neutron sources and equipment resulted in building clinical centers based on cyclotrons, linear or tandem accelerators which produce neutrons by interactions of protons, deuterium ions or other particles on various targets, such as ^{7}Li, ^{9}Be, etc. (IAEA TECDOC 2000). In all the above-mentioned cases the initial energies of neutrons are too high to be used directly for BNCT. Due to this fact, the thermalization, as well as focusing processes need to be performed before the treatment. The main goal of this PhD thesis was to design individual beam shaping assembly for the accelerator based BNCT neutron beam in the Armenian National Science Laboratory and for compact neutron generators based on Deuterium-Deuterium (DD) and Deuterium-Tritium (DT) reactions (I.Kadenko 2017). GEANT4 simulations were performed to find alternative materials for multipliers, moderators, reflectors and shielding purposes, which were not used to design beam shaping assemblies before. In this thesis, the first BSA is designed for the ^{9}Be(p,Xn) accelerator neutron source, where proton beam comes from the IBA C18/18 cyclotron with production of up to 100 μA of 18 MeV protons (V. Ivanyan 2020). The second and third BSA were designed for the DD compact neutron generators (CNG), with quasi - monochromatic neutron flux up to $5 \cdot 10^{12}$ n/s and energy of around 2.5 MeV and for the DT neutron generators,

with up to 10^{14} n/s flux and around 14.1 MeV energy. Details about different neutron sources with neutron applications for medical purposes are discussed in Chapter 2. In this chapter BNCT with additional details, such as recommendations by International Atomic Energy Agency (IAEA) and information about beam shaping assemblies by other researchers are described. It contains the specific information about the BNCT for brain tumor, with selection of the initial neutron source, estimation of the dose by fast and thermal neutrons, gamma rays and their correspondence to the recommendations of the IAEA. Also, results for the DT compact neutron generator based BNCT, with simulations of the brain phantom and usability of the exact BSA, are included in this Chapter. In Chapter 3 materials and methods, especially details about Cyclone 18/18 cyclotrons of IBA, DD and DT CNGs, as well as Monte Carlo codes used for the simulation studies are described. The design and optimization of a BNCT applicable neutron fluxes, with beam shaping assemblies on the base of C18/18 cyclotron, as well as on the base of DD and DT CNGs are discussed in Chapter 4, where all the components of the BSA, including moderators, back and side reflectors, as well as collimators are presented. Final discussion of the results with advantages and disadvantages of the designed BSAs for the treatment, as well as additional techniques for the simulation study are described in the Summary.

Author Contribution

It is relevant to describe the thesis by four main parts as contribution of the author. The first part is the BSA design and GEANT4 simulations for the cyclotron C18/18 based BNCT project. To make virtual model of the experiment, Monte Carlo calculations were performed by the author for the optimal selection of thicknesses and materials of the target for a 14.8 MeV proton beam. Based on the aforementioned simulation results the decision was made to use 2.5 mm thick ^{9}Be target with ^{9}Be (p, Xn) multibody reactions as source of neutrons. The C18/18 modified cyclotron of the IBA was installed in Armenia at the A. Alikhanian National Laboratory (AANL) for the medical purposes, especially for the development of the accelerator based BNCT. The simulation results obtained by the author are discussed in Chapter 3 and 4, as well as in the articles (V. Ivanyan 2020) and (R. Avagyan, V. Ivanyan et al. 2017, R. Avagyan, V. Ivanyan et al. 2018). The methodology of the optimization and designing of the BNCT applicable BSA was prepared in two ways. At first, as moderator two materials were used which at the same time served as fast neutrons filters. In the second method advantages of multipliers, such as nat-Bi or nat-Mo, were used and the simulations gave significant results. It is worth to mention that the achieved results were in high agreement with IAEA recommendations for BNCT, such as formed epithermal neutron flux and relatively low amount of thermal and fast components. Second and third parts of the thesis include designing and optimization of the beam shaping assemblies (BSA) for DD and DT neutron generator based BNCT performed by the author. As discussed with the leading experts, many types of BSAs were designed to achieve 10 keV energetic peak of neutrons, needed for the most aggressive malignant brain tumor Multiform Glioblastoma, in case if it is located even in the central part of the human brain. Moreover, the author performed quite useful GEANT4 simulations as fourth part of the thesis for the estimation and elaboration of the wide energy range (0.01 eV - 1 MeV) neutron reactions with the soft tissue (see Section 4.4 and Appendix). And as results the 10 keV neutron beam which is the edge of epithermal neutron energy range ($0.4\ \text{eV} < E_{epi} \leq 10\ \text{keV}$) had shown the best penetration ability through the tissue with the lowest number of gamma rays and additional nuclear reactions.

1. Basics of BNCT

1.1. Base Definitions and requirements by the IAEA for BNCT

The Boron Neutron Capture Therapy is based on the use of epithermal neutrons which thermalize while penetrating the tissues and interact with cancer cells. However, the neutron beams used in the clinical practice contain also initially thermal and fast neutrons components which should be minimized to decrease the dose delivered to the healthy tissues during the treatment. Thermal neutrons are in thermal equilibrium with a surrounding medium at 17°C (62°F) with Maxwellian distribution where mean velocity corresponds to the energy of about 0.025 eV (~2 km/s). Their energetic range is defined up to 0.5 eV by the International Atomic Energy Agency (IAEA), and for epithermal and fast neutrons the energy ranges from 0.5 eV to 10 keV and more than 10 keV, respectively (IAEA TECDOC 2001). As unit for the flux of each type of neutrons, the number of neutrons in a specific energy range passing through the surface within a second is used. For example as thermal ($\varphi_{thermal}$) and epithermal (φ_{epi}) neutron fluxes we define the number of neutrons with energies less than 0.5 eV and from 0.5 eV to 10 keV, which pass through 1 cm^2 area within a second, accordingly. Furthermore, the absorbed doses from fast neutrons and gamma rays are denoted by D_f and D_γ, respectively. These are the deposited energies per unit mass, and defined in respect to epithermal neutron fluence with the $Gy \cdot cm^2$ unit which is usable for the estimation of radiation risks. Historically, it is known as dose-area product (DAP), but it was currently renamed to kerma-area product (KAP) (W. Huda 2014).

The International Atomic Energy Agency (IAEA) is the central organization required to control and develop all the atomic/nuclear based technologies for the usage of safe and peaceful purposes in the world. BNCT being a method of malignant tumor therapy with neutron radiation is a subject of the IAEA recommendations (IAEA TECDOC 2001). They include both the types of neutron sources and also optimal epithermal flux production for the specific type of cancer. The clinical usage of different types of neutron sources has significant disadvantages due to their costs and sizes. Based on the depth, size and location of the tumor, BNCT applicable neutron flux can be specific, and one of the advantages of this therapy is based on deep penetration ability of neutrons. The quality of the incident beam depends on many parameters which include:

- dose of fast neutrons over epithermal neutrons flux,
- thermal and epithermal neutrons flux ratio,
- gamma ray dose over epithermal neutrons flux,
- ratio between the total epithermal neutron current and the total epithermal neutron flux.

They are the most important and should be in the core of the research for BNCT. It is necessary to differentiate epithermal neutron current from the epithermal neutron flux, where the flux means all the possible directions, while current is distributed directly, and it is way more important for decreasing the damage of healthy cells with targeted irradiation of tumor cells. It is accepted that intensity of the thermal neutron component should be around 20 times smaller than for epithermal neutrons to avoid massive damage on the scalp, while in the case of deep seated tumors the ratio of epithermal to thermal flux should exceed 100. As regards the KAP of fast neutrons and gamma rays per epithermal neutron, the best would be the achievement of a dose-area product lower than $2.0 \cdot 10^{-13}$ $Gy \cdot cm^2$ per neutron for both cases. Currently, the ratio of the dose for fast neutrons over epithermal neutron fluence is accepted to be from $2.5 \cdot 10^{-13}$ to

$13 \cdot 10^{-13}$ Gy·cm^2/n and from $1 \cdot 10^{-13}$ to $13 \cdot 10^{-13}$ Gy·cm^2/n in case of ratio of gamma rays dose over epithermal neutron fluence. The epithermal neutron flux, or number of epithermal neutrons passing through area of 1 cm^2 per second is one of the most important aspects to be investigated (R. Barth et al 1992, R. Brugger 1993, F. J. Wheeler et al. 1990). Here it is necessary to differentiate the neutron flux from fluence. In our research we use neutron fluence as number of neutrons passing through the surface area of the virtual detector during the whole irradiation time. Taking into account that the neutron yield of the source is a given number of neutrons per second then the estimation for the final neutron flux defined as number of neutrons passing through the surface area per unit time, as well. For example if from 10^6 simulated neutrons the registered/detected number of neutrons is equal to 100, then it will be divided by the surface area of the virtual detector. In case of 2.5 cm radius of the detector the surface area will be equal to ~19.625 cm^2 ($S = \pi \cdot R^2$), and the value of the detected neutrons per surface area ~5.1 n/cm^2. Assuming that the neutron yield is 10^{13} n/s and taking into account that from 10^6 initially simulated neutrons it was possible to achieve ~5.1 n/cm^2 then the neutron flux will be equal to ~$5.1 \cdot 10^7$ n/(s·cm^2) or number of detected neutrons per area surface per second. As for fluence, it is assumed the neutron flux integrated in the certain period of the time and its unit of measurement is cm^{-2}.

Also, as recommended by IAEA the ratio between total neutron current and total neutron flux should be ~ 0.7. The high value is needed to reduce the undesired irradiation as well as giving flexibility for the patient positioning. To understand its importance and differentiate from other types of fluxes, it is worth to note that in case of 0.5 the flux is isotropic and in case of 1 the flux is directly distributed .

1.2. Applications of Neutrons

With discovery of neutron, the progress of fundamental science followed with the creation of various new directions in applied nuclear physics. The research on different fields was based on wide diversity range of applications concentrating from the military to medical usages (J. Holmes et al. 1976, IAEA Report 2012, B. Jones 2020, I. Chatzis & M. Barbarino 2021, I. Kadenko 2017). Neutron imaging (N. Kardjilov 2011, G. McIntyre & P. Holden 2016) is a well-known method of radiography (Figure 2) (PSI 2016). Initially it was considered as better option to X-ray imaging, due to its high-quality images and attenuation possibilities. Nuclear reactions with neutrons are better options to get clear information about structures of different types of objects, and furthermore, they provide non-destructive techniques for analyzing the elemental content of a sample (C. Cristache et al. 2008, A. El-Taher et al. 2014, P. Moskal 2011). In comparison with X-rays, neutrons have deeper penetration and interaction level, which is a nucleus, whereas interactions of X-rays are limited to electrons at atomic levels. In Figure 2 one can see the advantage of neutrons when it comes to 2D or 3D visualization, due to their attenuation by light nucleus and deeper penetration inside heavy metals, such as Fe, Pb, Ti, etc.

Figure 2. *Example of a neutron imaging (left) of an analog camera in comparison with X-ray imaging (right), where neutrons make it possible to see not only heavier materials such as metals, but also some light materials such as hydrogenous substances, plastics etc. (Figure adapted from PSI website (see the link in the references)).*

Apart from imaging, the absorption and inelastic scattering of neutrons, being the basics of the neutron activation analysis, are widely used in nuclear engineering and fundamental studies (N. Dzysiuk 2010, 2015, I. Kadenko 2016). This technique allowed e.g. for deep underwater detection of hazardous materials. Such projects involve creation of small submarines, with equipped neutron source and gamma detector. The idea is the irradiation of the area on the bottom of the sea and detection of gamma ray which can characterize different chemical elements. One of these types of projects is SABAT (Figure 3), which is on the level of simulations study with quite successful results (M Silarski 2019, P Sibczyński et al. 2019) and

will be used for the investigation of the bottom of the Baltic Sea to find exact locations of hazardous gasses, which were sunk during the Second World War. Corrosion of these munitions could bring the spread of hazardous gasses and as a consequence depletion of flora and fauna of the sea.

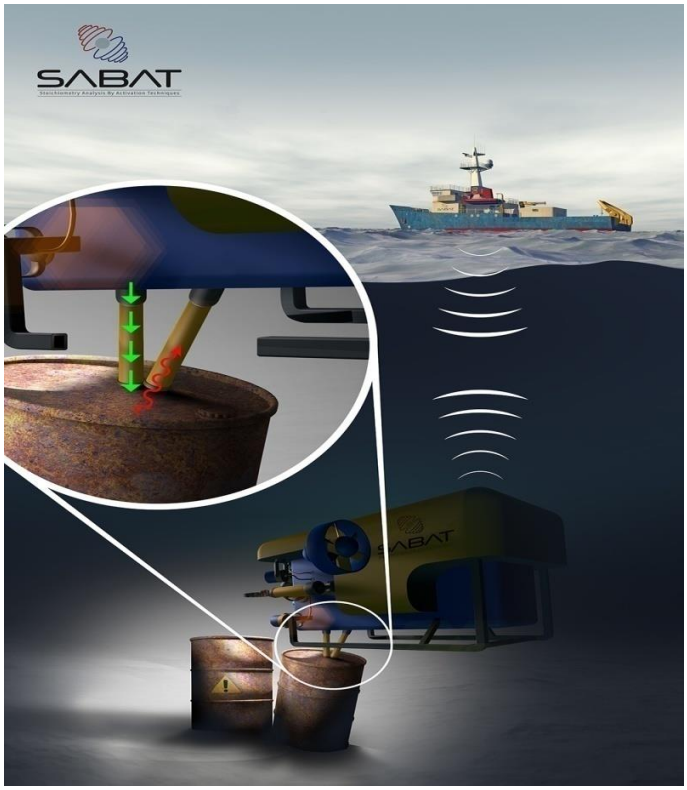

Figure 3. *Diagram of the localization of underwater hazardous gasses and materials by SABAT submarine (Figure adopted from (M. Silarski 2019))*

Applications of neutrons in medicine were concentrated mainly in neutron capture therapies (NCT) and on the research in this field (W. Sauerwein et al. 2012). The penetration of neutrons with possible secondary particle production could destruct the DNA of the tumor cells and kill them. The deeply detailed investigations showed that there can be more effective ways for cancer treatment with the usage of the technique of neutron capture reactions inside the tissue (Y. Kiyanagi et al. 2019). And one of them is boron neutron capture therapy (BNCT), which is mainly concentrated on head and neck cancers. The method is still under development and the importance of an appropriate neutron source selection is one of the key factors of the treatment. Besides shielding and security purposes, the amount and energy of used neutrons should be compatible with the therapy. The progress in BNCT requires an advanced research, which brings to development and investigation of special system called beam shaping assembly (BSA) for the thermalization and focusing of a neutron flux, before it will be used for the treatment.

1.3. Neutron sources

Currently, neutron sources (IAEA REPORTS 2012) exist on the base of nuclear reactors, cyclotrons or other type of accelerators, DD and DT CNGs, as well as some isotropic neutron sources, such as ^{252}Cf, AmBe, etc. (H. Vega-Carrillo & S. Martinez-Ovalle 2015). Besides initial neutron energies and yields the above-mentioned instruments differ with their compactness, costs, installation difficulties and other unique properties as a neutron source. The most problematic is the preparation of a nuclear reactor to be used for medical purposes, and until few years ago only fission nuclear reactors were available for the appropriate neutron flux production (Y. Kiyanagi et al 2019). One of the famous nuclear reactors, existing for the medical investigations and therapies, got another license in 2017 for joint research works. It is located at Kyoto University and called KUR as Kyoto University Reactor (Figure 4).

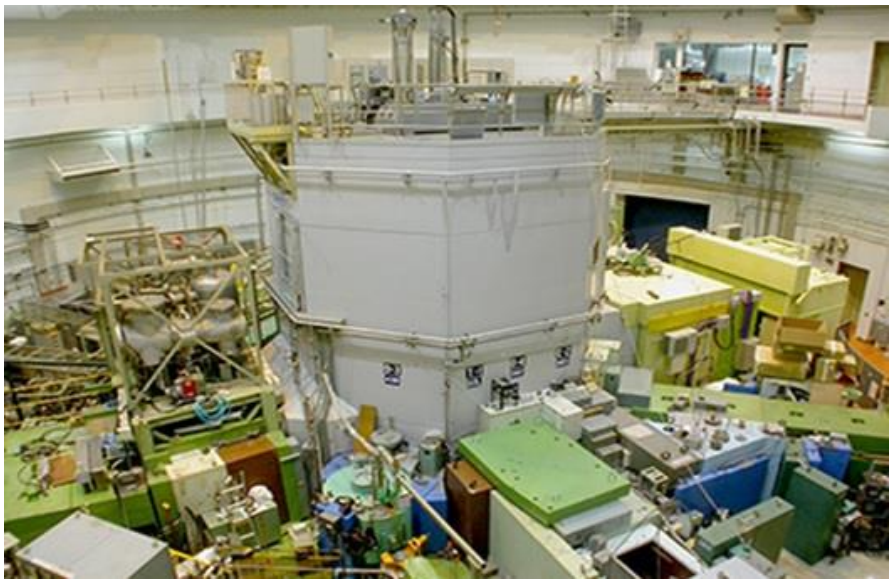

Figure 4. *Kyoto University Research Reactor (KUR) with various experimental setups according to the emitted neutrons (Figure adopted from Y. Kawabata and Y. Saito 2013)*

The base process in nuclear reactor is the neutron induced fission, when a heavy nucleus splits into lighter ones causing energy and particle emission (Figure 5). Natural Uranium, which is the key material for the fission process, contains up to 0.72 % of ^{235}U isotope. And it is the main multiplier of neutrons, where the fission proceeds due to the following nuclear reaction as one of the channels: $^{235}U+n \rightarrow {}^{141}Ba+{}^{92}Kr+3n$.

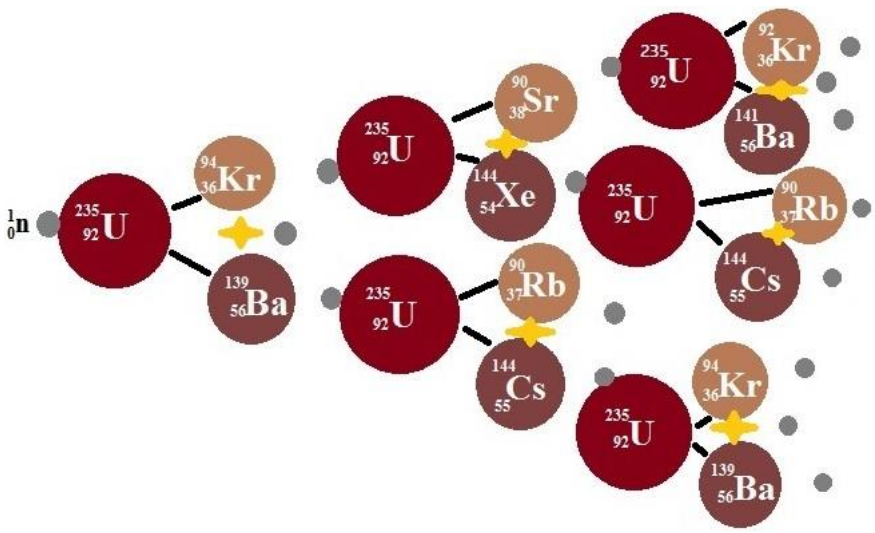

Figure 5. Nuclear Fission Process

Continuous multiplication process of neutrons gives a yield which may be sufficient for BNCT treatment. In case of KUR, more than 500 BNCT procedures have been performed, mainly for brain, head and neck cancer treatments (K. Kanda et al. 1993). BNCT clinics based on the nuclear reactors exist nowadays only in few countries worldwide. Most of nuclear reactor-based BNCT clinics are closed due to their difficulties of keeping them in working condition, cost and non-compactness, as well as problems with installation of this type of neutron sources in hospitals.

An alternative way to reactors are accelerator-based neutron sources which are progressing and will be used for BNCT more efficiently. Accelerators, which can be cyclotrons, linear accelerators or tandems in most cases accelerating protons and bombarding different targets to achieve secondary neutrons. There are two very well-known isotopes widely used as target material: lithium-7 and beryllium-9, for which the following many-body nuclear reactions are useful for neutron production: $^{7}Li(p,Xn)^{7}Be$ and $^{9}Be(p,Xn)^{9}B$ (S. Abramovich et al 1991). Currently, there are BNCT laboratories which already started experimental processes, such as world's first accelerator based BNCT industry for hospitals in many cities of Japan, Russian BNCT laboratory at Budker Institute of Nuclear Physics and Finish Neutron Therapeutics Incorporation (NTI) which has installed its compact accelerator-based neutron source for BNCT at Helsinki University Hospital (HUH) (S. Savolinen et al. 2013). Many other laboratories are just under construction or founding processes.

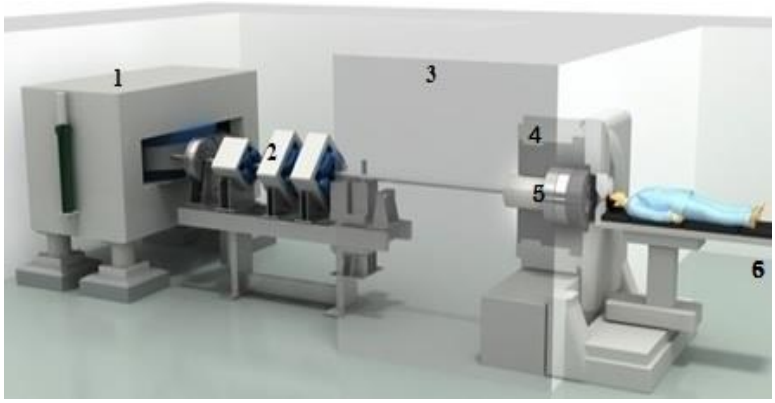

Figure 6. World's first accelerator based BNCT equipment with accelerator (1) beam transport line (2) a concrete wall (3) (separating the patient room (6)) with placed in beam shaping assembly (4) and an appropriate target (5) (Figure adapted from T. Mitsumoto et al. 2010)

The progress of compactness and usability of neutron sources in clinics doesn't stop on accelerator-based neutron sources which need additional construction works, and new buildings (Figure 6). Modern CNGs (Figure 7) based on DD/DT reactions can be also used for BNCT, as their properties are becoming more acceptable for the therapy. The energy and yield of neutrons from DD and DT CNGs are fixed, and it is an advantage for the research and progress towards fulfillment of the IAEA recommendations.

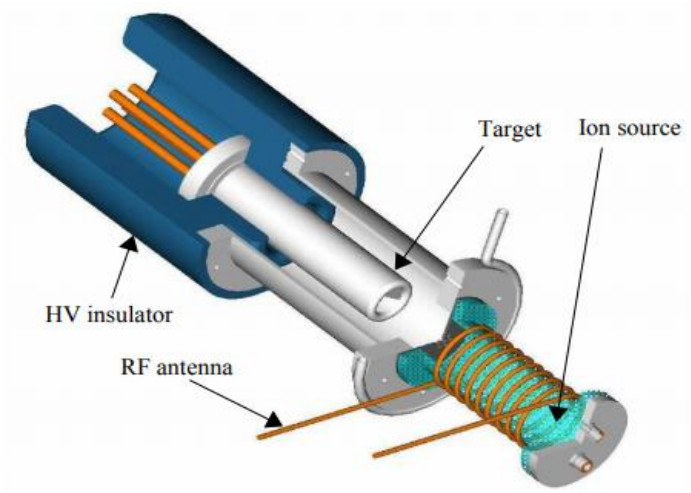

Figure 7. The axial extraction neutron generator (Figure adopted from T. Pui Lou 2003).

It is important to mention the compactness and ease of usability of CNGs in hospitals which does not need to have significant construction changes of buildings. The smallest known version of compact neutron generator (Neutrister) can be placed in a hand (Figure 8) (SANDIA National laboratory, see the link at references). In case of medical applications, the initial yield of neutrons should be high enough to fulfill the requirements of the therapy. In case of DD CNGs, where the energy of isotropic neutrons is 2.5 MeV (produced via reaction $d(d,n)^3He$), the initial yield should be at least 10^{13}n/s for its usage for BNCT, while the latest commercially

available devices can reach up to $5 \cdot 10^{12}$ n/s. The research progresses of the last years are quite promising and show that the expected yield (more than 10^{13} n/s resulting in around 10^{9} n/(s·cm)^2 epithermal neutrons (ref. at Table 2)) would be achieved in the nearest future.

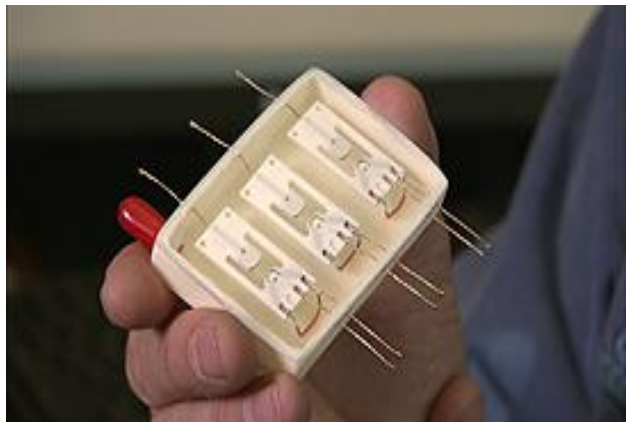

Figure 8. *World's smallest CNGs (neutristers) of Sandia National Laboratories mounted in a test box under vacuum (max yield is ~200 n/s per neutrister, Figure adopted from Sandia National Laboratory (see the link at references)).*

DT CNGs emit neutrons (via reaction d(t,n)α) with energies 14.1 MeV and the initial neutron yield can reach up to 10^{14}n/s. This does not yet mean that they can be easily installed in any hospital, because of the usage of thermalization system as for other cases, where the initial energies should be less, there is a need of moderation of the high energy neutrons with additional materials. The whole system with CNGs, which takes more space than the compact neutron generator itself, can be placed in clinics without significant changes, but by considering radiation safety issues.

Neutron Source	**Energy range**	**Achievable max. yield**	**Bibliography**
DD	2.5 MeV	~$5 \cdot 10^{12}$ n/s	Z. Song et al. 2014
DT	14.1 MeV	$1.45 \cdot 10^{14}$ n/s	F. Rasouli et al. 2012
^{252}Cf	2.35 MeV	$2.3 \cdot 10^{15}$ n/s/kg	Sh. Robinson 2020, Yu. Toporov 2004
^{241}AmBe (α, n)	<12 MeV (achromatic)	$6.8 \cdot 10^{3}$ n/s (per 1 mg ^{241}Am)	S. Mortazavi et al. 2010, T. Pui Lou 2003

Table 1. Technical details of some of the widely used neutron sources

Also, as neutron source it is worth to mention ^{252}Cf which has a half-life of around 2.7 years (I.W. Osborne-Lee & C. W. Alexander 1995) and provides neutrons with an average 2.35

MeV energy, which is result of the spontaneous fission leading to neutron emission with rate of 2.3×10^{15}n/s/kg.

$$^{252}Cf \rightarrow SF \rightarrow fragments + n + \gamma \ (3.1\%)$$
$$^{252}Cf \rightarrow {}^{248}Cm + {}^{4}He \ (96.9\%)$$

The above-mentioned material is produced in the high neutron flux reactors at Oak Ridge National Laboratory in the United States and at the Research Institute of Atomic Reactors in Russia (Sh. Robinson 2020, Yu. Toporov 2004). Besides the difficulties for the target production the spontaneous fission resulting in neutron emission, has 3.1% probability and significantly lower yield (10^9 n/s) than in the case of other neutron sources. In addition to the above mentioned general information, Table 1 gives details for some of the widely used neutron sources, their energies and yields which are highlighted in the scientific literature.

1.4. Boron neutron capture therapy

Boron-neutron capture therapy is a cancer treatment method which is mainly concentrated in deep sited tumors, such as head and neck cancers, while it is useful for the treatment of malignant tumors of other organs too (M. Suzuki et al. 2007, A. Zonta et al. 2009, E. Pozzi et al 2012, R. Farias et al. 2014, V. Trivillin et al. 2019, Malouff et al 2021, H. Fukuda et al. 2003). This method was proposed in 1936 by Gordon Locher (G. Locher 1936), with a hypothesis of concentrating the right amount of boron-10 isotopes inside of cancer cells and the following irradiation by an appropriate flux of thermal neutrons, causing nuclear capture reaction and emitting high linear energy transfer alpha particles which would destroy the tumor cell (Figure 9).

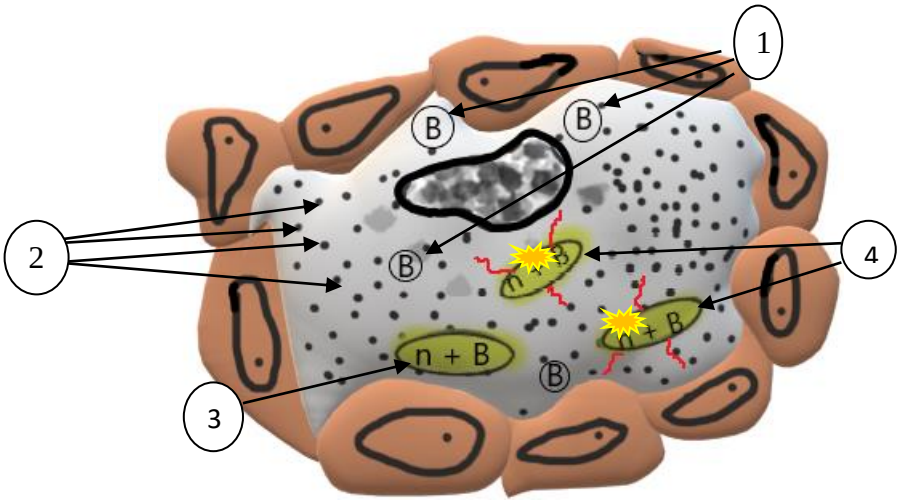

Figure 9. *BNCT in action 1) Boron compound (B) is selectively absorbed by cancer cell(s). 2) Neutron beam (n) is aimed at cancer site. 3) Boron absorbs neutron. 4) Boron disintegrates emitting cancer-killing radiation.*

The high cross section (3837 barn) of the $^{10}B(n,\alpha)^{7}Li$ reaction (for neutron energy E_n=0.025eV) (IAEA TECDOC 2001) makes this therapy a promising cancer treatment method. Most of the capture reactions:

$$^{10}B + n_{th} \rightarrow [^{11}B] \rightarrow {}^{4}He + {}^{7}Li + 2.79 \text{ MeV } (6\%)$$
$$^{10}B + n_{th} \rightarrow [^{11}B] \rightarrow {}^{4}He + {}^{7}Li + \gamma\ (0.48 \text{ MeV}) + 2.31 \text{ MeV } (94\%),$$

emit 478 keV gamma quanta which may be used for monitoring of the delivered dose. Due to the short path length of α particles (4-9 µm), the adjacent healthy cells are not damaged and the whole process results in the effective killing of the cancer cell containing boron-10 isotope. Since now all the research centers in this field, including preparation and production of different boron transport agents and thermal/epithermal neutron flux delivery, are working to make progress and select useful neutron sources, as well as, boron carriers with fewer disadvantages (W. Sauerwein et al. 2012). The boron carrier should be characterized by small toxicity, as well

as the delivery of the right amount of ^{10}B atoms into the right organs with less spreading over a patient body. It is worth to mention, that there is no such kind of boron transport agent, which will deliver the isotope only to the needed organ. This can cause later a neutron capture reaction outside of the malignant tumor, while for deep-sited brain cancer (multiform glioblastoma) there are stages, when other treatment methods are not useful (R. Barth et al. 2018, T. Yuan et al. 2019, IAEA TECDOC 2001) and thus, BNCT is the only effective method to prolong the patient life. To increase the impact and prolong the duration of a patient life as long as possible, this treatment method needs to be as perfect as possible in terms of selecting an appropriate boron-10 delivery agents as well as epithermal neutron flux with energy and angular spreads which confront the tumor position, size, and shape. If the preparation of an appropriate carrier relates to biological data, then the formation of the concrete neutron flux needs information about sizes and shapes of materials which will moderate, reflect, and after all focus the final neutron flux. Currently, modern beam shaping assemblies (BSA) for BNCT are able to form neutron beams which can be used with at least two boron-10 carriers. In the clinical practice: ^{10}B-4-boron-L-phenobarbital (BPA) and Borocaptate Sodium ($Na_2B_{12}H_{11}SH$) (W. Sauerwein et al. 2012, C. Gibson et al. 2003, H. Michiue et al. 2014, K. Nedunchezhian et al. 2016) are one of the bests. The uptake of each of the mentioned drugs depends on the type of tumor, thus research on new boron carriers for specific cancers is still lively ongoing (D. Alberti et al. 2015, W. Sauerwein et al. 2021). In case of neutron sources and BSA systems, the diversity of used materials for moderators, reflectors, shielding and some other important parts of the equipment, their thicknesses, shapes and sizes depend on many factors, and first of all on the initial energy and yield of neutrons. To focus a proper neutron flux in some cases heavy water is used (Figure 10) as the main component of the BSA, while other neutron moderators can include different types of isotopes which can be costly but effective to use in that unique case.

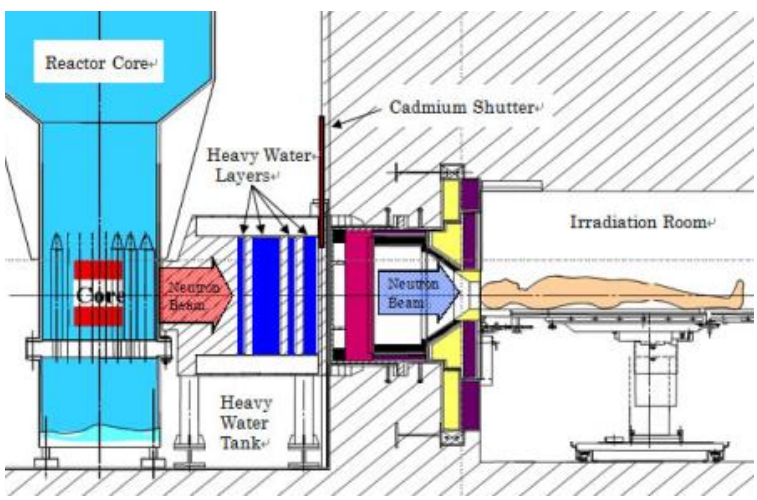

Figure 10. *Reactor based BNCT with a BSA made from heavy water layers of neutron moderator in JRR-4 (Figure adopted from (E. Bavarnegin et al. 2017)).*

1.5. Modern beam shaping assemblies (BSA) for BNCT

Neutron sources, which differ with their flux and energy, should have appropriate beam shaping assemblies (BSA) usable for BNCT. Their necessity in the way of the treatment is based on the type, size and depth of the tumor. The whole equipment (Figure 11) should be optimized and used considering neutron moderation, reflection and collimation.

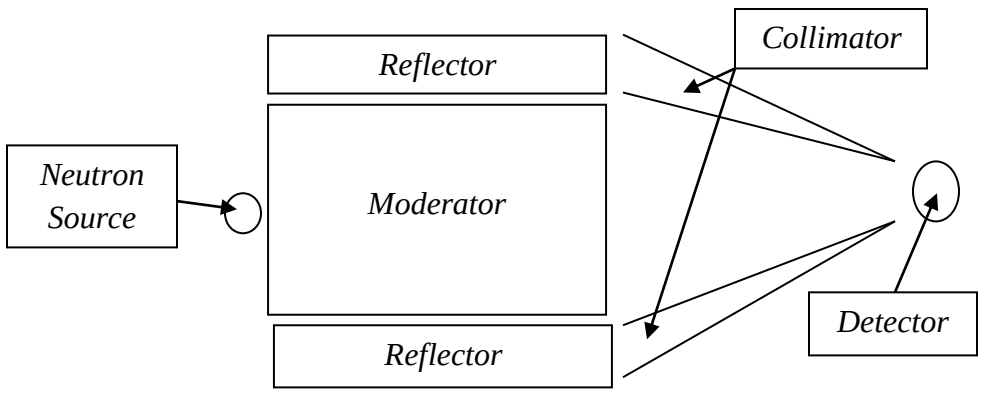

Figure 11. *Main parts of the BSA with additional components needed for the experimental setup.*

To separate the patient room from the rest of the experimental hall and partly solve the shielding problem, a thick concrete wall surrounding the BSA should be built. Besides the separating concrete wall, the whole building, which consists of the experimental hall and the patient room, should be isolated for the neighborhood safety reasons. The most optimal way for that, is the construction of a building from thick concrete or stone breaks. Same option would be the best for the ceiling or the floor, especially if there are any levels in that building/clinics.

Inside of each cell of the malignant tumor the capturing process is possible only if the energy of neutron is thermal (0.025 eV). Currently, all the existing neutron sources provide energies higher than the one needed for BNCT. Even if a neutron losses part of its energy during the penetration through the body to reach to the cell, the remaining energy is too high for the effective capture reaction in most of the cases. Thus, the initial energy moderation process is the key factor for the achievement of boron-neutron capturing process inside of the cancer cell. The construction of a BSA starts with its main component, which is the moderator of neutrons (Fig. 11). The selection of the moderator depends on the energy of neutrons, as well as, their angular distribution. In this thesis for the design of the BSA I have considered and performed simulations for the following materials as moderators: nat-Bi, ^{182}W, ^{186}W, nat-W, nat-U, nat-Al, nat-Fe, AlF_3, 40 % Al_2O_3 and 60 % AlF_3, 40% Al and 60 % AlF_3, 5 % Fe and 95 % AlF_3, Fe_2O_3, H_3BO_3, La_2O_3, LiF, TiF_4, salt, quartz.

Materials which reflect neutrons emitted from the source are necessary for focusing or collecting neutrons and for decreasing their number on the shielding materials. Back-reflectors are necessary in case of accelerator-based or DD/DT compact neutron generator-based neutron sources, as well as, based on the neutron sources from Californium-252 (^{252}Cf) or Americium-Beryllium (Am-Be) which neutron production source is the ^{9}Be(α, n)^{12}C nuclear reaction

followed by alpha ray emission of ^{241}Am ($T_{1/2}$ = 458 years). The need of back-reflectors usage comes mostly from the isotropic or quasi-isotropic distribution of the initial neutron yield. Besides back-reflectors, side-reflectors surrounding the moderator should be used. In this thesis I have considered in simulations lead and LiF reflectors and collimators with different dimensions and shapes.

The focusing procedure of neutrons, which starts from back and side reflectors, is followed with the installation of collimators to give a final direction to already thermalized neutrons. The selection of materials, shape and dimension of collimation system depends also on many factors, such as the angular distribution of neutrons expected after the moderation. In this thesis the main reflector material used for the GEANT4 simulations is natural lead, but for comparison LiF was examined as well, based on its thermal neutron filtering property.

As mentioned above the main difference between various BSAs comes from the requirements on the specific energy and yield of the final neutron flux. Currently, all the BNCT applicable neutron sources based on accelerators, DD/DT CNGs or nuclear reactors are unique because of the initial energy and yield of neutrons. The thermalization process should be differentiated depending on these factors, as well as on the final beam energy and number of neutrons per square centimeter.

Nuclear reactor-based neutron sources, equipped with BSA, are first thermal neutrons applied for BNCT (S. Altieri & N. Protti 2018). Currently they are in use only in a few research institutions worldwide, because of the expenses needed to keep the safety as well as for other reasons concerning its usage for medical purposes. In Figure 12 a map of some of the established nuclear reactor-based BNCT facilities is presented (Y. Kiyanagi et al. 2019). One of them is the Kyoto University reactor (KUR) which was installed in 1974 and which is one of the oldest reactors, being still in use as a multipurpose research reactor (Figure 13) with the BSA (Heavy water facility) for BNCT providing appropriate neutron flux for the medical treatment.

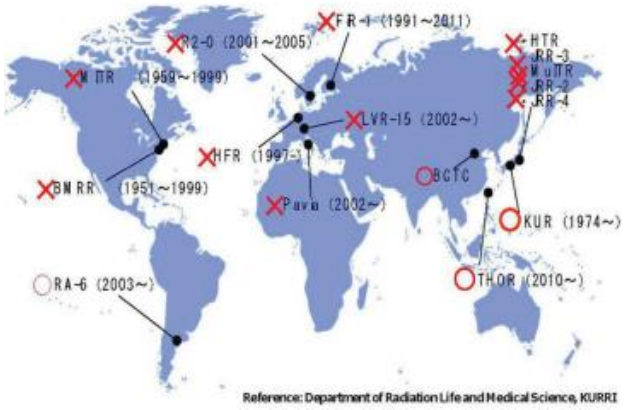

Figure 12. *Nuclear reactors used for BNCT which are still working (O) and were already shut down (X) (Figure adopted from* Y. Kiyanagi et al. 2019*).*

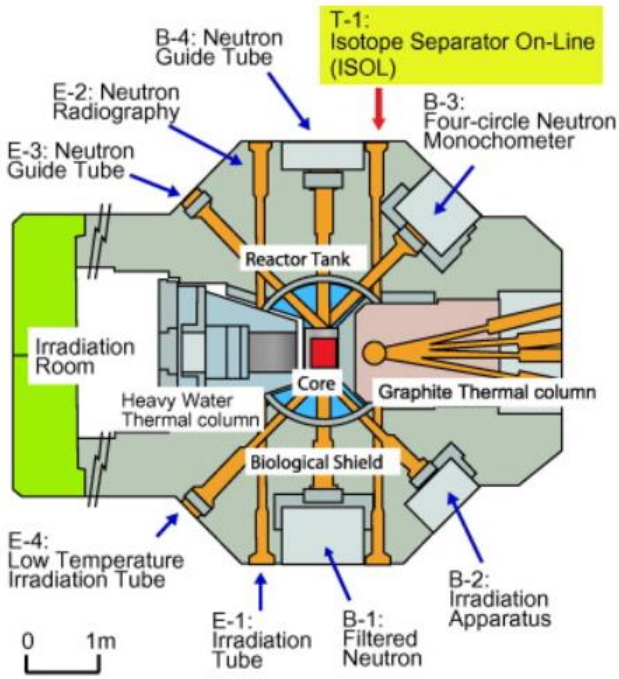

Figure 13. *Schematic view of the KUR reactor (Figure adopted from A. Taniguchi et al. 2013).*

The matter is completely different when the initial neutron source is based on accelerators with various energies and projectiles (Y. Kiyanagi et al. 2019).

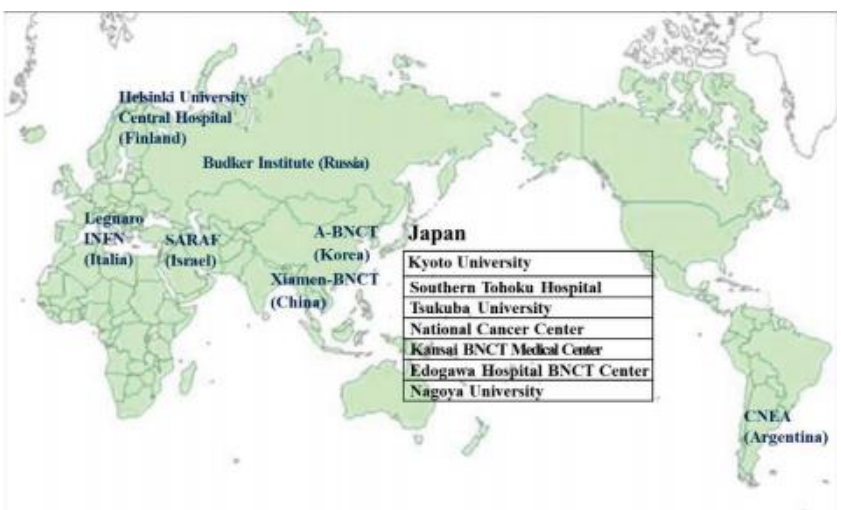

Figure 14. *Accelerator based BNCT facilities around the world (Figure adopted from Y. Kiyanagi et al. 2019).*

Initial energy and current of the projectile, as well as the material and thickness of the targets can be completely different when neutron source is based on accelerators (Figure 14). To produce mono-energetic or quasi-mono-energetic neutron beams, lithium-7 is widely in use as target for the low energy proton beams producing neutrons in the $^{7}Li(p,n)^{7}Be$ reaction with threshold energy of E_{th} = 1.881 MeV (Y. Kiyanagi et al. 2019). One of the main advantages of the low energy proton beam needed for the excitation and opening of the two-body (p,n) nuclear

channel is the production of low energy and quasi-monochromatic secondary neutron flux which is easier to thermalize. Here, there can be a problem connected with current or energy of protons to produce BNCT applicable neutron flux. This was possible to overcome at the BNCT laboratory in Budker Institute of Nuclear Physics (Novosibirsk, Russia), where a vacuum insulation tandem accelerator (VITA) is installed (S. Taskaev et al. 2021). It is suggested that ~2.5 MeV proton energy and ~15 mA current can be the best option for the BNCT (L. Zaidi et al. 2018). The BSA (Figure 15) used in this laboratory was constructed from 21 cm thick MgF_2 which provides BNCT applicable neutron flux, with additional layers of moderation such as Ti, Bi and Li-polyethylene (L. Zaidi et al. 2018).

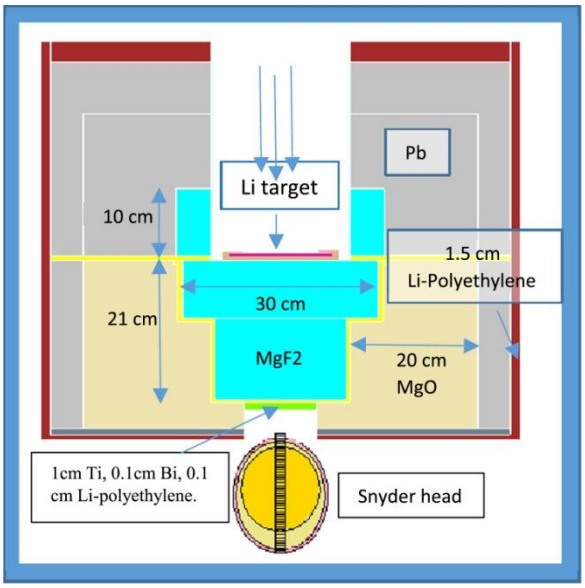

Figure 15. *Final design of the BSA used at the Russian BNCT laboratory in Novosibirsk (Figure adopted from (L. Zaidi et al. 2018)).*

In case of DT and DD CNGs where the initial energies are 14.1 MeV and 2.5 MeV, respectively, it is comparably easier to construct a BSA and apply it for all of such types of generators, if the initial neutron energies are the same. Here the difference of the BSA for various generators can be related to the purpose of the research, type of the cancer, as well as any other individual case. The compactness is one of the main advantages which makes these generators useful for clinical studies and for BNCT. The detailed discussion of BSA design and optimization based on the DD generator considered for BNCT is done in Section 4.2.

It is worth to mention that DD/DT compact neutron generator based BNCT studies are mostly under consideration based on the calculations with usage of different Monte-Carlo programs (J. Fantidis et al. 2015, F. Rasouli et al. 2012, S. Masoudi et al. 2017) and yet there is no such type of version of BSA which can be used together with generators in clinical BNCT cases.

2. State of the art of the BSA for CNG

2.1. BSA for BNCT based on DD CNG

Deuterium-deuterium (DD) CNGs, famous with their mobility, are one of the alternatives to accelerator based neutron sources. In Table 2 results for deuterium-deuterium compact neutron generator based investigations with comparison of IAEA recommendations for BNCT are presented. As research shows (see ref. in Table 2), in all of the cases the optimal BSA did not give a final suitability and yet need to be developed. The achievement of the BNCT applicable neutron flux is a step by step study, and the high amount of epithermal neutrons is one of the main goals to obtain. The research and development of a BSA for DD CNG based BNCT includes first of all the optimization of the final flux, filtered out from unnecessary thermal and fast neutrons, as well as gamma rays. Epithermal neutrons which will pass through the healthy tissue, can reach to the deep-seated tumor cells by losing part of their energy and already as thermal neutrons they can be captured inside the boron-10 containing cell. As this treatment method is mainly useful for the brain tumors like multiform glioblastoma, the energy distribution of neutrons should have 10 keV peak to reach the central area (at the 8 cm depth) of the brain (Durisi et al. 2007). The ratio between epithermal over thermal and epithermal over fast neutron components is important for the optimal treatment with less harm and damage of the healthy tissue.

BSA	***Yield [n/s]***	φ_{epi} ***[n/(cm²·s)]***	$\varphi_{epi}/\varphi_{thermal}$	$\varphi_{epi}/\varphi_{fast}$	D_f/φ_{epi} ***[Gy·cm²]***	$D_\gamma/\varphi_{epi.}$ ***[Gy·cm²]***
IAEA recommendations (in merit)	not fixed	$>10^9$	>20	fixed for BNCT (>20)	$<2\cdot10^{-13}$	$<2\cdot10^{-13}$
Susilowati et al. 2016	10^{11}	$8\cdot10^6$	52.91	-	$8.69\cdot10^{-13}$	$2.12\cdot10^{-14}$
Fantidis et al 2013	10^{11}	$1.17\cdot10^6$	128.81	20.81	$1.11\cdot10^{-17}$	$2.32\cdot10^{-17}$
Hsieh et al 2017	$5\cdot10^9$	$1\cdot10^5$	20	-	$5.5\cdot10^{-13}$	$2.4\cdot10^{-13}$
Kasesaz et al 2013	-	$1.19\cdot10^9$	573	20	$1.1\cdot10^{-14}$	$2.8\cdot10^{-13}$
Mu'alim et al 2018	$2.5\cdot10^{11}$	$3.16\cdot10^7$	-	-	-	-
Durisi et al 2007	10^{11}	$1.87\cdot10^6$	-	-	$1.82\cdot10^{-12}$	$2.98\cdot10^{-13}$

Table 2. *Comparison of different DD CNG-based BSAs for the BNCT.* $\varphi_{thermal}$, φ_{epi} *and* φ_{fast} *denote the flux of thermal, epithermal and fast neutrons, respectively.* D_f *and* D_γ*: are the doses of fast neutrons and gamma rays.*

The feasibility study of DD based BNCT for the achievement of a desirable epithermal neutron flux are performed mostly using MC simulations. To estimate the effect of the treatment method on the base of DD CNG simulations using the MCNP code were performed and described by different scientific groups worldwide, such as J. Fantidis et al. 2013 in Greece, M. Hsieh et al. 2017 in USA, Y. Kasesaz et al. 2013 in Iran. The investigation for a design of an appropriate BSA was carried out by the optimization of the studied material types, shapes and sizes for the moderator, reflector, and collimator respectively. Ten different materials with different thicknesses were discussed as energy spectrum shifters, such as Fluental, TiF_3, AlF_3, CF_2, MgF_2, Al_2O_3, D_2O, BiF_3, BiF_5 and CaF_2. According to the simulations the highest number of epithermal neutrons was possible to achieve in case of 10 cm thick heavy water (Figure 16).

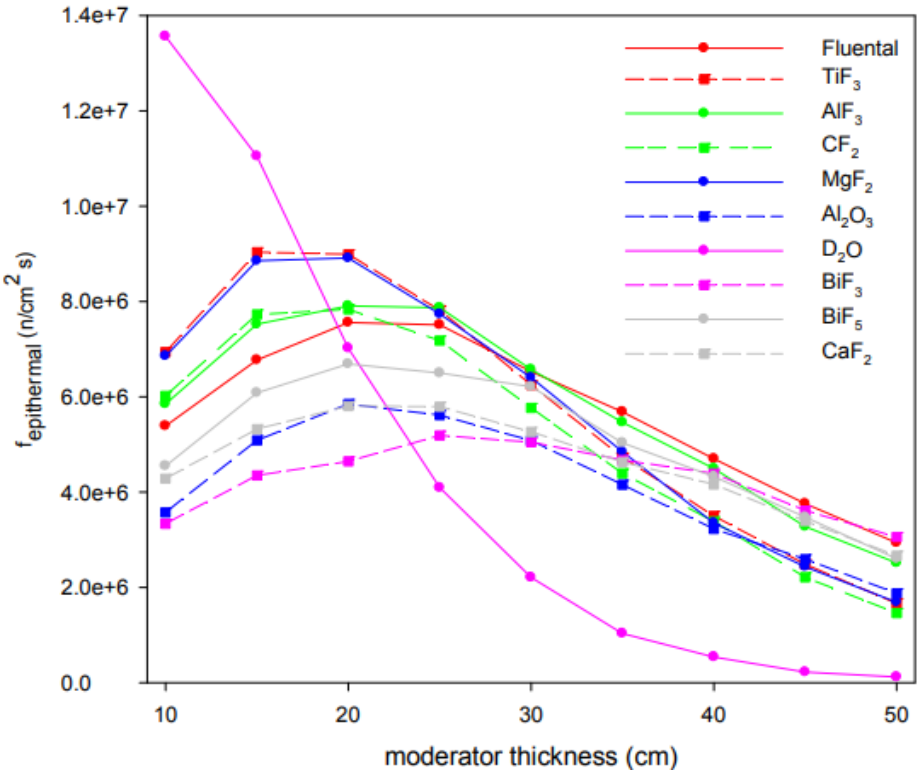

Figure 16. *Epithermal neutron flux dependence on various materials and thicknesses (Figure adopted from (J. Fantidis et al 2013)).*

The high amount of epithermal neutrons itself is not sufficient as recommended by IAEA for BNCT. The research for the estimation of the epithermal over thermal and epithermal over fast neutron flux ratios had shown that the best for the 1st moderator would be the usage of 18 cm thick TiF_3 (figures 16 - 18) (J. Fantidis et al. 2013). As presented in Figure 17 the epithermal over thermal ratio reaches the desirable value over 20 only for the TiF_3, while the ratio of epithermal over fast neutron fluxes yet need to be developed and the balanced ratios in

connection with epithermal neutron flux must be kept for further moderation, when the other moderators will be installed next to the TiF_3.

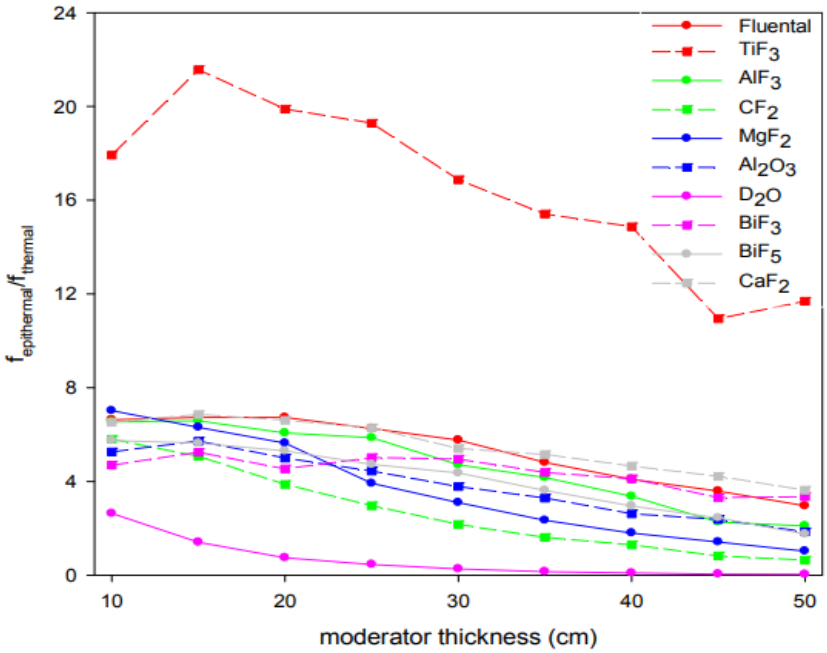

Figure 17. *Epithermal over thermal neutron flux ratio as a function of thickness of various materials (Figure adopted from J. Fantidis et al 2013).*

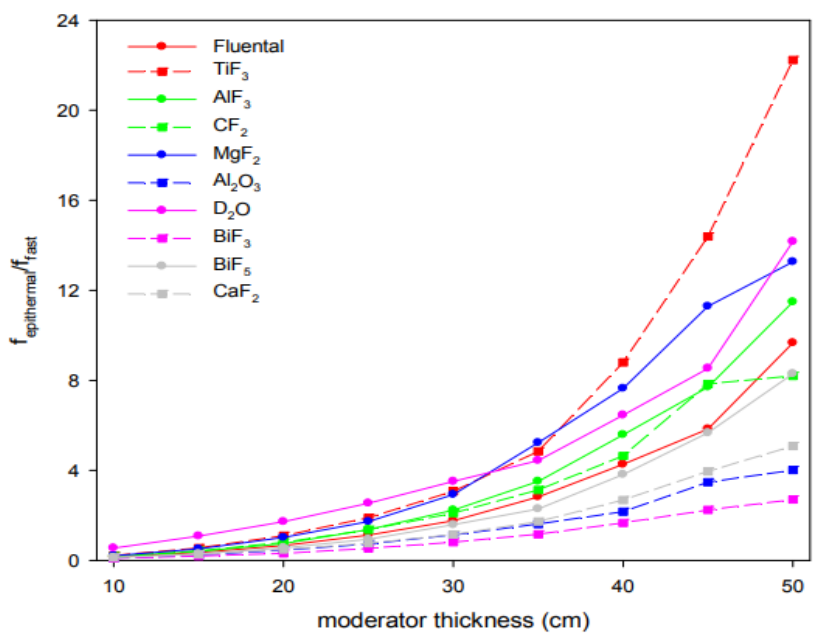

Figure 18. *Epithermal over fast neutron flux ratio as a function of thickness of various materials (Figure adopted from J. Fantidis et al 2013).*

For the selection of the second part of the moderator the other nine materials with different thicknesses were installed next to the 18 cm TiF_3 and simulated. The investigation for

the adequate ratios in comparison with epithermal neutron flux was performed and as depicted in Figure 19 the epithermal neutron flux is comparably higher when the second moderator is fluental or AlF_3.

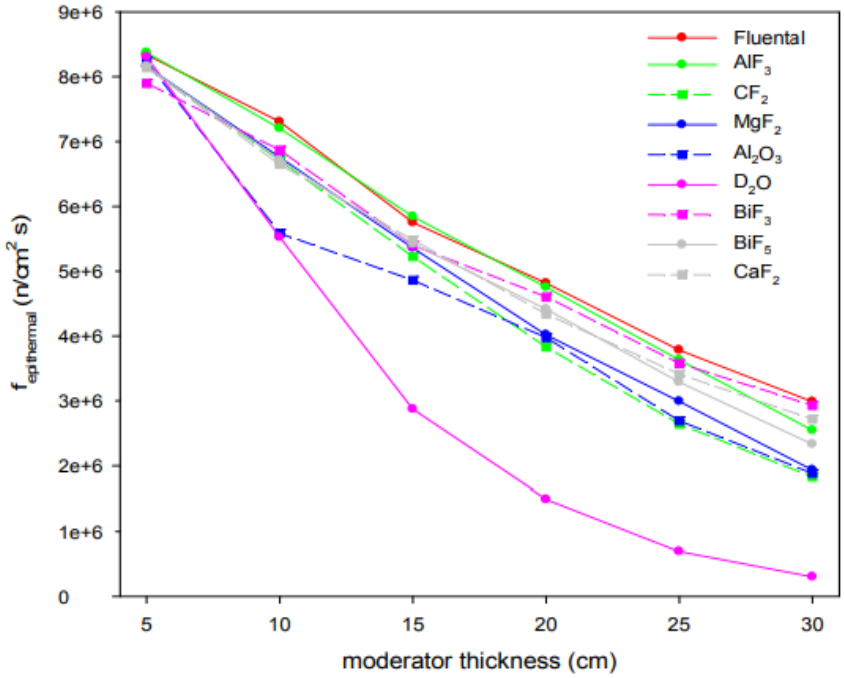

Figure 19. *Epithermal neutron flux as a function of thickness of various materials installed next to TiF_3 as second part of moderator (Figure adopted from J. Fantidis et al 2013).*

Study of the ratios of epithermal over thermal and epithermal over fast neutron components had shown that in case of 18 cm thick AlF_3 mixture installed next to the first moderator TiF_3 gives quite desirable results as presented in figures 20 and 21.

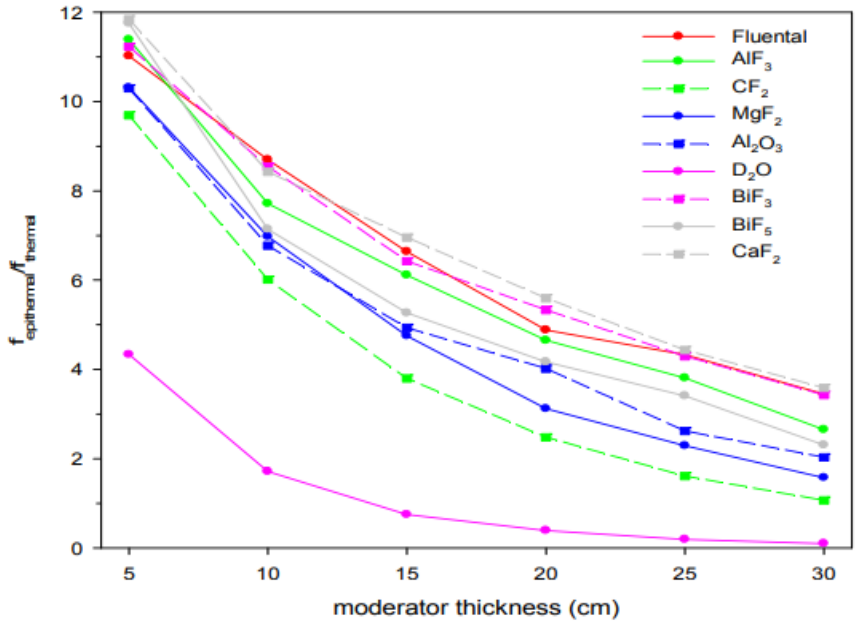

Figure 20. *Epithermal over thermal neutron flux ratio as a function of thickness of various materials installed next to TiF_3 as second part of moderator (Figure adopted from J. Fantidis et al 2013).*

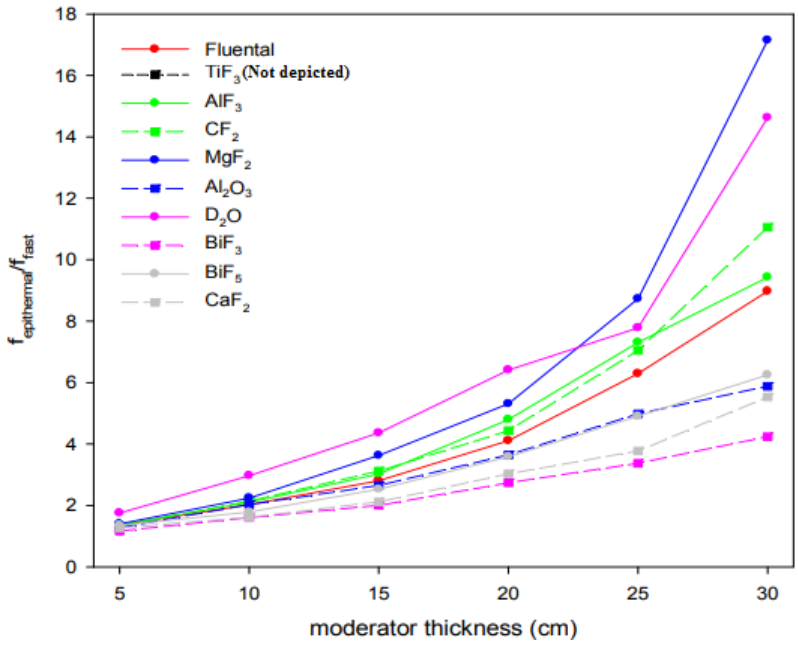

Figure 21. *Epithermal over fast neutron flux ratio as a function of thickness of various materials installed next to TiF_3 as second part of moderator (Figure adopted from J. Fantidis et al 2013).*

By taking into account the results shown in Figures 16-21 the first part of the moderator is decided to be made from heavy water and TiF_3. As can be seen in Figure 16 the amount of

epithermal neutrons is higher when D_2O is placed as moderator. Based on the optimization results the cone-shaped heavy water moderator with 6 cm length and radiuses of 5 cm and 4 cm, was placed inside of the 18 cm thick TiF_3 as first part of the moderator.

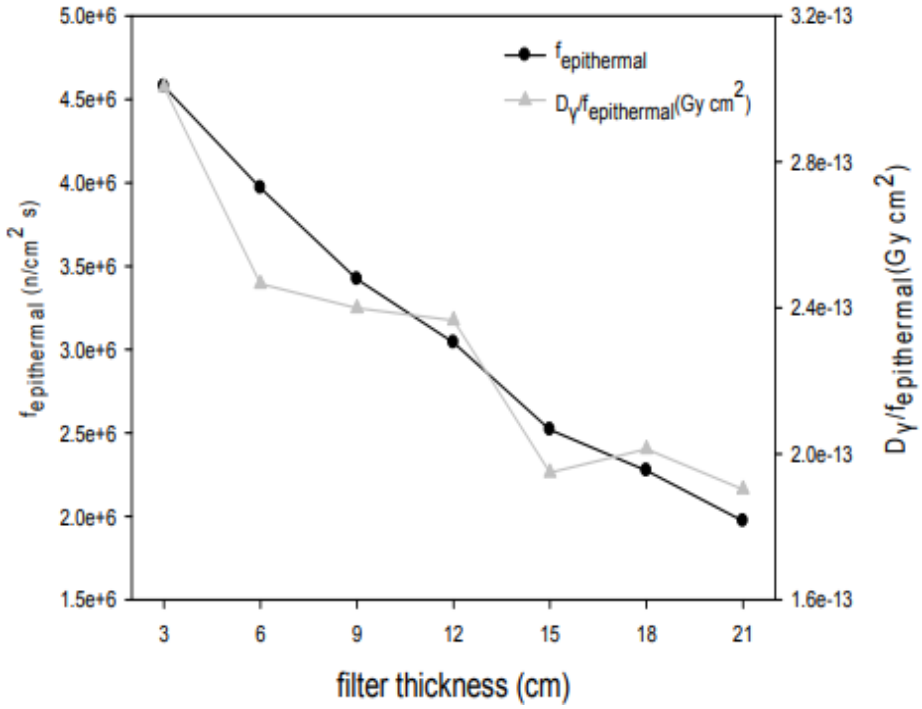

Figure 22. *Epithermal neutron flux and D_γ / $f_{epithermal}$ (same as D_γ/φ_{epi}) ratios in case of different thicknesses of Ti filter for the optimized BSA (Figure adopted from J. Fantidis et al 2013).*

The simulation results (Figures 19-23) had shown that in the optimal case the other moderation parts should be made from 18 cm thick AlF_3 as second moderator, and 18 cm thick BiF_3 as third moderation part and gamma-ray filter, followed by conical shaped 6 cm thick Ti layer as fast neutron filter (see Figures 22 and 23) where the radiuses are 45 cm and 12 cm. The last part of the optimized BSA is composed from 2 cm thick Li layers as thermal neutron filter and surrounded by 3cm thick Poly-Li delimiter as illustrated in Figure 24.

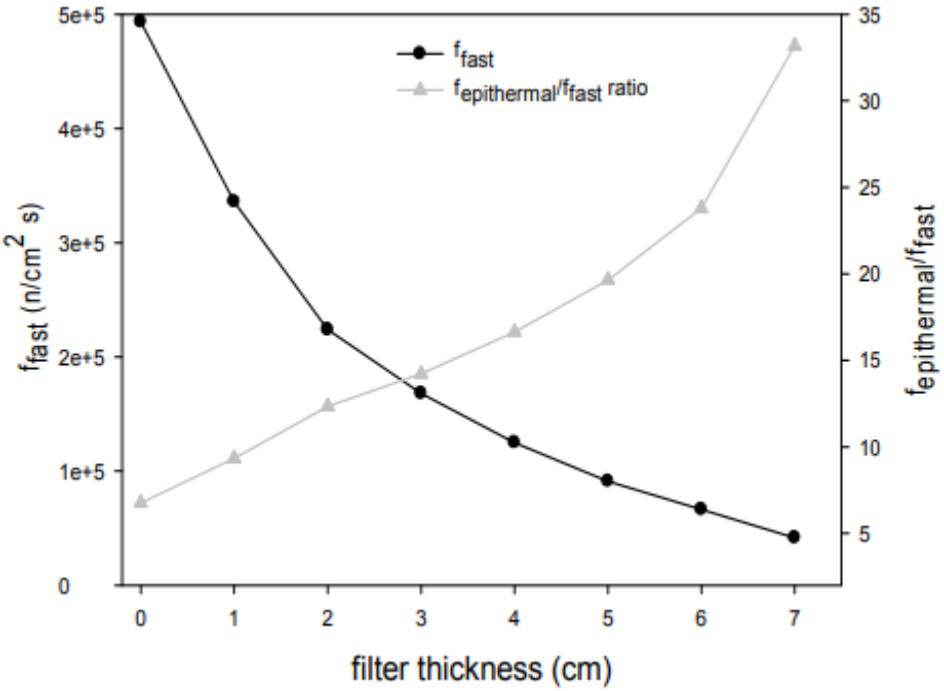

Figure 23. *Fast neutron flux and $f_{fast}/f_{epithermal}$ (same as $\varphi_{fast}/\varphi_{epi}$) ratio in case of different thicknesses of Ti filter of the optimized BSA, presented in Figure 24 (Figure adopted from J. Fantidis et al. 2013).*

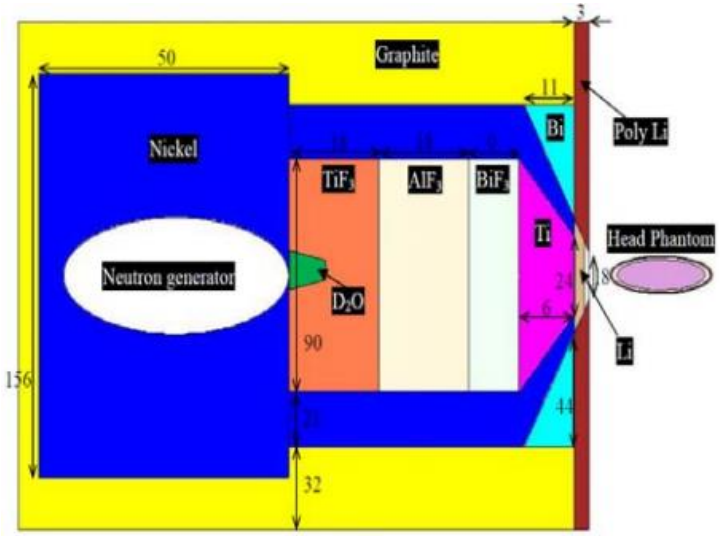

Figure 24. *Geometric configuration of the BNCT system not in scale (dimensions are given in cm) (Figure adopted from Fantidis et al. 2013).*

To sum up the achievement by the Greek research group and the optimization of the BSA(Figure 24), it is worth to mention that the recommendation of IAEA for BNCT were followed for the ratios of epithermal over thermal and epithermal over fast neutron fluxes with

values 128.81 and 20.81, respectively. Also the dose of gamma rays over the epithermal neutron flux and the dose of fast neutrons over the epithermal neutron flux with values $1.11 \cdot 10^{-17}$ Gy·cm^2 and $2.32 \cdot 10^{-17}$ Gy·cm^2, are in agreement with the recommendations. However, the obtained epithermal neutron flux is around $1.17 \cdot 10^6$ n/(s· cm^2), three orders of magnitude smaller than the needed 10^9 n/(s·cm^2). The described facility results are comparably better than many other scientific investigations in this field and, as previously was noted, the DD CNG neutron yield should be at least in order of 10^{13} n/s for the achievement of the desired amount of the epithermal neutron flux.

Taking into account in air parameters for BNCT recommended by IAEA (IAEA TECDOC 2001), as DD CNG based BSA design it is worth to describe the details of the work by the USA research team of M. Hsieh et al. 2017. In Table 3 results of the MCNPX simulations based on different thicknesses and mixtures as various parts of the moderator are presented and the assumed DD CNG maximum neutron yield amounts to $5 \cdot 10^9$ n/s. Optimization of the BSA configuration resulted in the thermal over epithermal ratio equal to 0.05, with $5.5 \cdot 10^{-13}$ Gy·cm^2 dose ratio of fast neutrons per epithermal neutron fluence and with dose of gamma rays per epithermal neutron fluence equal to $2.4 \cdot 10^{-13}$Gy·cm^2.

No.	**Moderator (cm)**	**φ_{epi} (n_{epi}/(cm^2·s)**	**$\varphi_{thermal}$ /φ_{epi}**	**D_f/φ_{epi} (Gy·cm^2)**	**D_γ/φ_{epi} (Gy·cm^2)**
1	AlF_3 (50)	$1.8 \cdot 10^5$	0.01	$1.4 \cdot 10^{-12}$	$1.8 \cdot 10^{-13}$
2	Li^7F (50)	$1.5 \cdot 10^5$	0.04	$6.6 \cdot 10^{-13}$	$1.8 \cdot 10^{-13}$
3	Li^7F (45) + MgF_2 (10)	$1.0 \cdot 10^5$	0.05	$5.5 \cdot 10^{-13}$	$2.4 \cdot 10^{-13}$
4	Li^7F (45) + AlF_3 (10)	$1.2 \cdot 10^5$	0.04	$5.6 \cdot 10^{-13}$	$3.4 \cdot 10^{-13}$
5	AlF_3 (55) + MgF_2 (10)	$8.3 \cdot 10^4$	0.025	$5.4 \cdot 10^{-13}$	$2.3 \cdot 10^{-13}$
6	CaF_2 (50)	$8.0 \cdot 10^4$	0.05	$6.4 \cdot 10^{-13}$	$2.7 \cdot 10^{-13}$
7	CaF_2 (50)	$1.5 \cdot 10^5$	0.01	$3.9 \cdot 10^{-12}$	$2.2 \cdot 10^{-13}$

Table 3. *Different moderator configurations of the BSA studied by M. Hsieh et al. 2017.*

To avoid in the simulation results question regarding the intersecting (fluence) and passing through the area (flux), it is important to note that the number of detected neutrons over the area and time is taken as neutron flux and its integrated value per certain period of time as fluence. To avoid the confusion and keeping things more understandable in some of the tables only the number of registered particles are presented mentioning the initial number of the simulated neutrons.

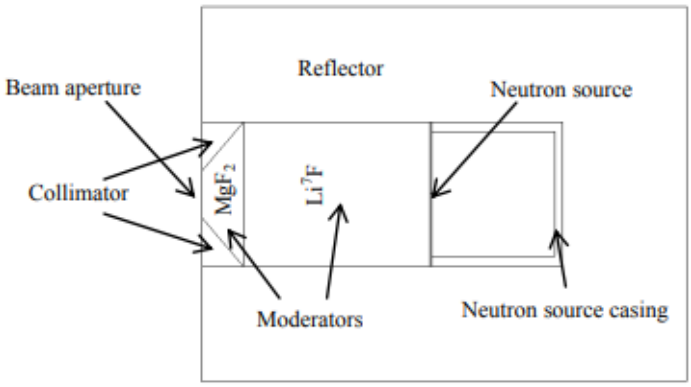

Figure 25. *Scheme of the optimized BSA configuration by M. Hsieh et al. (Figure adopted from M. Hsieh et al. 2017).*

In the described research the optimal BSA design for BNCT based on DD CNG was possible to achieve by using 45 cm thick ^{7}LiF as first part of the moderator and 10 cm thick MgF_2 as second part of the moderator, and the reflector was made of 30 cm thick Pb (Figure 25). For the best case the cone-shaped collimator with 10 cm length was also designed from lead, with aperture of 12 cm diameter closed by 0.1 mm thick Cd filter for the contribution of the final dose. As result of the simulations the obtained epithermal neutron flux was 10^5 n/(s·cm^2) (the neutron fluence is presented in Figure 26, details can be found in M. Hsieh et al. 2017) which requires $4.9\cdot10^{13}$n/s yield of initial neutrons for the formation of a desired 10^9 n/(s·cm^2) epithermal neutron flux.

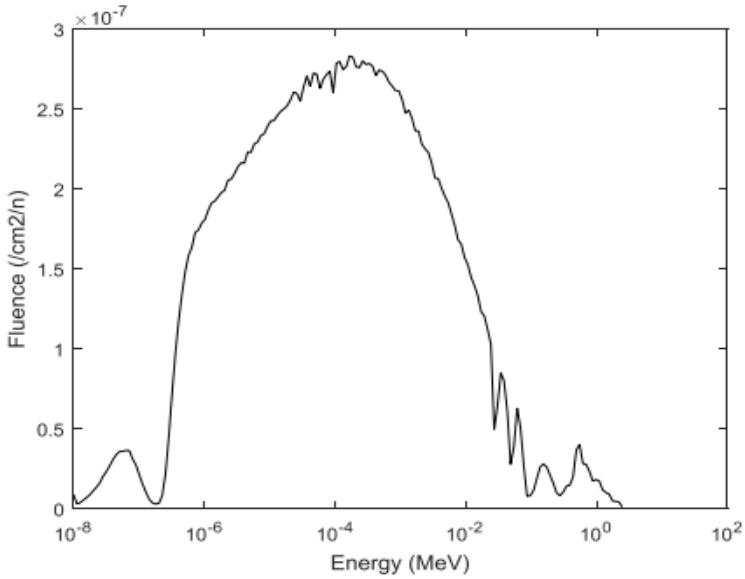

Figure 26. *Energy distribution of neutrons registered at the beam aperture (For the BSA presented in Figure 25) (Figure adopted from M. Hsieh et al. 2017).*

In case of sufficient initial neutron yield from DD CNG it was possible to achieve $1.19\cdot10^9$n/(s·cm^2) epithermal neutron flux with ratios 573 and 20 for epithermal over thermal

and epithermal over fast neutron fluxes, respectively. The Iranian group of Y. Kasesaz et.al, obtained the best agreement with the IAEA recommendation for BNCT, in case of 70 cm thick fluental moderator, 2 mm thick ^{6}Li thermal neutron filter and 2 mm thick Pb gamma ray filter, with 30 cm thick lead reflector (Figure 27) (Y. Kasesaz et al. 2013).

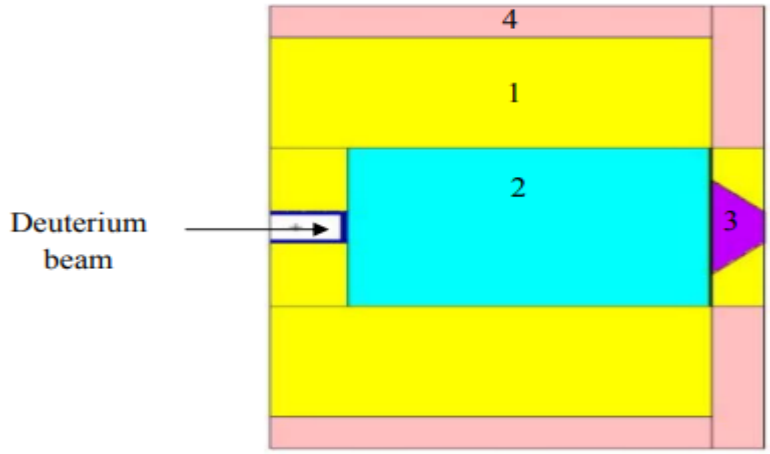

Figure 27. *DD based BSA configuration with (1) reflector, (2) moderator, (3) collimator and (4) gamma shield (Figure adopted from Y. Kasesaz et al. 2013).*

The registered neutron energy spectrum for the optimized BSA is mostly in the epithermal neutron energy region with 94 % epithermal neutrons (Figure 28).

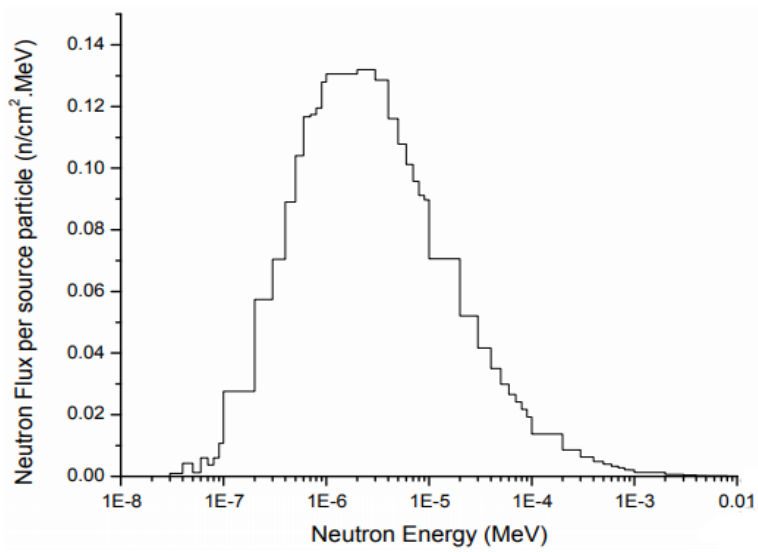

Figure 28. *Neutron energy distribution in case of the optimized BSA (Figure 27) (Figure adopted from Y. Kasesaz et al 2013)*

The detailed discussion is done for the estimation of the dose and its therapeutic influence using the head phantom. Also, the penetration depth of the formed neutrons by all of the above mentioned research groups is significant and mainly connected with the initial energy and direction of neutrons.

2.2. BSA for BNCT based on DT CNG

The study for the DT based BNCT as one of the important steps includes the optimal BSA designing for the moderation of the initial 14.1 MeV neutrons and the achievement of a neutron flux which will be consistent with IAEA recommendations for BNCT (IAEA TECDOC 2001). Modern DT CNG neutron yield can reach up to 10^{14} n/s, and taking into account the high initial energy, there is a chance to design a BSA which will thermalize neutrons in an adequate energy region and at the same time keep focused the correct amount of neutrons useful for the therapy. The achievement of 10^9 n/s/cm^2 epithermal neutron flux is highly possible in this case.

The feasibility study of a DT-based BNCT was done using MC codes as a part of the research to develop an appropriate BSA and estimate the consistency of a final flux with IAEA recommendations. The detailed explanation and step by step guide for the optimization of a DT based BNCT facility was provided by J. Fantidis and A. Antoniadis 2015. Due to the high energy of neutrons it is possible to use neutron multipliers and this can be one of the ways for the BNCT usable neutron flux achievement. The selected multiplier in this study was natural uranium and for a different parts of the moderator of the optimal BSA, fourteen materials with various combinations were considered.

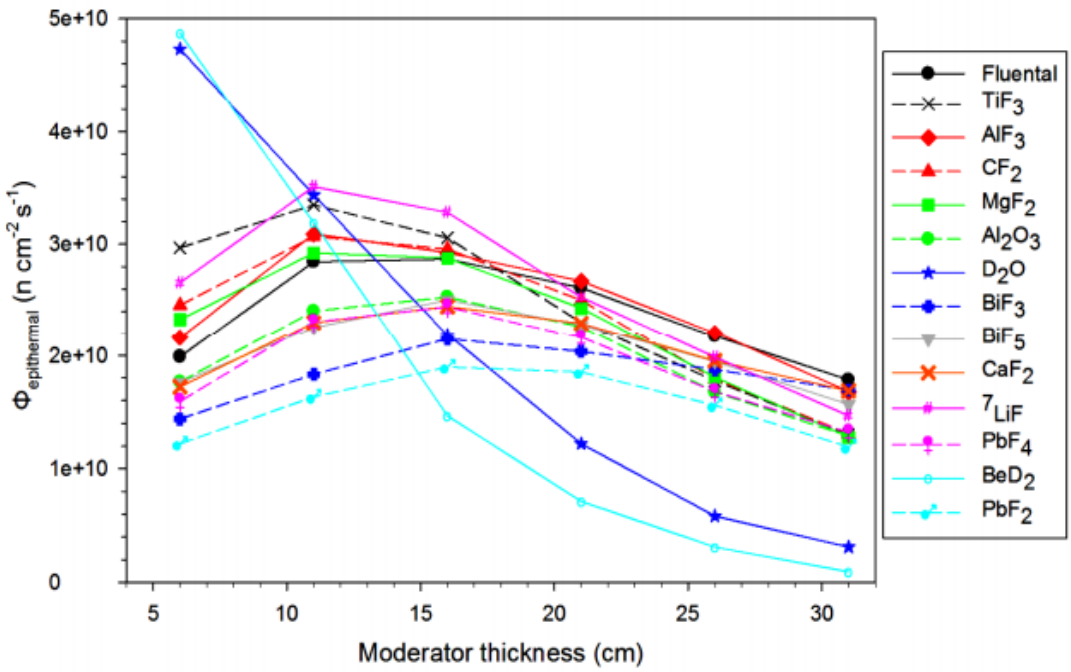

Figure 29. *Epithermal neutron flux after first part of moderator (for the BSA in Figure 34) (Figure adopted from J. Fantidis and A. Antoniadis 2015).*

As a first step of the study the epithermal neutron flux variation was discussed, as presented in Figure 29, for several materials with various thicknesses: Fluental, TiF_3, AlF_3, CF_2, MgF_2, Al_2O_3 D_2O, BiF_3, BiF_5, CaF_2, ^7LiF, PbF_4, BeD_2, PbF_2 for various thicknesses.

The epithermal neutron flux on its own is not yet enough to select the best material for the first part of the moderator and, as recommended by IAEA, there is a necessity to estimate the ratio of epithermal neutrons over thermal and fast components of the final flux, as well as gamma ray dose and fast neutron dose over the epithermal neutron flux. Thus, the highest registered epithermal neutrons flux for the thin layers of BeD_2 and D_2O should be considered in combination with other materials. Step by step investigation for the above-mentioned purposes, especially for the ratio of the epithermal over fast neutron fluxes, as result of the Monte Carlo simulations by MCNP-4B shows that the optimal version for the neutron energy shifter to the epithermal region is ^{7}LiF with 19 cm thickness. For that selection simulation results of epithermal neutrons and the ratio (Figure 30) of the epithermal over fast neutron components, were taken into account.

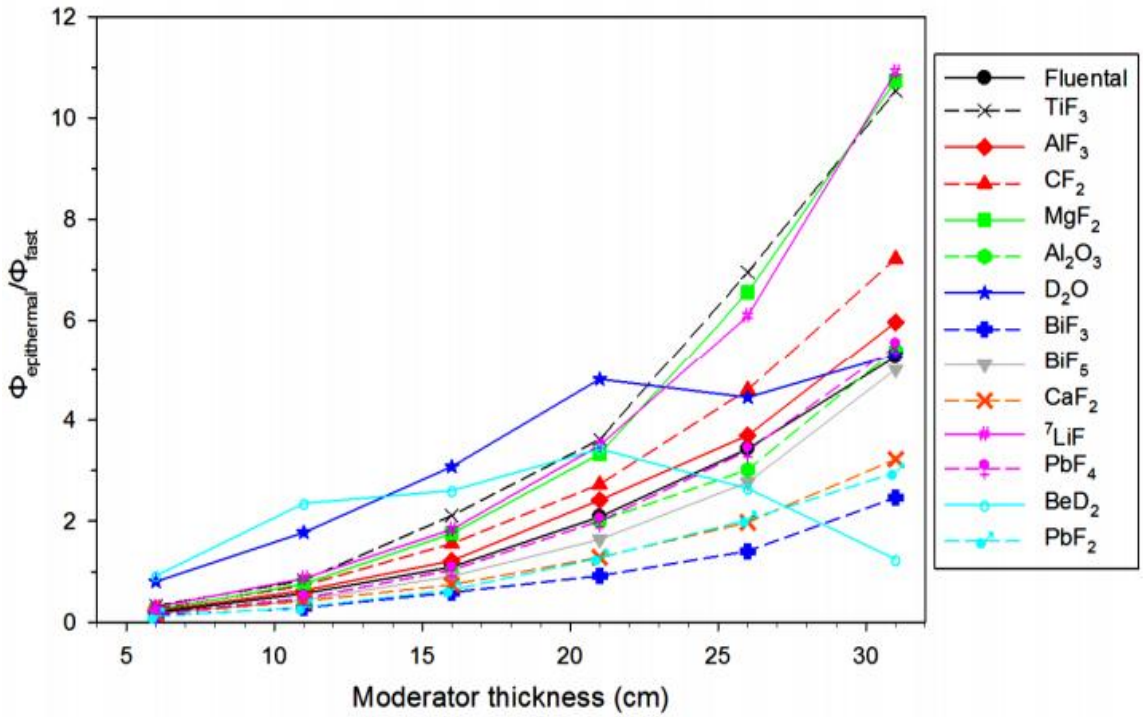

Figure 30. *Ratio of epithermal over fast neutron fluxes simulated for different thicknesses and materials for the DT neutron generator used as a source for BNCT (Figure adopted from Fantidis & Antoniadis 2015).*

The combination of uranium multiplier and lithium fluoride with conically shaped heavy water and seven other materials result in new intensities of epithermal neutrons. As presented in Figure 32 for the selection of the second part of the moderator all of the candidates can be useful, while the optimal material for the ratios of epithermal over thermal and fast neutron components is TiF_3 with 19 cm thickness. Figures 30 - 33 present the above mentioned ratios as function of thickness of different materials. Based on the simulations for fast as well as thermal neutrons 5 cm thick ^{60}Ni and 15 mm thick Cd were selected, respectively. As for gamma rays,

the best material to filter them out was decided to be 5.5 cm thick Bi and 2 cm thick delimiter made from Li-polyethylene to complete the design of the optimal BSA (Figure 34).

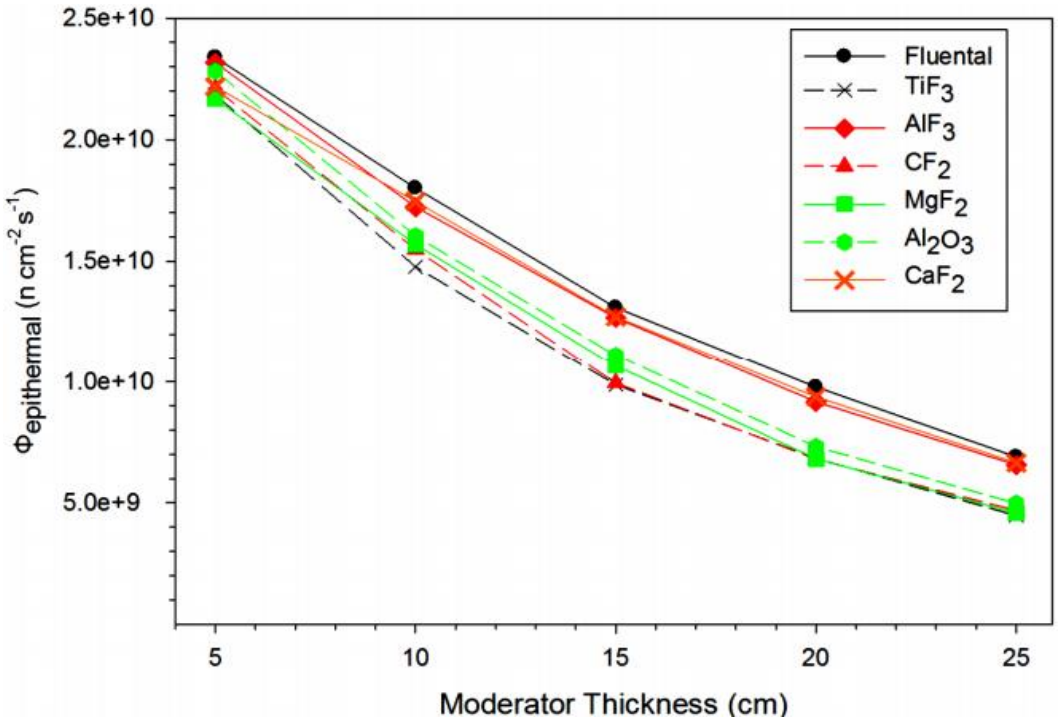

Figure 31. *Epithermal neutron flux dependence on various materials and thicknesses as second part of moderator installed next to ^{7}LiF with conical volume of D_2O (for the BSA in Figure 34) (Figure adopted from J. Fantidis and A. Antoniadis 2015).*

The resulting ratio of epithermal over thermal neutrons equals to 107.95 and epithermal to fast: 52.29, respectively. The dose of gamma rays and the dose of fast neutrons over the epithermal neutron flux were $0.179 \cdot 10^{-13}$ Gy-cm^2 and $1.27 \cdot 10^{-13}$ Gy-cm^2, respectively, with the final epithermal neutron flux equal to $3.94 \cdot 10^9$ n/(s·cm^2) as the best agreement with IAEA recommendations for BNCT.

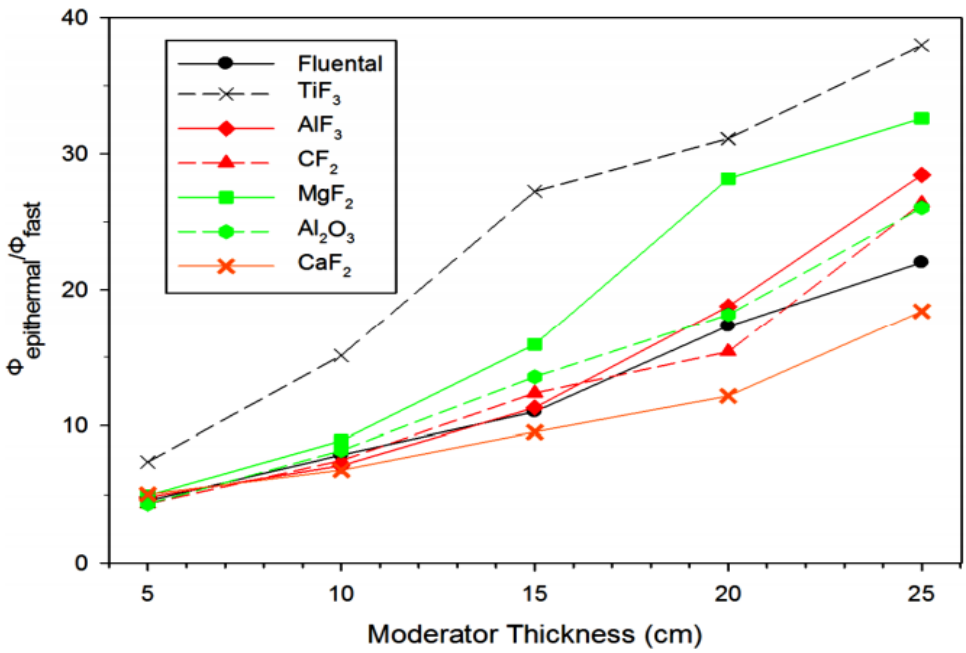

Figure 32. *Epithermal over fast neutron flux ratio dependence for various materials and thicknesses installed next to ^{7}LiF as second part of moderator (for the BSA in the Figure 34) (Figure adopted from J. Fantidis and A. Antoniadis 2015)*

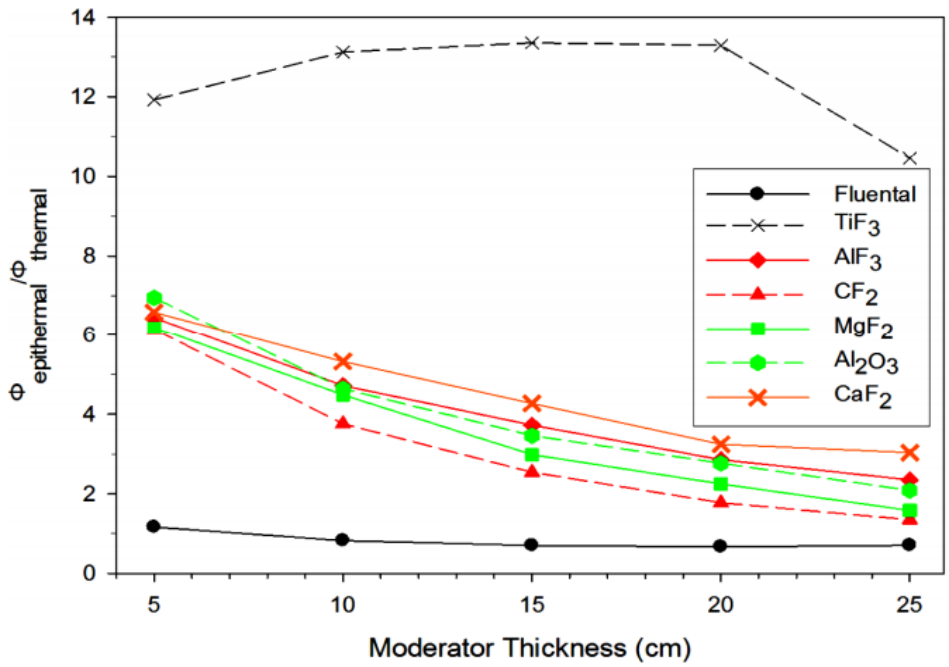

Figure 33. *Epithermal over thermal neutron flux ratio dependence for various materials and thicknesses as second part of moderator installed next to ^{7}LiF with conical volume of D_2O (for the BSA in Figure 34) (Figure adopted from J. Fantidis and A. Antoniadis 2015)*

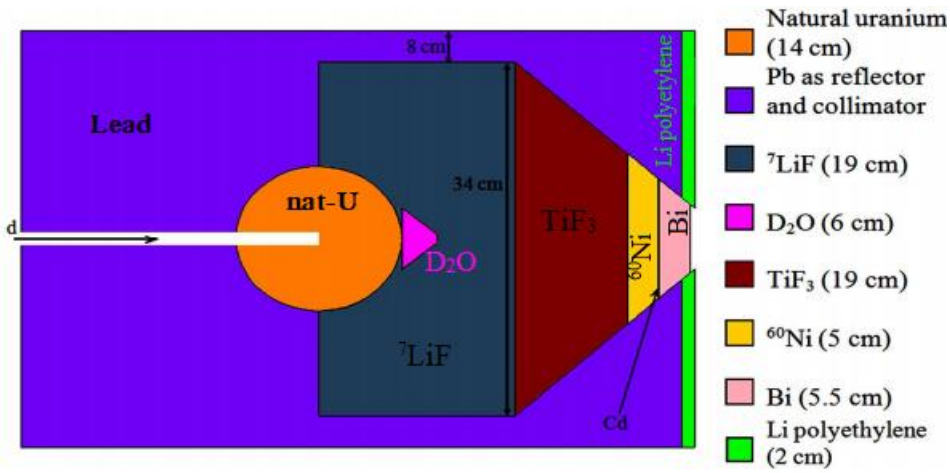

***Figure 34**. Optimized version of the BSA based on DT neutron generator (Figure adopted from J. Fantidis and A. Antoniadis 2015)*

Taking into account the research by J. Fantidis and A. Antoniadis described in their article from 2015 and the above presented details about their studies for the optimization of the BSA the final version of the DT neutron generator based BSA is shown in Figure 34 with its dimensions and types of the materials/compositions.

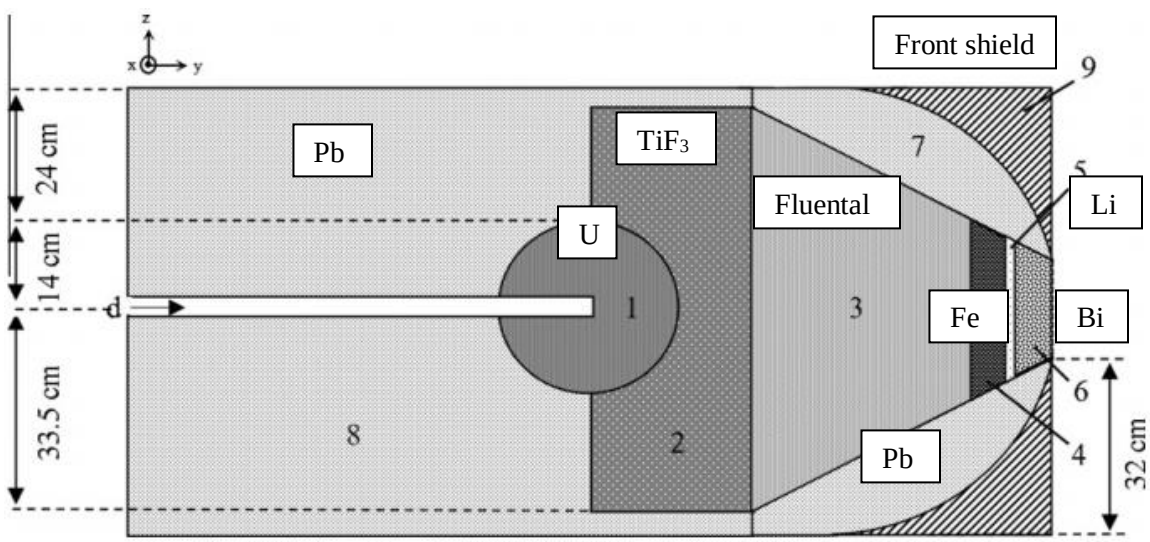

***Figure 35**. The Scheme of the Optimized BSA based on DT neutron generator, with 14 cm radius of Uranium multiplier (1), 23 cm thick TiF_3 (2), 36 cm thick Fluental (3), 4 cm thick Fe (4), 1 mm thick Li (5), 2.6 cm thick Bi (6), Pb as collimator (7) and reflector (8), with front shield (9) (Figure adapted from F. S. Rasouli 2012).*

To select the best solution for the optimal BSA design there is a necessity to consider other studies as part of the DT based BNCT research. As one of them it is important to mention the work of Rasouli et al 2012.

The final BSA designed with uranium multiplier of 14 cm radius, the moderator composed of 23 cm thick TiF_3 as first part and 36 cm thick Fluental as second part followed

with 4 cm thick Fe and 1 mm thick Li fast and thermal filters, accordingly and with 2.6 cm thick Bi as gamma ray filter (Figure 35). The collimator and reflector is lead and the shield is concrete for the optimal design of the BSA, resulting in the epithermal neutron flux equal to $4.43 \cdot 10^{9}$ n/(s·cm^{2}) from the $1.45 \cdot 10^{14}$ n/s initial neutron yield, with the ratios of 121.2 and 23.75 for the epithermal over thermal and fast components, accordingly.

The doses of gamma rays and fast neutrons over the epithermal neutron flux is also consistent with the recommendations of IAEA with values of $1.98 \cdot 10^{-13}$ Gy·cm^{2} and $0.59 \cdot 10^{-13}$Gy·cm^{2}, respectively, while the ratio of the epithermal neutron current over the epithermal neutron flux is 0.61 instead of 0.7 recommended value.

2.3. Selection of the source and BSA

The research in the field of BNCT showed that the accelerator based treatment is an optimal alternative to the reactor based therapy. Three BNCT laboratories in Finland, Japan and Russia have significant achievements and progress compared with other research centers which are not at the level of clinical or preclinical studies (Y. Kiyanagi et al 2019). Based on the above-mentioned studies it can be concluded that accelerator based BNCT can be applied for both shallow and deep-seated malignant tumors with successful treatments of tumors of various organs. The Japanese research center is leading with its accelerator based system which includes an accelerator with appropriate target and BSA for neutrons. It is known as the world's first accelerator based BNCT facility (T. Mitsumoto et al 2010).

The optimization of a DT neutron generator based BSA makes the realization of BNCT for clinical cases. Due to the latest results of the MC simulation studies the method has quite high consistency with IAEA recommendations, while it needs additional corrections for deep-seated tumors. The research shows that the inconsistency with IAEA recommendations is connected with the ratio of the epithermal neutron current over the epithermal neutron flux, which is quite close to the targeted 0.7 value, while it is not yet enough for practical cases (J. Fantidis & A. Antoniadis 2015, F. Rasouli 2012). It is also important to decrease energies of neutrons so they are as close as possible to 10 keV to make the final flux useful for the treatment of deep-seated cancers based on DT neutron generators.

The progress of the DD CNG development yet needs to be investigated in the way of increasing the initial neutron yield, to achieve the targeted minimum 10^9 n/(s·cm^2) epithermal neutron flux as discussed in Section 2.1 and recommended by IAEA. The low energy emission of neutrons after the BSA still can be useful for BNCT, but not for deep-seated malignant tumors. Comparably low cost, mobility and compactness of this type of neutron generators can be an alternative for reactors and accelerators to be used for shallow-seated tumors due to the existence of low energy peak of the epithermal neutrons closer to the thermal energetic region.

2.4. Estimation of absorbed dose

The estimation and determination of the absorbed dose is an important and at the same time-consuming or complex procedure. The influence of gamma rays and neutrons with different energy and angular distribution should be properly investigated by taking into account all of the factors for a successful treatment. For the BNCT performance the necessity of medical merits consideration is an asset. As main parts of the medical merits are considered: the ratio of the effective tumor dose to the effective maximum normal tissue dose known as Therapeutic Gain (TG), Advantage Depth (AD) and Therapeutic Depth (TD), where AD is the depth at which the normal tissue dose is equal to the tumor dose and TD is the depth at which the tumor dose decreased two times with respect to the dose of the normal tissue (details can be find in the Y. Kasesaz et al 2013), also the Advantage Depth Dose Rate (ADDR) which is the maximum dose rate to normal tissue. As defined by Y. Kasesaz et al 2013 for the weighted total dose (D_w):

$$D_w = W_g D_g + W_B D_B + W_N D_N + W_{fn} D_{fn},$$

where D_g is the gamma dose, D_B is the dose absorbed due to neuton capture on ^{10}B, D_N is the dose due to the neutrons captured on nitrogen and D_{fn} is the fast neutron dose. While Wg, W_B, W_N and W_{fn} are the corresponding weighting factors. For the calculations Wg was considered to be 1.0, W_B equals to 1.35 and 3.8 in the normal tissue and tumor respectively. And W_N, W_{fn} were taken as 3.2 (Y. Kasesaz et al 2013). Doses in the tumor and normal tissue were computed as a function of the boron concentration. The optimization of the dose computed in the tumor and normal tissue as a function of the boron concentration is an important stage of the treatment.

2.5. BNCT for brain tumor

The latest research for the brain tumor treatment based on the sufficient dose delivery for the malignant tumor shows that in some cases BNCT is the only solution prolonging the life of a patient (IAEA TECDOC 2001, R. Barth et al. 2018, Y. Kiyanagi et al. 2019). The calculations of the dose by different research groups as part of the investigations are another significant achievement. The simulation studies include the Snyder's head phantom presented in Figure 36. It has different layers for the skull, skin and brain as well as for the tumor, designed from ellipsoids and it is used for calculating the influence of the total dose for different depths of delivery.

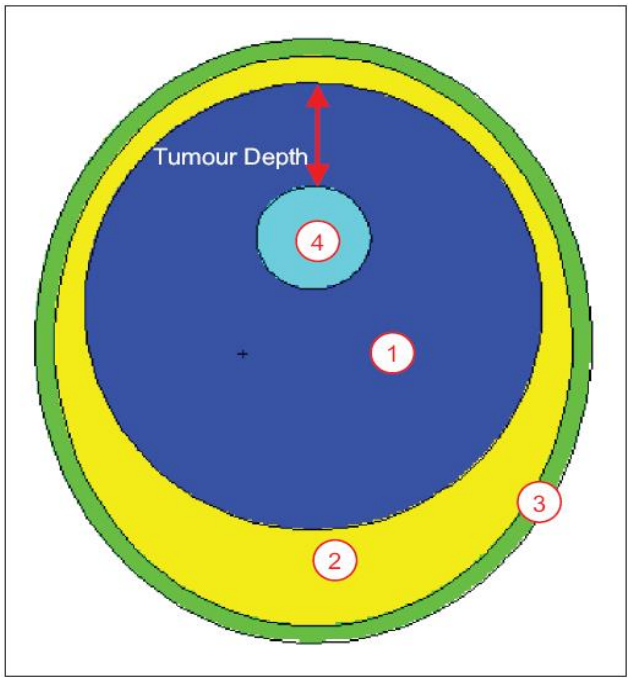

Figure 36. *The computational head phantom model, brain (1), skin (2), skull (3), tumor (4) (Figure adopted from R. Rasouli et al 2012)*

The simulation study for the final stage of the treatment is done with calculations of the total dose (Figures 37 - 39), taking into account thermal and fast neutron dose with gamma rays and boron dose for different depths. Based on the energy of the formed neutron flux, gamma ray and boron-10 dose, the peak of the absorbed total dose can have different depths in phantom. As simulation study by R. Rasouli et al. 2012 shows (Figure 39), for the initial neutron yield equal to $5 \cdot 10^{12}$ n/s in case of the DT neutron generator and the optimized BSA (Figure 35), the delivered total dose on the Snyder's head phantom has significant advantage in terms of the dose delivery on the tumor compared with normal tissue.

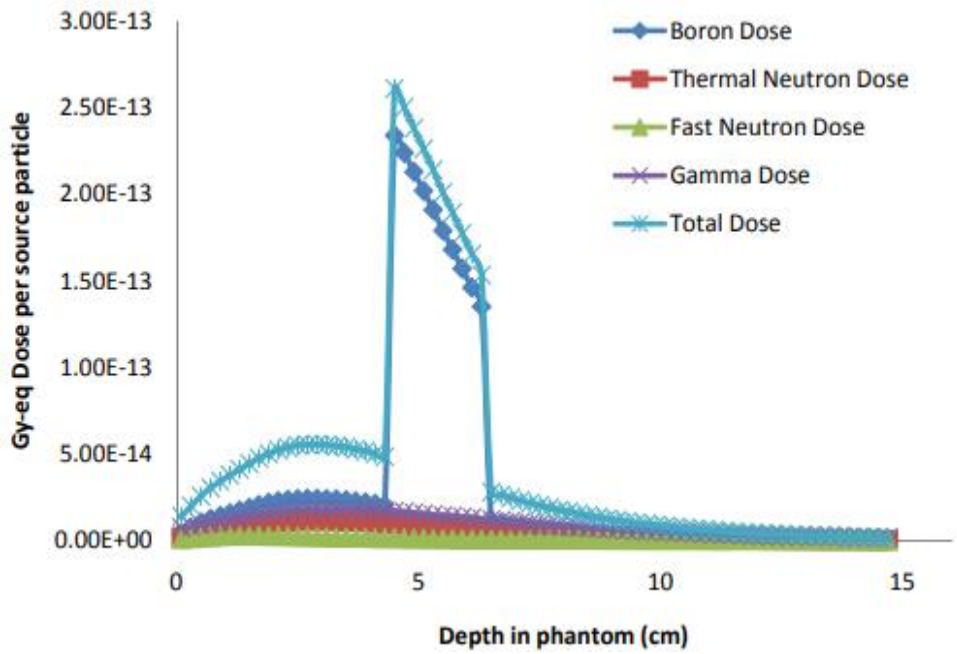

Figure 37. *The dose delivery dependence on the depth in Snyder's head phantom (Figure adopted from Y. Kasesaz et al. 2013)*

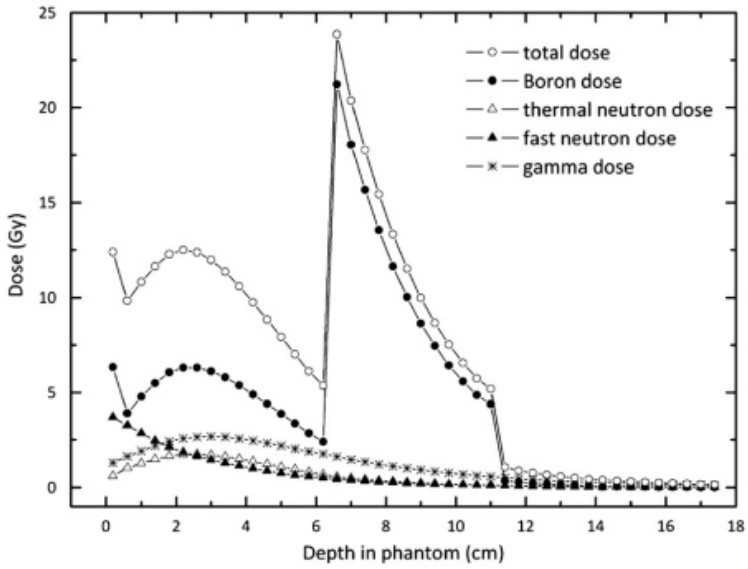

Figure 38.*.The dose delivery dependence on the depth in Snyder's head phantom (Figure adopted from Rasouli et al 2012)*

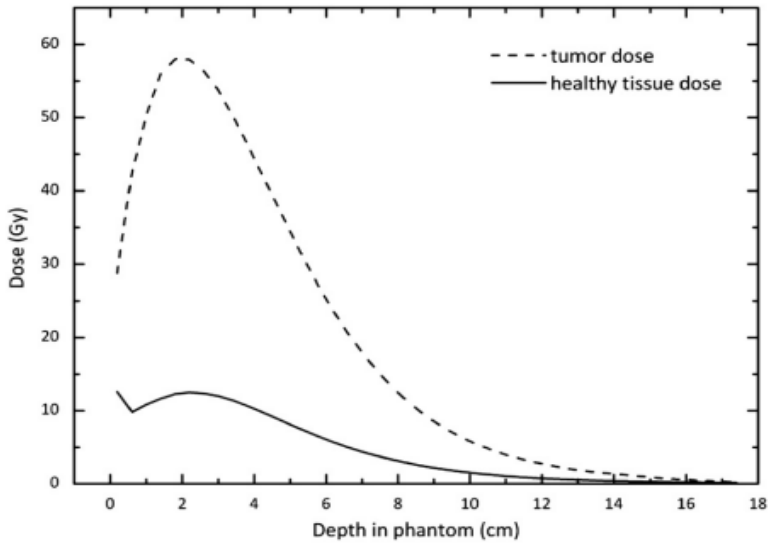

Figure 39. *Dose delivery dependence on the depth in tumor and in healthy tissue (Figure adopted from Rasouli et al 2012)*

R. Barth et al. in their studies for BNCT were periodically presenting results from different clinical investigations.

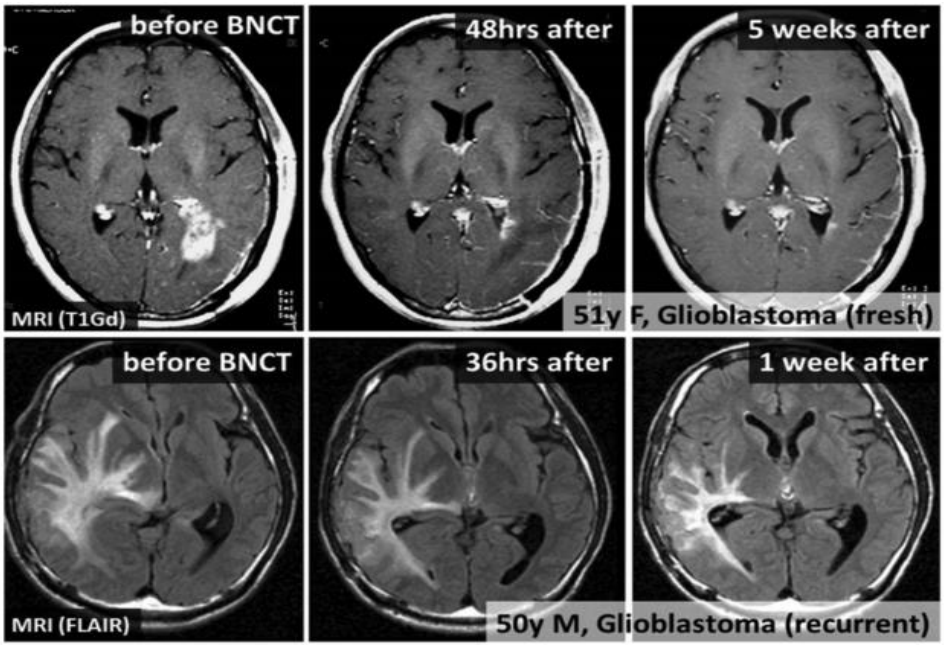

Figure 40. *Radiographic changes following BNCT for two representative patients with multiform glioblastoma (Figure adopted from R. Barth et al 2012).*

Figure 40 shows the difference in head BNCT results for two patients: 51 year old woman and 50 year old man with glioblastoma, whose head MRI shows radiographic changes before and after BNCT with significant changes resulting in life prolonging (R. Barth et al. *2012*).

3. Materials and Methods

3.1. Monte Carlo Codes

Computer simulation study is a necessity to describe a model of an experiment for the preparation of an accurate research. Monte-Carlo codes (MC codes) are an asset of detailed investigations of nuclear physics to check if any process is achievable experimentally or not. The nature of the MC code is based on methods usable in different areas such as finances, engineering, physics, etc. To explore the process in detail, it should be stressed the significance of the randomization, and to achieve the desirable process in reality, at first the virtual process should be randomized in the same way as it is possible in reality. Monte Carlo Simulations based on the realistic randomization give probabilities of outcomes in numerical representation. The code is named after the famous gambling destination in Monaco, and the technique sits in the core of the random outcomes of various games like roulette, dice, and slot machines. It was developed by a famous Polish-American mathematician and nuclear physicist Stanislaw Ulam in collaboration with John Von Neuman (N. Metropolis 1987). For Monte-Carlo simulations for scientific purposes, particularly in nuclear physics, there are programs for modeling realistic experiments, or in other words create virtual experiments based on previously achieved data and theoretical knowledge. In nuclear physics the acceptable randomization with all of the necessary tools can be described in MC codes, such as GEANT4 (particle interactions while passing through matter) (S. Agostinelli et al 2003, J. Allison et al 2006, J. Allison et al 2016), FLUKA (particle physics, high energy physics applications) (A. Fassò et al. 1993, G. Battistoni et al. 2007, T. Bohlen et al. 2014), MCNP (particle transport code) (T. Goorley et al. 2012, R. A. Schwartz et al. 2014, A. Berlizov 2006) and other programs based on the above-mentioned packages or separately developed in different programming languages.

3.2. GEANT4 Monte-Carlo Code

Studies presented in this thesis were performed using GEANT4 simulation package. In this chapter we will discuss few features of the GEANT4 which is the 4-th version of the program developed by C++ programming language (J. Allison et al 2016). GEANT4 (GEometry ANd Tracking) is a program to run or track particles through geometrical objects of different materials and make calculations for the nuclear reactions of interest. First, the virtual objects with materials must be defined, next one needs to select particles and run them through various materials or targets and register products of the nuclear reactions. Each part of the model for the experiment has to be programmed in C++ and for the simplicity they have unique names in all of the examples placed in the MC code. The geometrical part of the code is called detector construction, where all the necessary materials of a virtual experiment are created. Here a target and all of the important parts for the experiment can be modeled and placed in a so called world volume, which is a mother volume for all of the geometrical objects. Beside the geometrical part of the program, there are also developed classes (part of the code in object-oriented programming) for projectiles or initial sources, describing the particle type, position of the source, energy and angular distributions. This part of the model is called particle generator. All these can work properly by using physics which is known in GEANT4 as physics list class, as well as, stepping action, tracking action and event action classes, needed for the interactions between particles and materials. The data can be collected with help of run action class, which gets the necessary information about interactions and passes the exact data as text file or histogram, which can be programmed by the developer or user. To not go into details of other important parts of the GEANT4 MC code, it should be mentioned, that before each experiment, calculations by this code gives comparably achievable and predictable experimental result. The data which is used in the code is collected by the top level scientists and programmers of CERN and from all around the world. Some of the examples of the code describe the real experiments and the data is based on the achieved results. History or ReadMe files of the model can explain in detail and clarify what user needs to know. The ongoing updates of the GEANT4 MC code rises the quality of the program, by improving the styles of examples, inserting new data and avoiding the programming bugs, also with help of the worldwide GEANT4 collaborators. In the simulations by the author were taken into account all of the possibilities of the MC code in terms of visualization, histogram creation and physics list selection which was mostly based on hadronic interactions. At first the geometrical part of the materials used in the project were prepared, later it was followed with parts of particle generator and physics list. Other details were programmed based on the needs of the project.

3.3.Neutron sources based on Cyclone 18/18 cyclotrons and DD/DT CNGs

The compactness of different neutron sources became key factor for their usage for clinical purposes. Currently accelerators are becoming an alternative to reactors, also in some cases it is possible to produce isotopes for diagnostic purposes, and use an accelerator not only for therapeutic purposes. Cyclone 18/18 (Figure 41) of IBA, with fixed 18 MeV energies and up to 100 µA proton current is one of such type of examples (Adopted from IBA brochures, see the link in the references).

Figure 41. *A photo of the C18/18 cyclotron of IBA with proton beam transport line (Adopted from IBA brochures, see the link in the references).*

Besides internal 18 MeV proton beam required for isotope production, these type of cyclotrons have external beam-line, too. Usually the vacuum pipe for transporting protons is closed with 500 µm thick aluminum foil, which decreases the energy of protons from 18 MeV to 14.8 MeV. For neutron production it is optimal to use thick beryllium targets where the nuclear reaction with energy threshold less than 14.8 MeV can be used as presented in Table 4.

Reaction	Q-value [MeV]	Reaction threshold [MeV]
$p + {}^{9}Be \rightarrow {}^{9}B + n$	-1.8504	2.0572
$p + {}^{9}Be \rightarrow {}^{9}B + n + \gamma$	-1.8855	2.057
$p + {}^{9}Be \rightarrow {}^{8}Be + p + n$	-1.6645	1.8507
$p + {}^{9}Be \rightarrow {}^{8}Be + p + n + \gamma$	-1.7011	1.8507
$p + {}^{9}Be \rightarrow {}^{5}Li + \alpha + n + \gamma$	-3.5377	3.9333
$p + {}^{9}Be \rightarrow 2\alpha + p + n$	-1.5727	1.74859

Table 4. *Be (p,Xn) nuclear reactions with energy thresholds less than 14.8 MeV.*

To find optimal thickness for beryllium-9, GEANT4 simulations were performed. In the simulations all reactions listed in the Table 4 were taken into account as result of the usage QGSP_BERT_HP physics list. The modeling of the target in the GEANT4 program was done first as geometrical object representing cylinder with 1 cm radius and 2.5 maximal thickness for beryllium. The radius was selected taking into account the optimal dimensions of the proton beam emitted from the C18/18 pipeline. The energy of the simulated protons was fixed and equal to 14.8 MeV. This energy is remaining after passing through the 500 micrometer aluminum foil installed as exit-window for the pipeline. The energy of secondary neutrons, in all of the cases can reach up to 13 MeV, as can be seen in Figure 42, for three different thicknesses of ${}^{9}Be$. Based on the achieved results it is optimal to select 2.5 mm thick target for later simulations. The first reason for that is the loss of the energy of protons inside of the target. And second, the nuclear reactions with secondary neutrons resulting in the decrease of high energy neutrons. This can be seen in the energy spectra in Figure 43 numbered from 1 to 3, where the spectrum number 1 represents the 0.5 mm thick target, and accordingly 2 and 3 are 1mm and 2.5 mm thick beryllium targets. In all of the mentioned spectra, the highest amount of neutrons is in the energy region at up to 1 MeV. For the 2.5 mm and 1 mm targets, the number of neutron in the energy region from 4 MeV to 8 MeV is a proving fact that the thicker target is acting like a multiplier for the low energy neutrons, but it captures at the same time low energy neutrons as well. This can be seen in comparison between peaks of the spectra showing that the 2 times difference on the target thicknesses numbered 1 and 2 is resulting in ~1.7 times difference of the number of neutrons at the highest points of the spectra, while the difference between number of neutrons is ~1.2 times at the point of the peak in the 2.5 times difference on the 2.5 mm and 1 mm thick targets, numbered 3 and 2 accordingly. The simulations were done with relatively small number of generated projectiles later approximated with the highest possible current of protons equal to 100 μA or $6.25 \cdot 10^{14}$ protons per second.

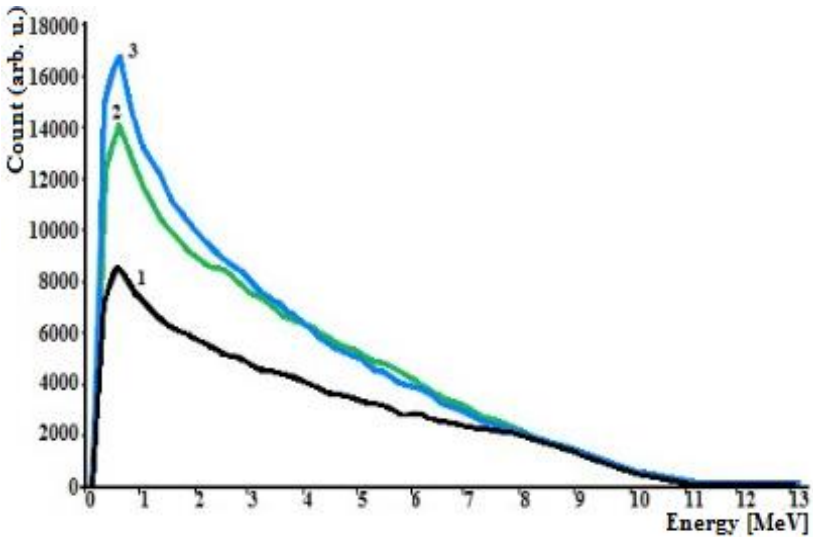

Figure 42. *Energy Spectra of neutrons obtained using 0.5 mm (1), 1 mm (2) and 2.5 mm (3) thick ^{9}Be (Figure adopted from R. Avagyan, V. Ivanyan et al. 2016).*

Neutron yield of the DD/DT CNG can be useful for BNCT after deeply detailed investigations. Taking into account the latest worldwide research, it can be concluded that based on the above-mentioned neutron sources it is realistic to prepare preclinical studies.

DD CNG has comparably lower yield with known maximum at up to $5{\cdot}10^{12}$ n/s, while most of the generators provide yield around 10^{11} n/s (ref. Table 2). The energy is fixed with 2.45 MeV peak and for higher yield of neutrons it can be selected as an alternative to any other neutron source due to its compactness, mobility and cost.

DT CNG provides higher energy neutrons with energy of 14.1 MeV, and it can be designed to generate up to 10^{14} n/s. As research shows (IAEA TECDOC 2001, F. Rasouli et al. 2012, J. Fantidis & A. Antoniadis 2015, S. Masoudi et al. 2017), the initial yield and energy of neutrons is sufficient for the achievement of a neutron flux suitable with IAEA recommendations, while its usage for deep-seated brain tumors yet needs to be studied additionally.

4. Designing of the optimal BSA for BNCT

4.1 GEANT4 simulation study of the BSA for BNCT based on C18/18 cyclotron

It is known that there is no neutron source which provides monochromatic neutron flux usable for BNCT. In the case of the ^{9}Be (p,Xn) nuclear reaction used at the C18/18 cyclotron to produce neutrons the enhancement of the epithermal neutrons energetic region can be done via appropriate BSA. One of the main goals is the moderation of neutrons with energies up to 13 MeV (R. Avagyan, V. Ivanyan et al 2016, 2017), while effectively selected reflecting and shielding materials will increase the number of epithermal neutrons after passing the BSA and will successfully irradiate the tumor located right after the exit window of the BSA. The process of the thermalization and the suitability of the flux according to the IAEA criteria for BNCT can be achieved in two ways. One of the methods is the usage of materials with high atomic number as moderators, resulting in elastic/inelastic scattering or capturing of fast neutrons. At the same time they increase the number of thermal/epithermal neutrons as result of elastic scatterings. In this case the final flux is not always possible to use in BNCT due to low amount of epithermal neutrons. Another way to decrease the energy of the generated neutrons is based on installation of materials which will increase the intensity of the low energy neutrons with (n,2n), (n,3n) reactions, when together with multiplication of neutrons their energy will be smaller compared with the energy of the initial ones. In the first case heavy materials as 5 cm thick bismuth, followed by 50 cm thick iron, were installed next to the 2.5 mm thick beryllium-9 target simulated for the design and optimization of a BSA based on the ^{9}Be (p,Xn) neutron source, were the proton beam is emitted from the C18/18 cyclotron installed at A. Alikhanian National Laboratory (AANL) (R. Avagyan, V. Ivanyan et al 2016, 2017).

Based on the step by step simulations (at least 2 per week for up to 3 years) on the way of the achievement of higher yield of low energy neutrons, which will be closer to the thermal/epithermal energetic region (up to 10 keV), different combinations of Bi, Iron, Al, graphite and $Li^{7}F$ were simulated.

In the simulations the thickness of the materials was varied in the range from few millimeters up to a meter. The step or selection of different thicknesses was based on the gained information making any positive change closer to the IAEA recommendation, especially for the increase of the number of epithermal neutrons and minimization of the influence by the higher energetic or fast neutrons. Some of the thicknesses and types of materials were resulting in worsening of the results achievements and due to that fact only the best cases are discussed.

Comparably better result, in case of the achievement of the desired goal, was possible to obtain after the usage of 5 cm thick Bi, 55 cm thick Fe, 10 cm thick Al, 5 cm graphite , 10 cm thick $Li^{7}F$ moderator installed next to the 2.5 mm thick ^{9}Be target. The scheme of the design is presented in Figure 43.

As presented in Figure 44 most of the neutrons after the moderation are in the range below 1.2 MeV with maximum of the distribution at about 200 keV.

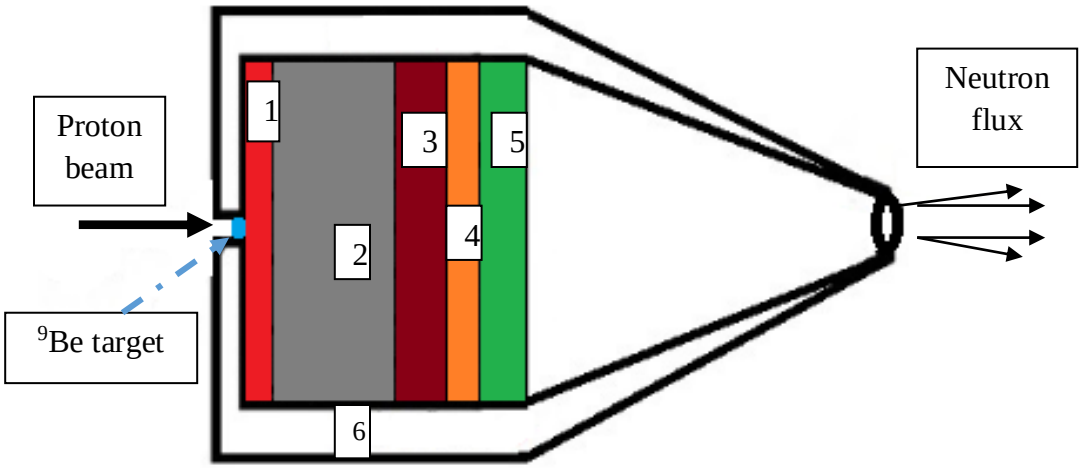

Figure 43. *BSA with 2.5 mm ^{9}Be target, 5 cm Bi (1), 55 cm Fe (2), 10 cm Al (3), 5 cm graphite (4), 10 cm ^{7}LiF (5), Pb reflector (6).*

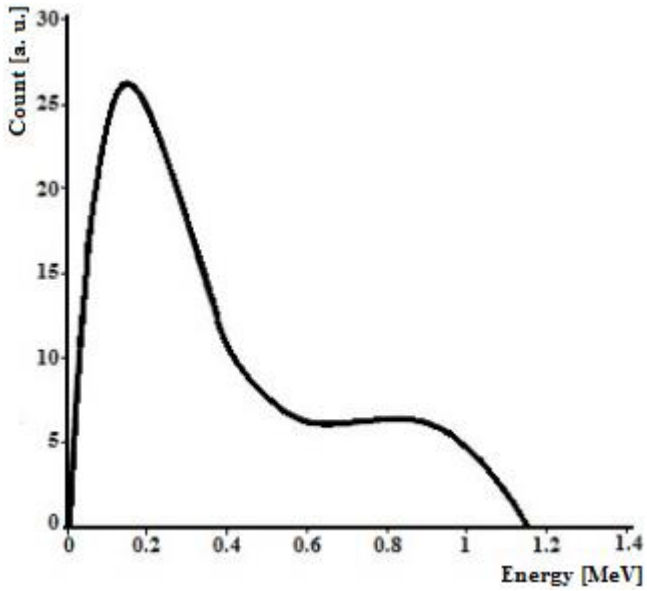

Figure 44. *Simulated neutron spectrum detected by 10 cm diameter virtual sensitive detector placed on the exit of the BSA. As presented in Figure 43 it is modeled from 5 cm Bi, 55 cm Fe, 10 cm Al, 5 cm graphite and 10 cm Li^{7}F with Pb reflector. (Figure adopted from R. Avagyan, V. Ivanyan et al. 2017).*

By the virtual sensitive detector, with 10 cm diameter, the simulation result is estimated to be $0.96 \cdot 10^6$ n/(s cm^2) from 100 μA proton current of the cyclotron. As presented in Figure 44 for the above-described BSA neutrons with energies at up to 200 keV are 61.1% of all the obtained flux out of which around 50% are thermal or epithermal.

As a second example it is worth to discuss another BSA (Figure 45) designed for C18/18 cyclotron of AANL. Here, secondary neutrons with up to 12 MeV energies pass through 20 cm

thick natural molybdenum which multiplies neutrons and next in a line used iron and paraffin boric acid, both with 45 cm thickness were used, this BSA provides a flux of ~$0.968 \cdot 10^9$ n/(s·cm^2) being in high agreement with the IAEA recommendations for BNCT (IAEA TECDOC 2001).

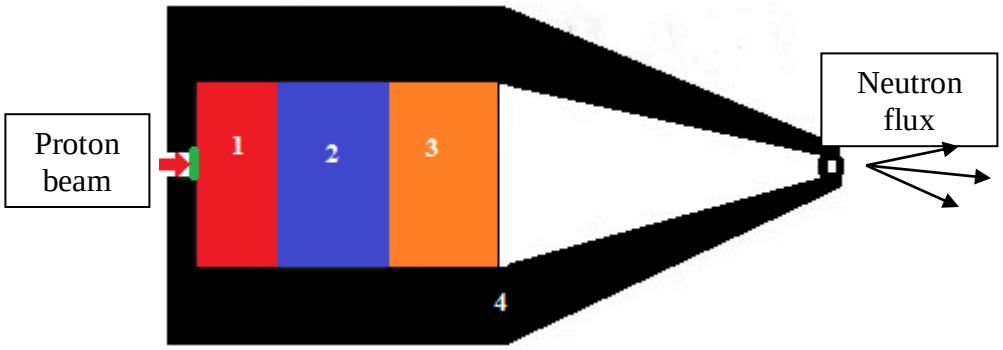

Figure 45. *Proton beam (red arrow) bombarding a 2.5 mm thick ^{9}Be (green) target followed by the BSA consisting of 20 cm thick Mo (1. red), 45 cm Fe (2. blue) and 45 cm paraffin boric acid (3. orange) as moderators, and 20 cm thick Pb (4. black) as reflector (V. Ivanyan 2020).*

In this model, the whole BSA system is installed in a concrete wall which will separate the room for patients from the rest of the experimental hall. With the designed BSA the agreement of the achieved neutron flux with the IAEA recommendations for BNCT is quite high. Based on the simulations, in case of the detailed investigations, the possible experiment can result in the neutron flux greater than 10^9 n/(s·cm^2) consisting in more than 69% of epithermal neutrons, less than 17% of fast neutrons, and the thermal neutrons amount not exceeding 14% (*V. Ivanyan 2020)*. Also, it will be necessary for the future steps to work on higher suitability with IAEA recommendations. In Figure 46 energy distribution of neutrons when BSA consisted of 20 cm thick nat-Mo, 45 cm thick nat-Fe and 45 cm thick paraffin boric acid is presented.

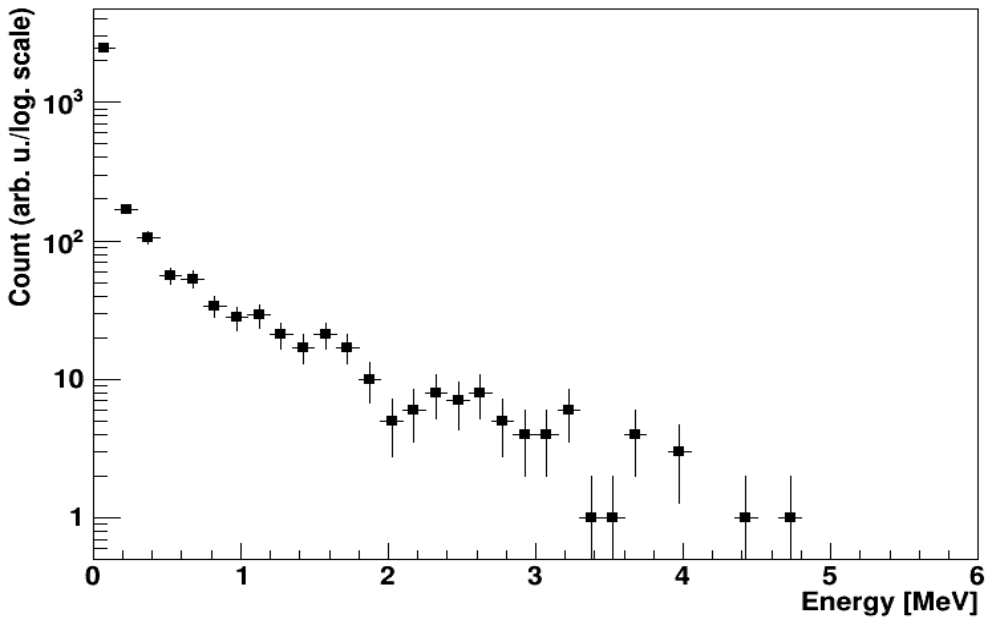

Figure 46. *Energy distribution of neutrons after the BSA of 20 cm thick nat-Mo, 45 cm thick nat-Fe and 45 cm thick paraffin boric acid moderator as shown in Figure 20, simulated after the bombardment of 2.5 mm ^{9}Be by protons. (Figure adopted from (V. Ivanyan 2020)).*

Experimentally the results should be proven at the A. Alikhanian National Science Laboratory (AANL, Yerevan, Armenia), where the Cyclone 18/18 is installed. Later expectations require deeply detailed investigations for the number of epithermal neutrons, their energetic and angular distributions, and ratios over thermal and fast neutron components based on the specific case. As for this part of the research it is significant to achieve the high neutron flux consisting mainly from thermal and epithermal neutrons. Figure 47 shows energy and angular distributions of epithermal neutrons registered at the edge of the BSA's collimator, where the radius of the virtual sensitive detector is 2.5 cm. The energetic distribution (Figure 47 (a)) shows that most of the epithermal neutrons have energies up to 1 keV. From the research done for the capturing neutrons in the soft tissue it can be seen that neutrons within this energetic region will be captured not reaching deeper in the soft tissue target (Section 4.4). Based on the angular distribution (Figure 47 (b)) of neutrons detected on the surface of the virtual detector one can see that mostly centralized movement of neutrons will give less harming. In this stage the research is still under development to improve the achieved results for clinical cases as well.

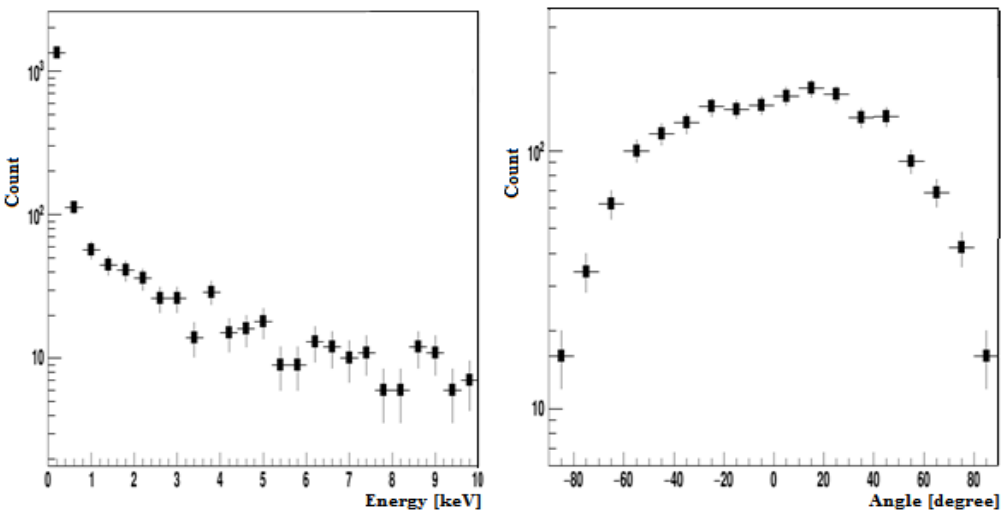

a) *b)*

Figure 47. *Energy (a) and angular (b) distribution of epithermal neutrons after the BSA shown in Figure. 46. The spectra were obtained based on 10^8 simulated events.*

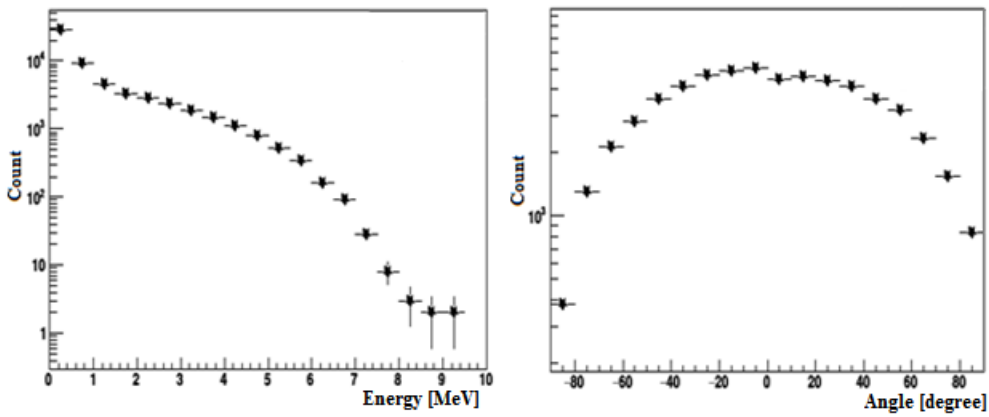

a) *b)*

Figure 48. *Energy (a) and angular (b) distribution of gamma rays after the BSA shown in Figure 45. The spectra were obtained based on 10^8 simulated events.*

It is required by IAEA to maximize the diameter of the outcoming neutron flux to 12 cm for brain, head and neck tumor treatment with BNCT, while for small tumors as well as for the research and development of BNCT in Armenia, it is possible to use the narrow beam outlet/exit of neutrons. The energetic and angular distributions presented in Figure 48 prove that the total dose on the patients will be increased because of gamma rays and it is necessary to keep all of the recommendations of IAEA for BNCT. The spectrum shows also that relatively high number of gamma rays are in the energy range up to 1 MeV (~80 %) which is an additional asset to continue progress in the creation of the BNCT facility based on C18/18 cyclotron at AANL.

4.2 GEANT4 simulation study of BSA for BNCT based on DD CNG

Based on the investigations of other researchers discussed in Chapter 2, I have done complementary studies of the BSA for the DD neutron generators considering new materials and dimensions as well as 1 cm^2 hollow size for the point source. The distribution of 10^6 to 10^8 neutrons with 2.5 MeV energies were generated isotropically during the initial emission. The designed 23 different BSAs by GEANT4.10.04 simulations, with combinations of different materials and thicknesses are presented in Tables 4-6. The BSAs grouped in the tables differ with their shape, moderator and reflector types and thicknesses, as well as outlet or exit window radiuses. Each geometry and material was implemented in the code as part of construction of the logical and physical volumes, shapes and dimensions were changed and developed later on. Particularly BSAs in table 4 and 5 differ not only in their material types but first of all in the outlet radius which is 2.5 cm in case of BSAs in Table 4 and 6 cm in Table 5. The generation of 2.5 MeV isotropically distributed neutrons were done as a point source in the place as indicated in the scheme (Figure 49).

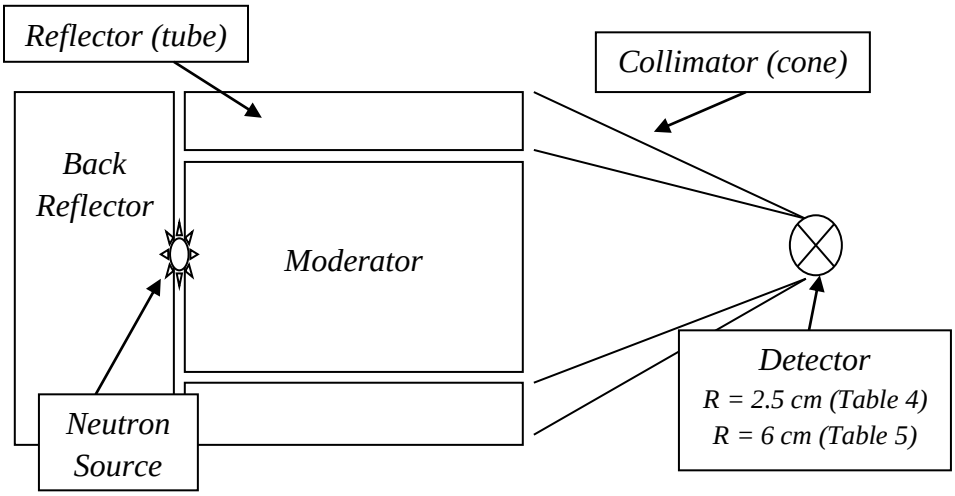

***Figure 49**. General scheme of a DD CNG based BSA with its main components where the hollow for the point source is 1 cm^3 tube .Thicknesses and materials of the BSA designing components were varied to obtain the optimal neutron flux characteristics.*

The virtual detector is designed with the same radius as the outlet of the collimator and has imaginary material called G4Galacticum which can be associated with vacuum, but it is programmed to detect neutrons if they will pass through its circular volume. As first version for the BSA design which is presented in Table 4, the tube shape for moderators is followed with conical reflector/collimator to focus the neutron flux to the outlet with 2.5 cm radius. This value is not in agreement with the IAEA recommendations, but it was a preliminary version assuming possible usage of a BSA for relatively small and not deep seated tumors. As first part of the moderator natural uranium, natural tungsten, as well as tungsten-182 and tungsten-186 were investigated. As presented in Table 4 the second part of the moderator was considered mainly in combination with tungsten-186 isotope as first part, as well as with filters of gamma rays and thermal neutrons. Namely, aluminum fluoride, paraffin-boric acid, quartz, $FeAlF_3$, La_2O_3 and

Fe_2O_3, bismuth cadmium and lithium fluoride were discussed for the above-mentioned purposes. Comparably better result is obtained in case of the BSA #14, (Scheme of BSA#14 is presented in Figure 50), where the reflector is lead and the radius of the virtual sensitive detector is 2.5 cm. The BSA is designed inside of the concrete wall, surrounding it from the sides. As result of the usage of 20 cm thick back and 10 cm thick side Pb reflectors with 8cm thick ^{186}W, 45 cm thick mixture of Fe (5%) AlF_3 (95%) moderator and 1.25 cm thick Cd filter, the obtained neutron flux had ratios of epithermal over thermal and epithermal over fast components equal to 174 ± 62 and 24 ± 3, respectively. The ratios are consistent with the IAEA recommendations, while the recommended radius of the exit window of the BSA should be 6 cm. Also, the epithermal neutron flux should be 10^9 n/(s·cm^2), instead of the ~$6.8 \cdot 10^7$ n/(s·cm^2), estimated in case of $5 \cdot 10^{12}$n/s initial neutron yield of the DD compact neutron generator.

BSA #	***Moderator part 1***	***Moderator part 2***	***Filter***	$\varphi_{epi}/\varphi_{thermal}$	$\varphi_{epi}/\varphi_{fast}$
1	8cm ^{186}W	47.5 cm AlF_3	1.25 cm Cd	107 ± 30	24.5 ± 3.2
2	8cm nat-U	47.5 cm AlF	1.25 cm Cd	102 ± 25	16.7 ± 1.7
3	8cm ^{186}W	47.5 cm 40% Al_2O_3& 60 % AlF_3	1.25 cm Cd	67 ± 17	25 ± 4
4	8cm ^{186}W	45 cm 40% Al & 60 % AlF_3	1.25 cm Cd	96 ± 22	4.1 ± 0.2
5	8cm ^{186}W	45 cm 5% Fe & 95 % AlF_3	1.25 cm Cd	94 ± 22	26.0 ± 3.6
6	8cm nat-W	47.5 cm AlF_3	1.25 cm Cd	72 ± 18	17.8 ± 2.2
7	8cm ^{186}W	45 cm 40% Al_2O_3& 60 % AlF_3	1.25 cm Cd	47.7 ± 9.3	23 ± 3
8	8 cm ^{186}W	47.5 cm AlF_3	1.25 cm H_3BO_3	40 ± 10	26 ± 5
9	8 cm ^{186}W	47.5cm H_3BO_3	1.25 cm Cd	0.43 ± 0.51	0.33 ± 0.39
10	8 cm ^{186}W	47.5 cm Quartz	1.25 cm Cd	71 ± 16	4.0 ± 0.3
11	8 cm ^{186}W	47.5 cm Salt	1.25 cm Cd	49± 12	0.37 ± 0.02
12	8 cm ^{186}W	47.5 cm Fe_2O_3	1.25 cm Cd	57 ± 24	2.5 ± 0.3
13	8 cm ^{182}W	47.5 cm AlF_3	1.25 cm Cd	78 ± 20	18.3 ± 2.3
14	8cm ^{186}W	45 cm mixture of 5% Fe &95 % AlF_3	1.25 cm Cd	174 ± 62	24 ± 3

Table 4. *List of GEANT4 modeled moderation systems for BNCT with 10 cm thick Pb back reflector and 5 cm thick Pb side reflector assuming that the DD CNG hollow is a tube with 5 cm radius and 10 cm length (BSA 1 - BSA 13) and with 20 cm thick Pb back reflector and 15 cm thick Pb side reflector assuming that the DD CNG hollow is a tube with 1 cm diameter and 1cm length (BSA 14 in Figure 50).*

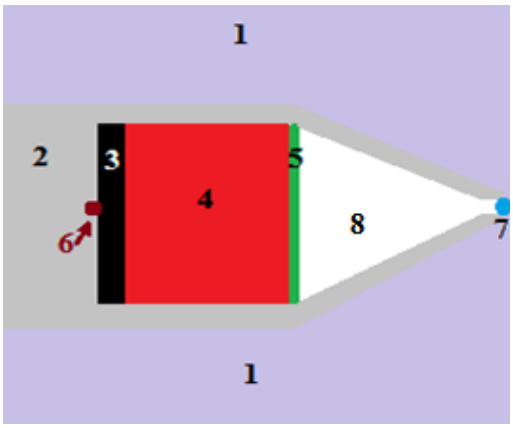

Figure 50. *Scheme of one of the simulated Beam Shaping Assemblies (BSA #14): Concrete shielding (purple)(1), 20 cm thick back and 10 cm thick side Pb reflectors (gray) (2), 8cm thick ^{186}W (black) (3), 45 cm thick mixture of Fe(5%) AlF_3 (95%) (red) (4), 1.25 cm thick Cd (green) (5), neutron source hollow (dark red) (6), R = 2.5 cm virtual sensitive detector (blue) (7) and vacuum (8) is inside the lead collimator (white).*

The other designs of the BSA were studies assuming 6 cm radius of the exit window as a step forward to the required parameters for the BNCT. In Table 5 simulation results in respect to the ratios of epithermal over thermal and epithermal over fast neutron fluxes were presented. Besides the outlet radius, the differences between BSA #14 and BSA #15, which are comparably better BSAs listed in Table 4 and 5, respectively, is the additional third part of moderator which is LiF for BSA #15. Moreover, there is a vacuum closing window, which is 1 mm thick Pb.

BSA	Moderator part 1	Moderator part 2	Moderator part 3	Filter 1	Filter 2	$\varphi_{epi}/\varphi_{thermal}$	$\varphi_{epi}/\varphi_{fast}$
15	8 cm ^{186}W	45 cm mixture of 5% Fe & 95 % AlF_3	1.25 cm LiF	0.5 mm Bi	1 mm Lead	107 ± 10	19 ± 1
16	8 cm ^{186}W	45 cm mixture of 5% Fe & 95 % AlF_3	1.25 cm LiF	1 mm Bi	1mm Lead	102 ± 10	19 ± 1
17	8 cm nat-W	45 cm mixture of 5% Fe & 95 % AlF_3	1.25 cm LiF	1 mm Bi	1 mm Lead	104 ± 10	17 ± 1
18	8 cm nat-W	45 cm Quartz	1.25 H_3BO_3	1.25 cm LiF	1 mm Lead	257 ± 49	17 ± 1
19	15 cm nat-W	45 cm Quartz	1.25 H_3BO_3	1.25 cm LiF	1 mm Lead	107 ± 20	6.1 ± 0.3

Table 5*.GEANT4 modeled BSAs with 20 cm thick back and 15 cm thick side Pb reflectors. The outlet diameter of the collimator is 12 cm. Moderator parts 1, 2 and 3 are layers from left to right, and the point source is located on the left side of the 1st part of the moderator. Filters 1 and 2 are for thermal neutrons (LiF) and gamma rays (Bi and lead), also Filter 2 is installed as closing window for the collimator. The quantities φ_{epi}, $\varphi_{thermal}$, and φ_{fast} are thermal, epithermal and fast neutron fluxes, accordingly.*

As presented in Figure 51 BSA # 15 is designed inside of the concrete wall with 20 cm thick back and 10 cm thick side Pb reflectors 8cm thick ^{186}W 45 cm thick mixture of Fe (5%) and AlF_3 (95%) parts of moderator with 1.25 cm thick LiF and 0.5 mm Bi thermal neutron and gamma ray filters, and 1 mm Pb outlet window. Also, the neutron source hollow has 1 cm^3 volume, and virtual sensitive detector has 12 cm diameter. The lead collimator is designed to have deep vacuum inside with negligible pressure and density. As result of the simulations it is estimated to achieve epithermal flux ~$6.12 \cdot 10^8$ n/(s·cm^2) in case of $5 \cdot 10^{12}$n/s initial neutron yield of the DD compact neutron generator.

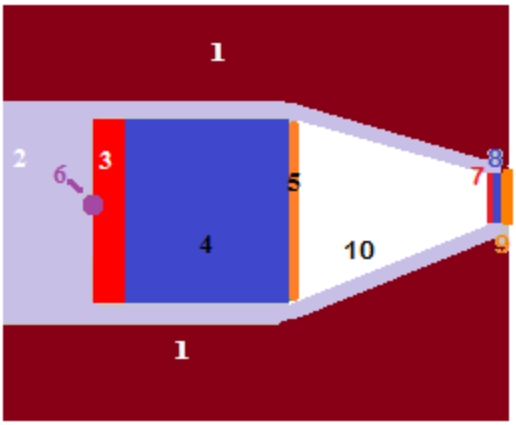

Figure 51. *Scheme of the BSA # 15 placed in concrete wall (1) with 20 cm thick back and 10 cm thick side Pb reflectors (2), 8cm thick ^{186}W (3), 45 cm thick mixture of Fe (5%) and AlF_3 (95%) (4), 1.25 cm thick LiF (5), 1 cm^3 neutron source hollow (6), 0.5 mm Bi (7), 1 mm Pb outlet window (8), virtual sensitive detector (D = 12 cm) (9) and vacuum inside of (10) the collimator with same natural Pb material as all of the reflectors .*

Another aspect of the design was the new shape of the moderator parts, as presented in Figure 52, with moderators in a conical shape and with relatively smaller length for lead collimator with ratios of epithermal over thermal neutron fluxes presented in Table 6.

BSA	**Moderator part 1**	**Moderator part 2**	**Moderator part 3**	**Filters**	$\varphi_{epi}/\varphi_{thermal}$
20	10 cm W	15 cm Fe_2O_3	35 cm Al	1.25 cm LiF, 1 mm Bi, 1 mm Pb	26 ± 2
21	10 cm W	15 cm Fe_2O_3	35 cm Al	1.25 cm LiF, 2cm Bi, 1 mm Pb	27 ± 6
23	10 cm W	15 cm Fe_2O_3	35 cm La_2O_3	1.25 cm LiF, 1 mm Bi, 1 mm Pb	29 ± 7

Table 6. *GEANT4 modeled Beam Shaping Assemblies with moderators in conical shapes and with the outlet diameter D=12 cm. The whole BSA was set in air, filters placed inside of the tube-collimator and the moderators are 10 cm thick W, 15 cm Fe_2O_3, 35 cm Al, followed with 1.25 cm thick LiF thermal neutron filter, 1 mm thick Bi gamma ray filter, also 1 mm thick Pb outlet window filters gamma rays. And neutron source hollow is tube with 1cm length and 1 cm radius.*

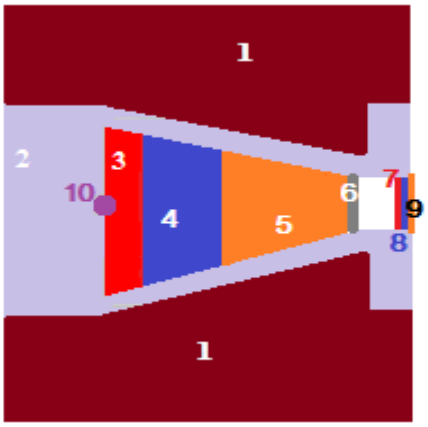

Figure 52. *Scheme of the purely conical BSA #20 inside of the concrete wall (1) with back and side lead reflectors and in air lead collimator (filters placed inside of the tube-collimator) (2), 10 cm thick W (3), 15 cm Fe_2O_3 (4), 35 cm Al (5), 1.25 cm thick LiF (6), 1 mm thick Bi (7), 1 mm thick Pb outlet window (8), virtual sensitive detector (D = 12 cm) (9) and neutron source hollow (10) with 1 cm^3 volume.*

The achievable epithermal neutron flux is estimated to be ~3.85 $\cdot 10^7$n/($cm^2 \cdot$s) with ratio of epithermal over thermal neutrons equal to 26 ± 2 in case of the 10 cm thick W, 15 cm thick Fe_2O_3 , 35 cm thick Al parts of the moderator with 1.25 cm thick LiF and 1 mm thick Bi filters placed in the tube-collimator of 6 cm radius and 10 cm length and closed with 1 mm Pb outlet window and assuming the initial neutron production rate at the level of $5 \cdot 10^{12}$ n/s for DD compact neutron generator. In Figure 53 energy distributions of thermal and epithermal neutrons are presented, and in Figure 54 simulation results for the angular distributions of epithermal and fast neutrons are depicted.

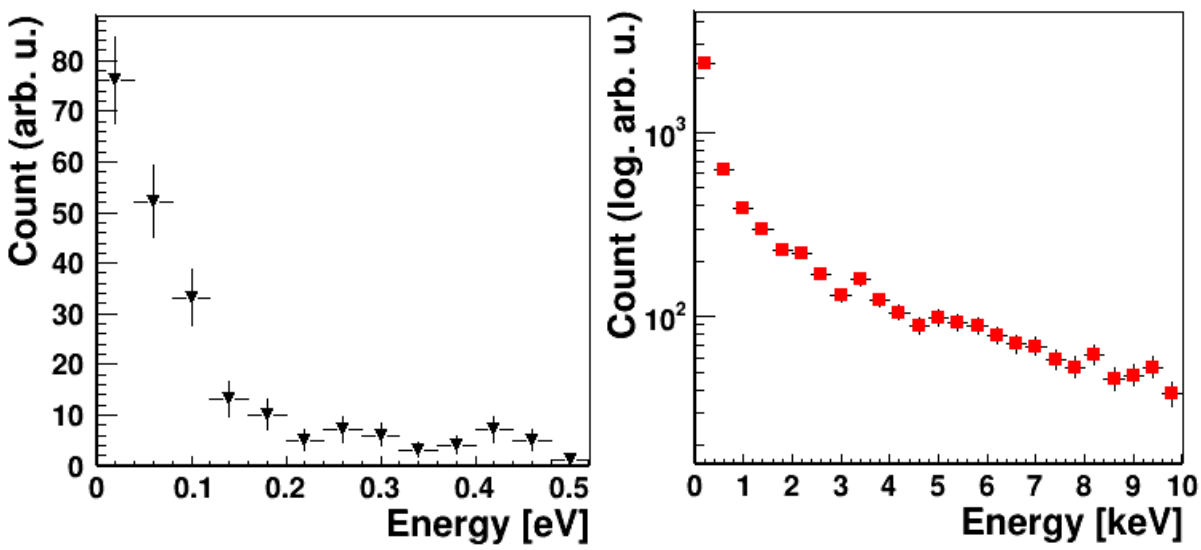

a) b)

Figure 53. *Energy distributions of (a) thermal and (b) epithermal neutrons obtained in the case of BSA #20.*

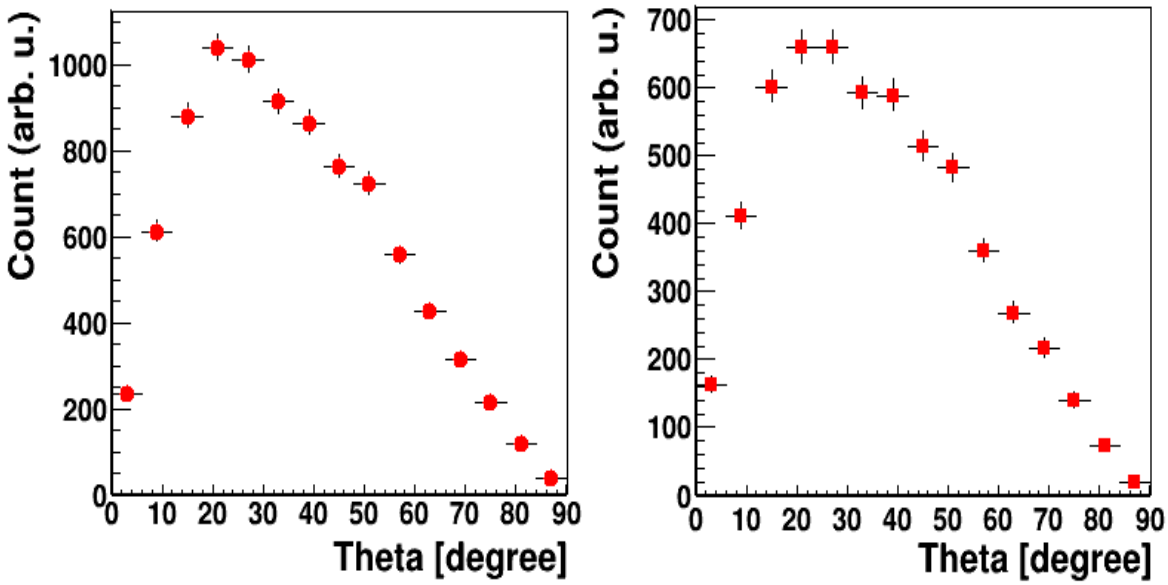

a) b)

Figure 54. *Angular distributions of neutrons in case of the BSA #20. (a) For neutrons with energies up to 2.5 MeV and (b) for neutrons in the energy range from 0.5 eV to 10 keV. The angle is defined with respect to the main axis of the BSA.*

As can be seen in Figure 54, neutrons are mostly emitted closer to the central axis of the virtual sensitive detector as θ is the angle between the particle direction and the longitudinal axis of the BSA. Relatively small number of epithermal neutrons is emitted closer to the edges of the virtual detector (closer to 90 degree). This means, that the Pb reflector and collimator, as well as the shape of the moderation system which is focusing neutrons, is quite significant, especially for epithermal neutrons.

4.3 BSA for BNCT based on DT CNG

Besides the designs for the DT based BSAs discussed in Chapter 2 which are optimized by other researchers, GEANT4 simulations were performed to estimate possible new BSA versions and achieve neutron flux with higher suitability of the IAEA requirements. For a DT based BSA (Figure 55) the thermalization and higher epithermal neutron flux achievement of two methods were taken into account. First, usage of heavy materials with high atomic number and second, performing simulations with neutron multipliers were considered. In Tables 8-10 some of the BSAs with comparably successful agreement with IAEA requirements are listed. First 8 BSA had different geometry compared to more canonical 11 BSAs as shown in Figures 56-57. In Tables 7 and 8 moderators for the BSA which have almost the same scheme as presented in Figure 56 are listed. Table 7 contains some of the versions/compositions of the moderators which were not giving any success and in Table 8 one can see values which are more or less step forward. Later by changing the design of the BSA (Figure 57) and making corrections, as well as using different combinations and materials it was possible to obtain better results. At first the simulations were done with materials listed in Table 9 and the improved results are presented in Table 10.

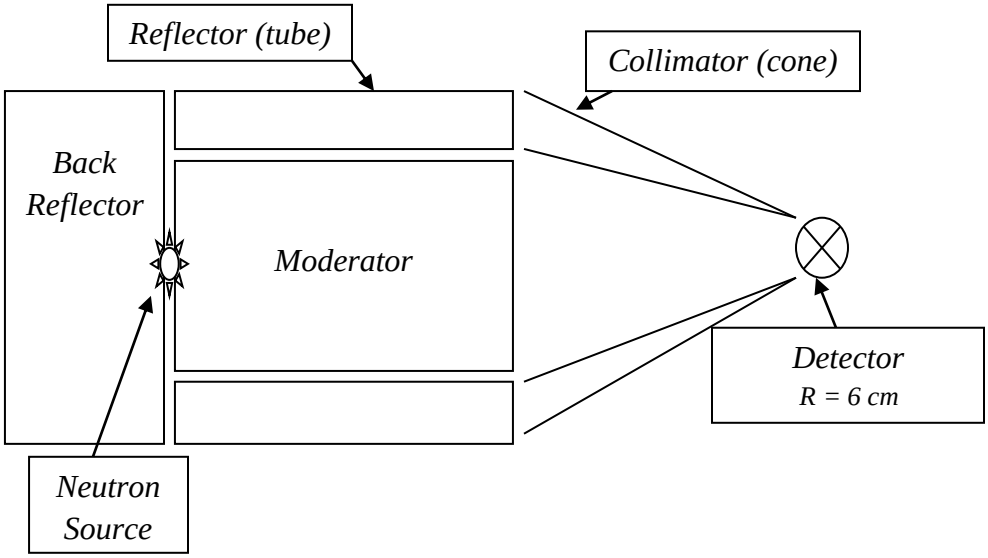

Figure 55. *General scheme of a DT CNG based BSA with its main components, where the hollow for the point source is 1 cm^3 tube. Thicknesses and materials of the BSA designing components were varied to obtain the optimal neutron flux characteristics.*

Simulations with the usage of multipliers were in higher consistency with IAEA recommendations. As presented in Figures 56-57 using different materials widely known as neutron multipliers together with other parts of the moderator (Table 9) and the usage of heavy materials as different parts of the moderator (Table 8-9) without multipliers gives completely

different result. As one of the best design of the BSA it is worth to be mentioned the usage of the 27 cm thick Bi multiplier with 53 cm $FeAlF_3$ as first part of the moderator with 3 cm thick Aluminum as the second part of the moderator next to multiplier, and with additional 1 cm thick LiF filter.

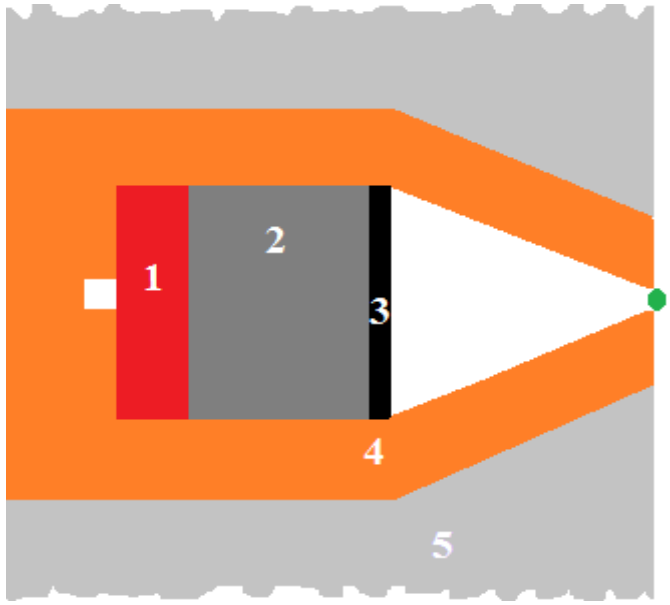

Figure 56. *Scheme of the BSA based on DT neutron generator. As listed in Table 7 moderator parts are numbered (1), (2) and Filter (3), while in Table 8 with same scheme of the BSA Multiplier (1), Moderator (2) and Filter (3) are listed. In both cases 20 cm thick lead side and back reflectors as well as collimator with same material and thickness (4) were simulated. For shielding purposes the BSA is placed in a concrete wall (5).*

BSA #	Moderator Part 1[cm]	Moderator Part 2 [cm]	Filter [cm]
1	MoF (20)	$FeAlF_3$ (40)	LiF (1)
2	MoF (20)	TiF_3 (40)	LiF (1)
3	MoF_6 (30)	Al (28)	Co (1)
4	MoF_6 (30)	AlF_3 (28)	Cd [1)
5	MoF_6 (35)	Al (30)	Co (1)
6	MoF_6 (35)	Iron (30)	Co (1)
7	MoF_6 (35)	Paraffin Boric Acid (30)	Co (1)
8	MoF_6 (35)	$FeAlF_3$ (30)	Co (1)

Table 7. *Moderator parts of the BSA (presented in Figure 56) based on DT neutron generator with 14.1 MeV neutrons (numbers in the parenthesis are thicknesses of the compositions/ materials in cm)*

Based on the results one can conclude that it is still not enough to get thermal or epithermal fluxes which will meet the IAEA recommendations, but also all of the possible ratios, between thermal, epithermal and fast neutron components should be studied. Also, the gamma ray influence should be taken into account which still needs to be optimized.

BSA #	***(1) Multiplier [cm]***	***(2) Moderator [cm]***	***(3) Filter [cm]***	$n_{epi}/n_{thermal}$	n_{epi}/n_{fast}	***Total Number of Gamma Rays***
1	Mo (25)	AlF_3 (25)	Cd (0.2)	1913/116 [16.5]	1913/703 [2.72]	518
2	Mo (25)	AlF_3 (30)	Cd (0.2)	1677/79 [21.23]	1677/424 [3.95]	455
3	Mo (26)	AlF_3 (25)	Cd (0.4)	1723/83 [20.76]	1723/581 [2.97]	525
4	Mo (26)	AlF_3 (44)	Cd (0.4)	760/49 [15.51]	760/66 [11.51]	292
5	Mo (28)	AlF_3 (27)	Co (0.4)	1350/61 [22.13]	1350/401 [3.37]	419
6	Mo (30)	AlF_3 (28)	Cd (1)	1066/59 [18.1]	1066/271 [3.93]	345
7	W (20)	$FeAlF_3$ (40)	LiF (1)	596/22 [27.1]	596/71 [8.4]	not defined
8	W (20)	$FeAlF_3$ (40)	Pb (1)	774/135 [5.73]	774/69 [11.22]	not defined

Table 8. *DT based BSA (Figure 56) moderator design simulated for 10^7 neutrons with 14.1 MeV energy. Numbers in parenthesis are the thicknesses of the compositions/materials, and $n_{epi}/n_{thermal}$ are the registered total numbers of epithermal neutrons over the registered total number of thermal neutrons with approximated ratios presented in the square brackets.*

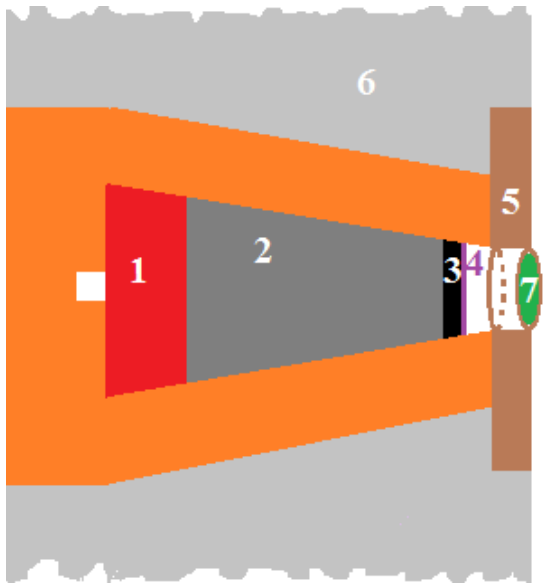

Figure 57. *Scheme of the BSA based on DT neutron generator. As listed in Table 9 and 10 with multiplier or first part of the moderator (1), second part of the moderator (2) with last part of the moderator (3) with filters (4). Collimator is Lead or LiF (Table 9) (5) with virtual sensitive detector (7) at the exit window. The system is placed in a concrete wall (6).*

BSA #	***Multiplier [cm]***	***Moderator Part 1 [cm]***	***Moderator Part 2 [cm]***	***Filter [cm]***	***Reflector [cm]***	***Collimator length [cm]***
1	-	*Fe (27)*	*Al (56)*	*LiF (1)*	*LiF(25)*	*Lead (10)*
2	-	*Fe (27)*	*Al (53)*	*Bi(3) and LiF(1)*	*LiF (25)*	*Lead (10)*
3	-	*Fe (27)*	*TiF_4 (53)*	*Bi(3) and LiF(1)*	*LiF (25)*	*Lead (10)*
4	-	*$FeAlF_3$ (27)*	*Al (56)*	*LiF (1)*	*LiF (25)*	*Lead (10)*
5	-	*Al (83)*	-	*LiF (1)*	*LiF (25)*	*Lead (10)*
6	-	*LiF (27)*	*$FeAlF_3$ (53) and Al (3)*	*LiF (1)*	*LiF (25)*	*Lead (10)*
7	*Mo (27)*	*TiF_4 (53)*	-	*Bi (3) and LiF(1)*	*LiF (25)*	*Lead (10)*
8	*U (27)*	*Al (57)*	-	-	*Lead (25)*	*Lead (10)*

9	*U (27)*	*Fe (57)*	-	-	*Lead (25)*	*Lead (10)*
10	*W (27)*	*$FeAlF_3$ (3)*	*Al (3)*	*LiF (1)*	*LiF (25)*	*LiF (10)*
11	*Bi (27)*	*$FeAlF_3$ (53)*	*Al (3)*	*LiF (1)*	*Lead (25)*	*Lead (10)*

Table 9. *DT based BSA configuration, where the diameter of the BSA outlet is 12 cm (BSAs based on Figure 57 with thicknesses of the compositions/materials presented in parenthesis).*

BSA #	$n_{epi}/n_{thermal}$	n_{epi}/n_{fast}	γ_{total}	n_{total} ***(up to 50 keV)***
1	217/2.33(93.13)	217/218 (0.995)	not defined	not defined
2	197/2.33 (84.54)	197/202 (0.97)	not defined	not defined
3	265/2.33 (113.734)	265/34 (7.8)	not defined	not defined
4	1947/2.33 (835.62)	1947/1041 (1.87)	342	2714
5	309/2.33 (132.62)	309/301 (1.03)	83	519
6	17/2.33 (7.3)	17/2 (8.5)	22	18
7	112/2.33 (48.07)	112/20 (5.6)	not defined	not defined
8	44/11 (4)	44/109 (0.404)	13	139
9	6/2.33 (2.6)	6/83 (0.07)	1	not defined
10	11/2.33 (4.72)	11/1 (11)	3	12
11	439/4 (109.75)	439/75 (5.85)	163	504

Table 10. *Results obtained for BSAs presented in Table 7 in case of the detector with 12 cm diameter (Figure 57) , when 10^6 isotropically distributed neutrons with 14.1 MeV energy were simulated (the 2.33 value of $n_{thermal}$ corresponds to the upper limit on the thermal flux which in the simulations was in some cases equal to 0).*

4.4 Irradiation of a soft tissue by wide range energetic neutrons

To describe the influence of neutrons on the soft tissue GEANT4 simulations were performed assuming neutrons with energies from 0.01 eV to 1 MeV increasing the energy by a factor of 10 at each step. As a target for the neutrons a cube of 12 cm side length was modeled. The density of the tissue is taken as 1.0 g/cm^3, with mass fractions of 13 elements listed in Table 11.

#	Chemical Element	Mass Fraction in the soft tissue
1	Hydrogen (H)	0.104472
2	Carbon (C)	0.23219
3	Nitrogen (N)	0.02488
4	Oxygen (O)	0.630238
5	Sodium (Na)	0.00113
6	Magnesium (Mg)	0.00013
7	Phosphor (P)	0.00133
8	Sulfur (S)	0.00199
9	Chlorine (Cl)	0.00134
10	Potassium (K)	0.00199
11	Calcium (Ca)	0.00023
12	Iron (Fe)	0.00005
13	Zink (Zn)	0.00003

Table 11: *Mass Fraction of each of the elements contained in the GEANT4 designed soft tissue. The fractions are as given in reference M. Adrian et al. 2016.*

The beam of neutrons is irradiating the soft tissue which has cubical volume with side length equal to 12 cm. During the GEANT4 simulation study secondary gamma rays being product of the reactions were calculated. The components of the soft tissue are listed in Table 11 and in Table 12 are the results from 10^6 simulated neutrons, were the highest number of gamma rays is achieved in case of 0.01 eV neutrons. Below nuclear reaction with isotopes of the elements contained in the soft tissue target are listed:

1) $n + {}^{1}H \rightarrow N_{(gamma\ or\ e-)} + d$,
2) $n + {}^{39}K \rightarrow N_{(gamma\ or\ e-)} + {}^{40}K$,
3) $n + {}^{39}K \rightarrow n + {}^{39}K$,
4) $n + {}^{41}K \rightarrow n + {}^{42}K$,
5) $n + {}^{41}K \rightarrow n + {}^{41}K$,
6) $n + {}^{24}Mg \rightarrow n + {}^{24}Mg$,
7) $n + {}^{25}Mg \rightarrow n + {}^{25}Mg$,
8) $n + {}^{14}N \rightarrow N_{(gamma\ or\ e-)} + {}^{15}N$,

9) $n + {}^{14}N \rightarrow n + {}^{14}N$,
10) $n + {}^{14}N \rightarrow p + {}^{14}C$,
11) $n + {}^{15}N \rightarrow n + {}^{15}N$,
12) $n + {}^{23}Na \rightarrow N_{(gamma\ or\ e-)} + {}^{24}N$,
13) $n + {}^{23}Na \rightarrow n + {}^{23}Na$,
14) $n + {}^{16}O \rightarrow N_{(gamma\ or\ e-)} + {}^{17}O$,
15) $n + {}^{16}O \rightarrow n + {}^{16}O$,
16) $n + {}^{17}O \rightarrow n + {}^{17}O$,
17) $n + {}^{18}O \rightarrow N_{(gamma\ or\ e-)} + \alpha + {}^{15}C$,
18) $n + {}^{18}O \rightarrow n + {}^{18}O$,
19) $n + {}^{31}P \rightarrow N_{(gamma\ or\ e-)} + {}^{32}P$,
20) $n + {}^{31}P \rightarrow n + {}^{31}P$,
21) $n + {}^{32}S \rightarrow N_{(gamma\ or\ e-)} + {}^{33}S$,
22) $n + {}^{32}S \rightarrow \alpha + {}^{29}Si$,
23) $n + {}^{32}S \rightarrow n + {}^{32}S$,
24) $n + {}^{33}S \rightarrow n + {}^{33}S$,
25) $n + {}^{34}S \rightarrow n + {}^{34}S$,
26) $n + {}^{64}Zn \rightarrow n + {}^{64}Zn$.

In the listed reactions "$N_{(gamma\ or\ e-)}$" is the number of gamma rays or electrons. The number of gamma rays and electrons will be separated in the upgraded versions of GEANT4. Here it also can be done by simple coding and avoiding the detection of electrons. While in the previous versions "N" was only the number of gamma rays. The rest of the details of the output from the simulations can be found in the Appendix with additional information and for all of the mentioned energies.

E_n	0.01 eV	0.1 eV	1 eV	10 eV	100 eV	1 keV	10 keV	100 keV	1 MeV
$N_{g/n}$	$1.4196 \cdot 10^{-1}$	$7.434 \cdot 10^{-2}$	$2.729 \cdot 10^{-3}$	$8.43 \cdot 10^{-4}$	$2.39 \cdot 10^{-4}$	$6.8 \cdot 10^{-5}$	$2.6 \cdot 10^{-5}$	$1.6 \cdot 10^{-5}$	$9.2 \cdot 10^{-5}$

Table 12: *Number of secondary gamma rays per neutrons ($N_{g/n}$) originating from neutron interactions with energies (E_n) from 0.01 eV to 1 MeV.*

In Figure 58 - 59 the spectra of the energies of gamma quanta, originating from neutron reactions with a soft tissue are presented. The detailed output of the simulation results are presented in the Appendix including all of the reaction channels.

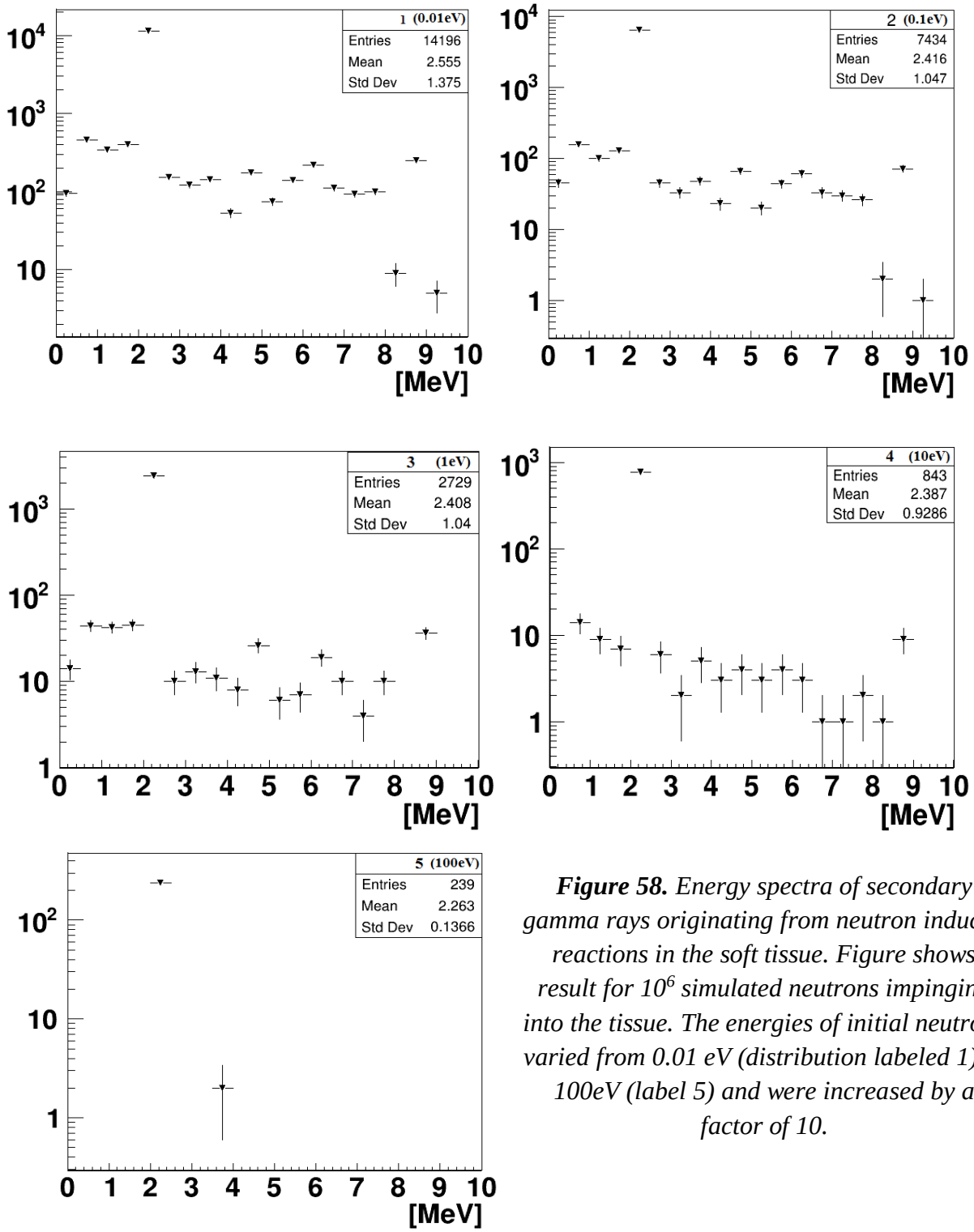

Figure 58. *Energy spectra of secondary gamma rays originating from neutron induced reactions in the soft tissue. Figure shows result for 10^6 simulated neutrons impinging into the tissue. The energies of initial neutrons varied from 0.01 eV (distribution labeled 1) to 100eV (label 5) and were increased by a factor of 10.*

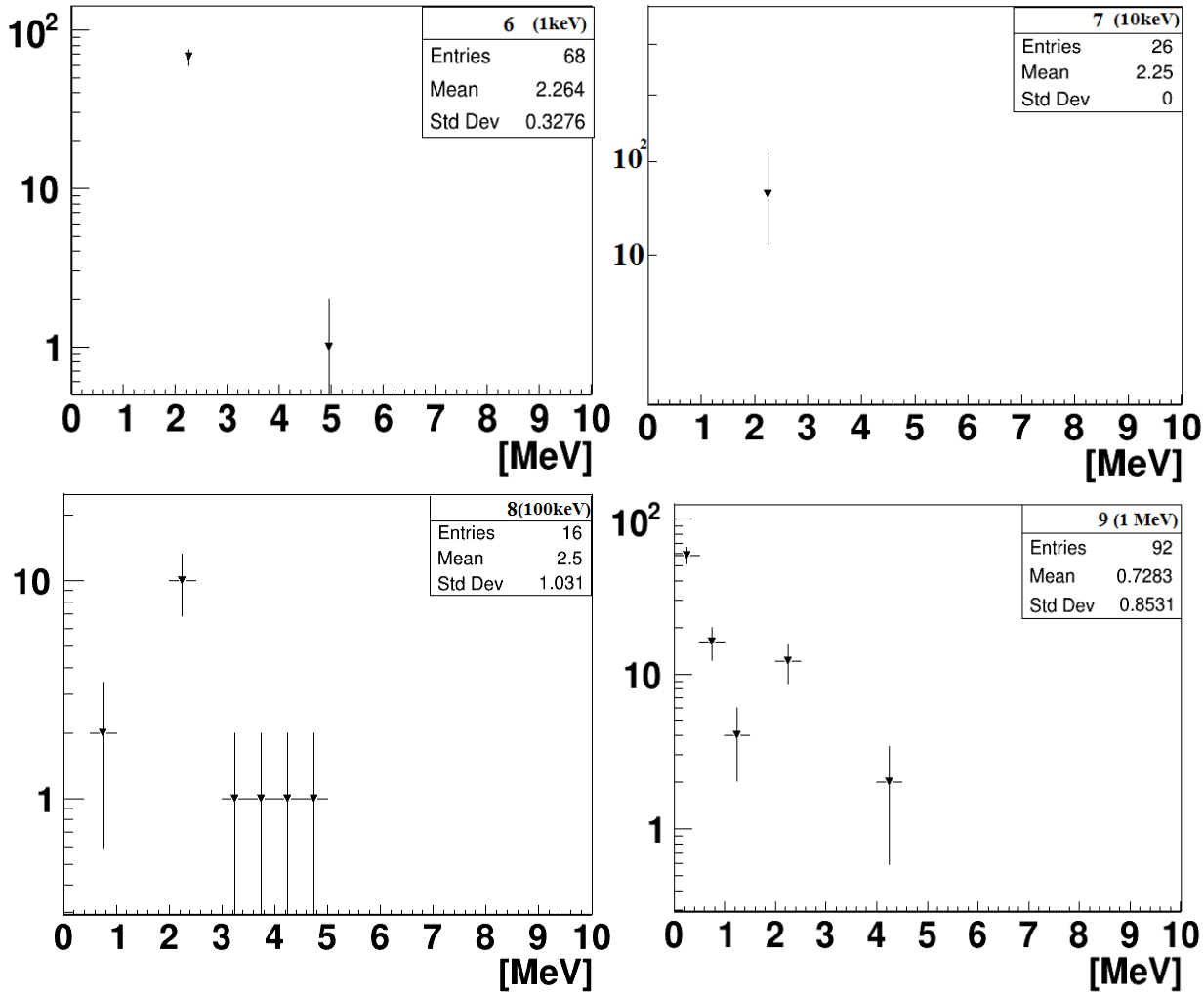

Figure 59. *Energy spectra of secondary gamma rays originating from neutron induced reactions in the soft tissue. Figure shows result for 10^6 simulated neutrons impinging into the tissue. The energies of initial neutrons varied from 1 keV (distribution labeled 6) to 1 MeV (label 9) and were increased by a factor of 10.*

Based on different initial energies from 0.01 eV up to 100 keV less neutrons are being captured and in case of 1 MeV additional neutron induced reactions occur (Figure 59) as can be seen in the list below and in detail in the Appendix:

1. $n + {}^{12}C \rightarrow n + {}^{12}C$,
2. $n + {}^{13}C \rightarrow n + {}^{13}C$,
3. $n + {}^{40}Ca \rightarrow n + {}^{40}Ca$,
4. $n + {}^{35}Cl \rightarrow n + {}^{35}Cl$,
5. $n + {}^{35}Cl \rightarrow p + {}^{35}S$,
6. $n + {}^{37}Cl \rightarrow n + {}^{37}Cl$,
7. $n + {}^{56}Fe \rightarrow N_{(gamma\ or\ e-)} + n + {}^{56}Fe$,
8. $n + {}^{56}Fe \rightarrow n + {}^{56}Fe$,

9. $n + {}^{1}H \rightarrow N_{(gamma\ or\ e-)} + d$,
10. $n + {}^{1}H \rightarrow n + p$,
11. $n + {}^{2}H \rightarrow n + d$,
12. $n + {}^{39}K \rightarrow n + {}^{39}K$,
13. $n + {}^{41}K \rightarrow n + {}^{41}K$,
14. $n + {}^{24}Mg \rightarrow n + {}^{24}Mg$,
15. $n + {}^{25}Mg \rightarrow n + {}^{25}Mg$,
16. $n + {}^{26}Mg \rightarrow n + {}^{26}Mg$,
17. $n + {}^{14}N \rightarrow \alpha + {}^{11}B$,
18. $n + {}^{14}N \rightarrow n + {}^{14}N$,
19. $n + {}^{14}N \rightarrow p + {}^{14}C$,
20. $n + {}^{15}N \rightarrow n + {}^{15}N$,
21. $n + {}^{23}Na \rightarrow N_{(gamma\ or\ e-)} + n + {}^{23}Na$,
22. $n + {}^{23}Na \rightarrow n + {}^{23}Na$,
23. $n + {}^{16}O \rightarrow N_{(gamma\ or\ e-)} + {}^{17}O$,
24. $n + {}^{16}O \rightarrow n + {}^{16}O$,
25. $n + {}^{17}O \rightarrow N_{(gamma\ or\ e-)} + n + {}^{17}O$,
26. $n + {}^{17}O \rightarrow \alpha + {}^{14}C$,
27. $n + {}^{17}O \rightarrow n + {}^{17}O$,
28. $n + {}^{18}O \rightarrow N_{(gamma\ or\ e-)} + \alpha + {}^{15}C$,
29. $n + {}^{18}O \rightarrow N_{(gamma\ or\ e-)} + n + {}^{18}O$,
30. $n + {}^{18}O \rightarrow n + {}^{18}O$,
31. $n + {}^{31}P \rightarrow n + {}^{31}P$,
32. $n + {}^{32}S \rightarrow \alpha + {}^{29}Si$,
33. $n + {}^{32}S \rightarrow n + {}^{32}S$,
34. $n + {}^{33}S \rightarrow n + {}^{33}S$,
35. $n + {}^{34}S \rightarrow n + {}^{34}S$,
36. $n + {}^{66}Zn \rightarrow n + {}^{66}Zn$,
37. $n + {}^{68}Zn \rightarrow n + {}^{68}Zn$.

This result somehow can be represented as neutron capture therapy, which proves once more that the lower the energy of neutrons the better they can be captured. In case of BNCT additional interactions exist with boron-10 and due to this fact, most usable neutron energy for deep seated tumors becomes 10 keV (R. Barth et al. 2012).

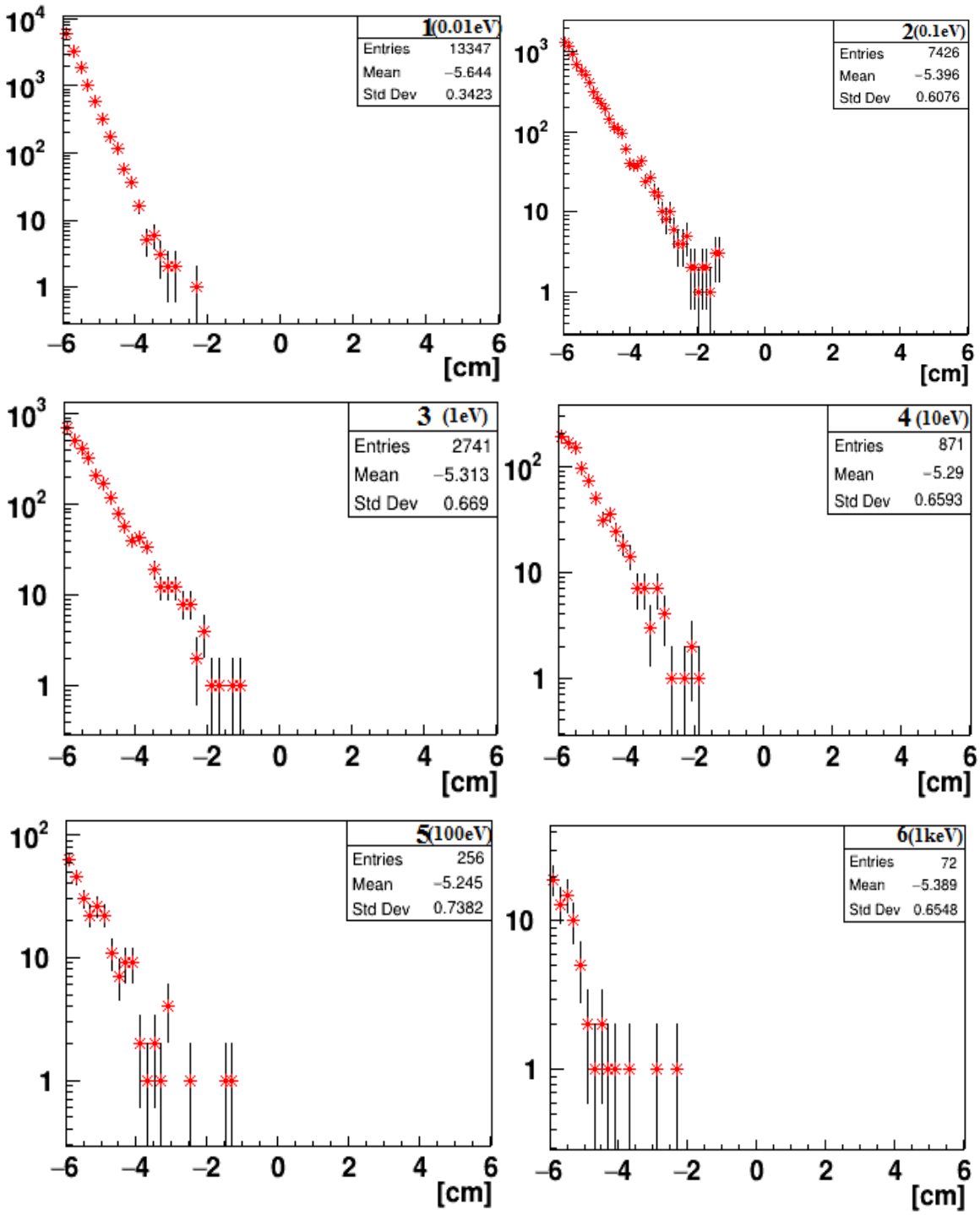

Figure 60. *Neutron induced reactions occurred at different depths in the soft tissue with number of neutron reactions (each represents also one neutron participating in the reaction) as function of the penetration depth. Initial energies for separately simulated neutrons in the energy range from 0.01 eV to 1 keV and with 10 time increment of each step numbered from (1) to (6) on figures .*

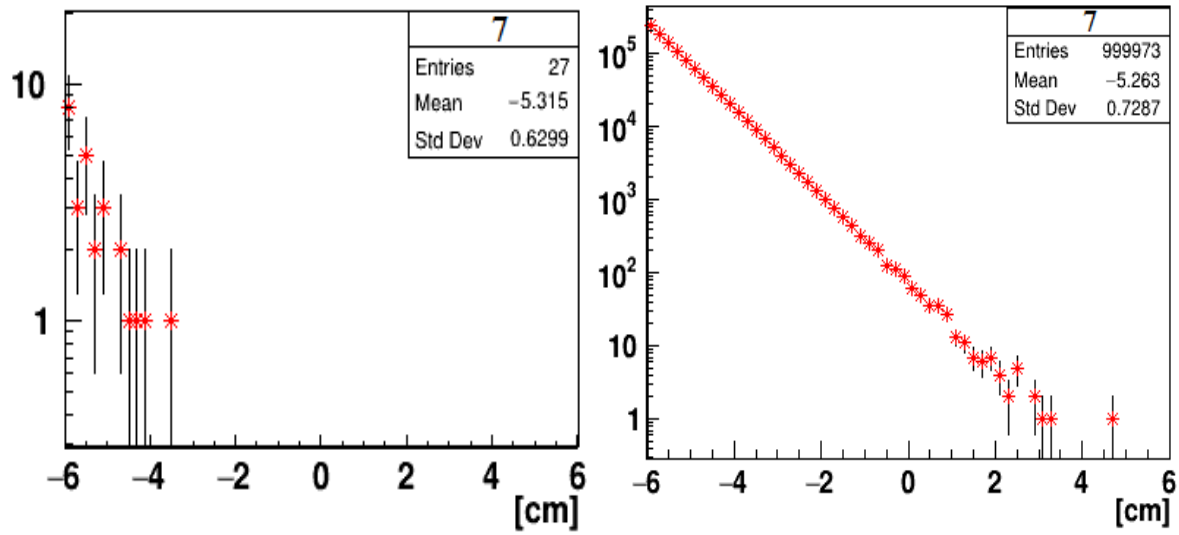

a) ***b)***

Figure 61. *Neutron induced reactions occurred at different depths in the soft tissue with* ***(a)*** *number of neutrons captured during the penetration in the soft tissue* ***(b)****. and participating in non absolutely elastic scatterings for separately simulated neutrons with initial 10 keV energies.*

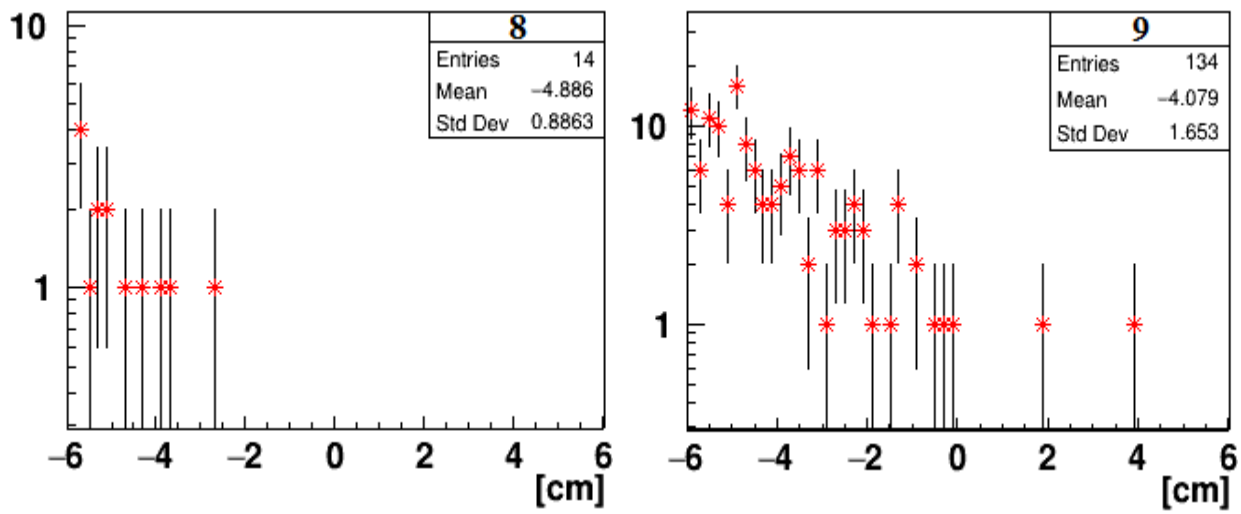

Figure 62. *Neutron induced reactions occurred at different depths in the soft tissue with number of neutron reactions (each represents also one neutron participating in the reaction) as function of the penetration depth. Initial energies for separately simulated neutrons in the energy range from 100 keV (label 8) to 1 MeV (label 9) .*

In figures 60-62 the scales from -6 to 6 are due to the placing of the 12 thick cube from soft tissue at the center of the box with (0, 0, 0) coordinate, with the left (negative) and right (positive) directions.

5. **Summary and Conclusions**

The aim of this thesis was the development, design and optimization of the beam shaping assemblies for the BNCT based on C18/18 cyclotron were the neutron source is ^{9}Be (p, Xn) nuclear reaction, as well as for BNCT based on DD and DT neutron generators. The feasibility study for the development of BNCT based on the Armenian C18/18 cyclotron as well as DD and DT compact neutron generators were performed using GEANT4 simulation package.

Chapter 1 discussed some of the neutron applications for non-military purposes, as well as the importance of the neutron usage in cancer treatment, particularly the need for the development of BNCT. As an example some of the necessary equipments which are already in use worldwide for BNCT were presented.

Chapter 2 presented most of the valuable scientific achievements by other researchers, particularly in Greece, Russia, Finland, Japan and Iran. Most of the above mentioned countries are already famous with clinical or experimental achievements in the development of BNCT.

Chapter 3 and 4 describe materials and methods and their successful usage for studies. Neutron sources on the basis of C18/18 cyclotron, DD and DT based BSA design and optimization were modeled by GEANT4.10.04 program with the usage of QGSP_BERT_HP physics list. On the base of C18/18 cyclotron there is a need to estimate neutron flux of the nuclear reaction with 14.8 MeV proton beam and 2.5 mm thick ^{9}Be target where the 14.8 MeV is the remaining energy of protons after passing through the 500 µm thick Al window of the particle transporting pipe line. After preliminary MC simulations (R. Avagyan, V. Ivanyan et al. 2017, R. Avagyan, V. Ivanyan et al. 2018) the successful GEANT4 study resulted in the design and optimization of a BNCT applicable BSA modeled from assuming moderator parts of 20 cm thick nat-Mo, 45 cm thick nat-Fe, and 45 cm paraffin boric acid. The tube shape moderator is covered with 20 cm thick nat-Pb as reflector (Figure 19 Section 3.1, details: V. Ivanyan 2020). The epithermal neutron flux is more than 10^{8} n/(s·cm^{2}) achieved after the BSA and yet could be examined for higher suitability level with the IAEA requirements. The high neutron flux was possible to obtain based on the multiplication property of the thick natural molybdenum placed as first layer for the moderation, while used/designed BSA was confined only to the thermalization of neutrons using not successful combinations and thickness of bismuth, iron or other materials. The DD compact neutron generator based BNCT was next for which GEANT4 simulations were performed to investigate its usability as a neutron source for the medical applications. The research and development study resulted in the design of 23 different BSAs with various parameters (Section 4.2), taking into account the recommendations of the IAEA. For the non-clinical investigations a BSA with 2.5 cm radius of the outlet and moderator of 8 cm thick ^{186}W, 45 cm thick mixture of nat-Fe (5%) AlF_3 (95%) and 1.25 cm thick nat-Cd with lead reflector surrounding the moderator was designed. As a result the ratio of the achieved epithermal neutron flux over thermal and fast neutrons were ~174 and ~24, respectively.

In case of head and neck cancers based on the depth of the tumor the aforementioned requirements can be usable for the BNCT treatment with life-saving or prolonging results, as

BNCT is suggested, being the most promising method for the multiform glioblastoma (the most active brain tumor) treatment. The obtained result is in agreement with the IAEA recommendations. The ratio of epithermal over thermal neutrons should be more than 100 and in case of epithermal over fast components of the final flux the ratio should be at least 20 as recommended by IAEA for the BNCT.

The next part of the thesis dealt with the design of the BSA for DT generator. The requirements of the IAEA were taken into account to design 27 BSAs for the DT based BNCT. The recommended in merit ratio (more than 20) for epithermal over thermal neutrons was possible to achieve in most of cases, especially with the usage of thick multipliers, such as nat-Bi, nat-W, nat-U and nat-Mo installed separately as first part of the moderation system. In addition various simulations were performed with different combinations of more than 10 materials namely Al, Fe, Co, Cd, AlF_3, LiF, MoF, MoF_6,TiF_3,TiF_4 paraffin boric acid as well as $FeAlF_3$ with 5%/95% mixture of iron and AlF_3 (Section 4.3). It is worthwhile noting that the need for the specific 10 keV neutron peak for the deep seated tumors will be an important step towards the development of a progressive treatment based on BNCT. In Section 4.4, results based on the simulation of neutrons in wide energy range of neutron interactions with soft tissue were discussed. While the edge of the epithermal neutron energy range 10 keV gives the lowest number of gamma production in the soft tissue, as can be seen from the simulations provided partly in the Section 4.4 and in the Appendix with the total output of the program.

In conclusion, in this thesis the BSAs were designed for the C18/18, DD and DT based neutron sources. The various combinations of materials and geometries for moderators, reflectors and collimators were investigated using GEANT4 simulation package. One of the latest versions for C18/18 based BSA gave a chance to obtain neutron flux in higher agreement with IAEA recommendations for BNCT. The composition of materials such as 20 cm thick nat-Mo, 45 cm thick nat-Fe and 45 cm thick paraffin boric acid were designed as moderator shown in Figure 20. Here the shielding concrete wall is simulated along the BSA axis. Besides the negative expectations about the possible high epithermal neutron flux the results of the GEANT4 simulations were promising. First time it was possible to achieve almost 10^9 n/(s·cm^2) flux containing ~70 % epithermal neutrons and less than 14% percent thermal neutrons. This results are an asset to continue the development of the BNCT projects on the base of C18/18 cyclotrons of IBA as well as began non-clinical investigations.

The best established version of the DD based BSA includes moderator consisting of 8 cm thick ^{186}W, 45 cm thick mixture of 5% Fe and 95 % AlF_3, 1.25 cm thick LiF, 0.5 mm Bi and 1 mm thick lead, and the 20 cm thick back and 15 cm thick side Pb reflectors with 15 cm thick lead collimator. As for DT neutron generator based BSA the best design consisted from 27 cm thick Bi, 53 cm thick $FeAlF_3$, 3 cm thick Al, and 1 cm thick LiF moderator with 25 cm thick back and side lead reflectors and 10 cm thick lead collimator. The achieved epithermal over thermal neutron ratio was larger than 100.

Appendix

The Box is 12 cm of SoftTissue

Material: SoftTissue density: 1.000 g/cm3 RadL: 37.630 cm Nucl.Int.Length: 74.643 cm
Imean: 68.126 eV temperature: 293.15 K pressure: 1.00 atm

---> Element: Hydrogen (H) Z = 1.0 N = 1 A = 1.010 g/mole
---> Isotope: H1 Z = 1 N = 1 A = 1.01 g/mole abundance: 99.989 %
---> Isotope: H2 Z = 1 N = 2 A = 2.01 g/mole abundance: 0.011 %
ElmMassFraction: 10.45 % ElmAbundance 62.99 %

---> Element: Hydrogen (C) Z = 6.0 N = 12 A = 12.000 g/mole
---> Isotope: C12 Z = 6 N = 12 A = 12.00 g/mole abundance: 98.930 %
---> Isotope: C13 Z = 6 N = 13 A = 13.00 g/mole abundance: 1.070 %
ElmMassFraction: 23.22 % ElmAbundance 11.78 %

---> Element: N (N) Z = 7.0 N = 14 A = 14.007 g/mole
---> Isotope: N14 Z = 7 N = 14 A = 14.00 g/mole abundance: 99.632 %
---> Isotope: N15 Z = 7 N = 15 A = 15.00 g/mole abundance: 0.368 %
ElmMassFraction: 2.49 % ElmAbundance 1.08 %

---> Element: O (O) Z = 8.0 N = 16 A = 15.999 g/mole
---> Isotope: O16 Z = 8 N = 16 A = 15.99 g/mole abundance: 99.757 %
---> Isotope: O17 Z = 8 N = 17 A = 17.00 g/mole abundance: 0.038 %
---> Isotope: O18 Z = 8 N = 18 A = 18.00 g/mole abundance: 0.205 %
ElmMassFraction: 63.02 % ElmAbundance 23.99 %

---> Element: Na (Na) Z = 11.0 N = 23 A = 22.990 g/mole
---> Isotope: Na23 Z = 11 N = 23 A = 22.99 g/mole abundance: 100.000 %
ElmMassFraction: 0.11 % ElmAbundance 0.03 %

---> Element: Mg (Mg) Z = 12.0 N = 24 A = 24.305 g/mole
---> Isotope: Mg24 Z = 12 N = 24 A = 23.98 g/mole abundance: 78.990 %
---> Isotope: Mg25 Z = 12 N = 25 A = 24.99 g/mole abundance: 10.000 %
---> Isotope: Mg26 Z = 12 N = 26 A = 25.98 g/mole abundance: 11.010 %
ElmMassFraction: 0.01 % ElmAbundance 0.00 %

---> Element: P (P) Z = 15.0 N = 31 A = 30.974 g/mole
---> Isotope: P31 Z = 15 N = 31 A = 30.97 g/mole abundance: 100.000 %
ElmMassFraction: 0.13 % ElmAbundance 0.03 %

```
---> Element: S (S)   Z = 16.0   N =    32   A = 32.066 g/mole
---> Isotope:   S32   Z = 16   N =  32   A =  31.97 g/mole   abundance: 94.930 %
---> Isotope:   S33   Z = 16   N =  33   A =  32.97 g/mole   abundance:  0.760 %
---> Isotope:   S34   Z = 16   N =  34   A =  33.97 g/mole   abundance:  4.290 %
---> Isotope:   S36   Z = 16   N =  36   A =  35.97 g/mole   abundance:  0.020 %
ElmMassFraction:   0.20 %  ElmAbundance   0.04 %

---> Element: Cl (Cl)   Z = 17.0   N =    35   A = 35.453 g/mole
---> Isotope:  Cl35   Z = 17   N =  35   A =  34.97 g/mole   abundance: 75.780 %
---> Isotope:  Cl37   Z = 17   N =  37   A =  36.97 g/mole   abundance: 24.220 %
ElmMassFraction:   0.13 %  ElmAbundance   0.02 %

---> Element: K (K)   Z = 19.0   N =    39   A = 39.098 g/mole
---> Isotope:   K39   Z = 19   N =  39   A =  38.96 g/mole   abundance: 93.258 %
---> Isotope:   K40   Z = 19   N =  40   A =  39.96 g/mole   abundance:  0.012 %
---> Isotope:   K41   Z = 19   N =  41   A =  40.96 g/mole   abundance:  6.730 %
ElmMassFraction:   0.20 %  ElmAbundance   0.03 %

---> Element: Ca (Ca)   Z = 20.0   N =    40   A = 40.078 g/mole
---> Isotope:  Ca40   Z = 20   N =  40   A =  39.96 g/mole   abundance: 96.941 %
---> Isotope:  Ca42   Z = 20   N =  42   A =  41.96 g/mole   abundance:  0.647 %
---> Isotope:  Ca43   Z = 20   N =  43   A =  42.96 g/mole   abundance:  0.135 %
---> Isotope:  Ca44   Z = 20   N =  44   A =  43.96 g/mole   abundance:  2.086 %
---> Isotope:  Ca46   Z = 20   N =  46   A =  45.95 g/mole   abundance:  0.004 %
---> Isotope:  Ca48   Z = 20   N =  48   A =  47.95 g/mole   abundance:  0.187 %
ElmMassFraction:   0.02 %  ElmAbundance   0.00 %

---> Element: Fe (Fe)   Z = 26.0   N =    56   A = 55.845 g/mole
---> Isotope:  Fe54   Z = 26   N =  54   A =  53.94 g/mole   abundance:  5.845 %
---> Isotope:  Fe56   Z = 26   N =  56   A =  55.93 g/mole   abundance: 91.754 %
---> Isotope:  Fe57   Z = 26   N =  57   A =  56.94 g/mole   abundance:  2.119 %
---> Isotope:  Fe58   Z = 26   N =  58   A =  57.93 g/mole   abundance:  0.282 %
ElmMassFraction:   0.01 %  ElmAbundance   0.00 %

---> Element: Zn (Zn)   Z = 30.0   N =    65   A = 65.396 g/mole
---> Isotope:  Zn64   Z = 30   N =  64   A =  63.93 g/mole   abundance: 48.630 %
---> Isotope:  Zn66   Z = 30   N =  66   A =  65.93 g/mole   abundance: 27.900 %
---> Isotope:  Zn67   Z = 30   N =  67   A =  66.93 g/mole   abundance:  4.100 %
---> Isotope:  Zn68   Z = 30   N =  68   A =  67.92 g/mole   abundance: 18.750 %
```

---> Isotope: Zn70 Z = 30 N = 70 A = 69.93 g/mole abundance: 0.620 %
ElmMassFraction: 0.00 % ElmAbundance 0.00 %

0.01 eV neutrons

The run is 1000000 neutron of 0.01 eV through 12 cm of SoftTissue (density: 1 g/cm3)

List of nuclear reactions:

neutron + C12 --> N gamma or e- + C13: 64 Q = 7.4375 MeV
neutron + C12 --> neutron + C12: 37492 Q = 0.040321 eV
neutron + C13 --> N gamma or e- + C14: 1 Q = 8.179 MeV
neutron + C13 --> neutron + C13: 441 Q = 0.037025 eV
neutron + Ca40 --> N gamma or e- + Ca41: 4 Q = 5.6097 MeV
neutron + Ca40 --> neutron + Ca40: 15 Q = 0.044949 eV
neutron + Cl35 --> N gamma or e- + Cl36: 852 Q = 10.404 MeV
neutron + Cl35 --> neutron + Cl35: 254 Q = 0.039241 eV
neutron + Cl35 --> proton + S35: 9 Q = 615.23 keV
neutron + Cl37 --> N gamma or e- + Cl38: 2 Q = 5.2796 MeV
neutron + Cl37 --> neutron + Cl37: 6 Q = 0.06517 eV
neutron + Fe56 --> N gamma or e- + Fe57: 1 Q = 3.0736 MeV
neutron + Fe56 --> neutron + Fe56: 4 Q = 0.014193 eV
neutron + H1 --> N gamma or e- + deuteron: 11085 Q = 2.2257 MeV
neutron + H1 --> neutron + proton: 877446 Q = 0.047774 eV
neutron + H1 --> proton: 1 Q = 0.0046918 eV
neutron + H2 --> neutron + deuteron: 18 Q = 0.049771 eV
neutron + K39 --> N gamma or e- + K40: 61 Q = 7.7999 MeV
neutron + K39 --> neutron + K39: 38 Q = 0.038527 eV
neutron + K41 --> N gamma or e- + K42: 1 Q = 7.5338 MeV
neutron + K41 --> neutron + K41: 8 Q = 0.035445 eV
neutron + Mg24 --> neutron + Mg24: 7 Q = 0.056083 eV
neutron + Mg25 --> neutron + Mg25: 2 Q = 0.070824 eV
neutron + N14 --> N gamma or e- + N15: 108 Q = 13.853 MeV
neutron + N14 --> neutron + N14: 7315 Q = 0.040687 eV
neutron + N14 --> proton + C14: 1121 Q = 626.34 keV
neutron + N15 --> neutron + N15: 12 Q = 0.036123 eV
neutron + Na23 --> N gamma or e- + Na24: 12 Q = 5.4724 MeV
neutron + Na23 --> neutron + Na23: 73 Q = 0.038422 eV
neutron + O16 --> N gamma or e- + O17: 6 Q = 4.0343 MeV
neutron + O16 --> neutron + O16: 63228 Q = 0.039935 eV
neutron + O17 --> neutron + O17: 13 Q = 0.036904 eV
neutron + O18 --> N gamma or e- + alpha + C15: 5 Q = 1.7352 keV

neutron + O18 --> neutron + O18: 145 Q = 0.035721 eV
neutron + P31 --> N gamma or e- + P32: 6 Q = 7.9364 MeV
neutron + P31 --> neutron + P31: 85 Q = 0.040676 eV
neutron + S32 --> N gamma or e- + S33: 28 Q = 8.6421 MeV
neutron + S32 --> alpha + Si29: 1 Q = 1.529 MeV
neutron + S32 --> neutron + S32: 24 Q = 0.037936 eV
neutron + S33 --> neutron + S33: 2 Q = 0.010895 eV
neutron + S34 --> neutron + S34: 3 Q = 0.015608 eV
neutron + Zn64 --> neutron + Zn64: 1 Q = 0.013626 eV

number of gamma or e- (ic): N = 1 --> 6

List of generated particles:
C12: 37492 Emean = 0.037371 eV (9.0949e-06 eV --> 0.27671 eV)
C13: 505 Emean = 179.18 eV (0.00073487 eV --> 7.0265 keV)
C14: 1122 Emean = 41.969 keV (2.5337 keV --> 42.143 keV)
C15: 5 Emean = 0.028984 eV (0.014386 eV --> 0.058473 eV)
Ca40: 15 Emean = 0.045339 eV (0.0054424 eV --> 0.089312 eV)
Ca41: 4 Emean = 0.5127 eV (0.24844 eV --> 0.83636 eV)
Cl35: 254 Emean = 0.038627 eV (0.0005457 eV --> 0.18962 eV)
Cl36: 852 Emean = 894.51 eV (5.8277 eV --> 11.189 keV)
Cl37: 6 Emean = 0.063845 eV (0.0068321 eV --> 0.18183 eV)
Cl38: 2 Emean = 290.87 eV (55.407 eV --> 526.33 eV)
Fe56: 4 Emean = 0.014197 eV (0.0038126 eV --> 0.032429 eV)
Fe57: 1 Emean = 52.273 eV (52.273 eV --> 52.273 eV)
K39: 38 Emean = 0.038426 eV (0.0020736 eV --> 0.12035 eV)
K40: 61 Emean = 284.81 eV (0.18839 eV --> 832.39 eV)
K41: 8 Emean = 0.033991 eV (0.0010987 eV --> 0.054271 eV)
K42: 1 Emean = 0.43996 eV (0.43996 eV --> 0.43996 eV)
Mg24: 7 Emean = 0.058141 eV (0.015105 eV --> 0.12368 eV)
Mg25: 2 Emean = 0.066042 eV (0.060008 eV --> 0.072076 eV)
N14: 7315 Emean = 0.038092 eV (0.00011823 eV --> 0.25175 eV)
N15: 120 Emean = 3.5532 keV (0.0016262 eV --> 27.155 keV)
Na23: 73 Emean = 0.037828 eV (0.00082946 eV --> 0.1312 eV)
Na24: 12 Emean = 413.01 eV (5.6463 eV --> 1.9467 keV)
O16: 63228 Emean = 0.037737 eV (1.4552e-05 eV --> 0.32705 eV)
O17: 19 Emean = 61.183 eV (0.0045111 eV --> 536.73 eV)
O18: 145 Emean = 0.033434 eV (0.0016771 eV --> 0.12199 eV)
P31: 85 Emean = 0.038652 eV (0.0014588 eV --> 0.18621 eV)
P32: 6 Emean = 712.32 eV (303.32 eV --> 1.0531 keV)

S32: 24 Emean = 0.036076 eV (0.00037107 eV --> 0.11848 eV)
S33: 30 Emean = 422.65 eV (0.0098407 eV --> 1.2309 keV)
S34: 3 Emean = 0.015199 eV (0.0015498 eV --> 0.028416 eV)
S35: 9 Emean = 17.255 keV (17.202 keV --> 17.311 keV)
Si29: 1 Emean = 185.47 keV (185.47 keV --> 185.47 keV)
Zn64: 1 Emean = 0.013955 eV (0.013955 eV --> 0.013955 eV)
alpha: 6 Emean = 223.92 keV (0.003507 eV --> 1.3435 MeV)
deuteron: 11103 Emean = 1.3168 keV (0.0015746 eV --> 1.3441 keV)
gamma: 14196 Emean = 2.5641 MeV (1.2362 keV --> 10.833 MeV)
proton: 878577 Emean = 751.72 eV (3.979e-06 eV --> 598.02 keV)

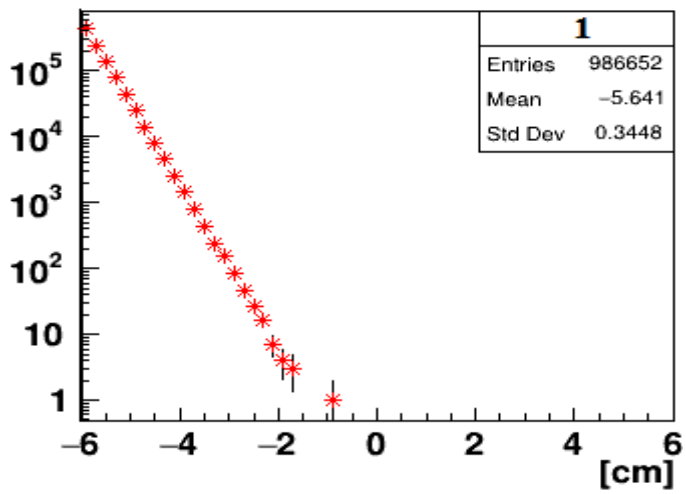

0.01 eV Neutron Penetration into the soft tissue (12 cm thick)

0.1 eV neutrons

The run is 1000000 neutron of 0.1 eV through 12 cm of SoftTissue (density: 1 g/cm3)

Process calls frequency:

hadElastic= 992567 nCapture= 6788 neutronInelastic= 645

List of nuclear reactions:

neutron + C12 --> N gamma or e- + C13: 16 Q = 6.8749 MeV
neutron + C12 --> neutron + C12: 37764 Q = 0.03827 eV
neutron + C13 --> N gamma or e- + C14: 1 Q = 8.179 MeV
neutron + C13 --> neutron + C13: 383 Q = 0.035127 eV
neutron + Ca40 --> neutron + Ca40: 3 Q = 0.011967 eV
neutron + Cl35 --> N gamma or e- + Cl36: 255 Q = 10.443 MeV
neutron + Cl35 --> neutron + Cl35: 233 Q = 0.037877 eV
neutron + Cl35 --> proton + S35: 3 Q = 615.23 keV
neutron + Cl37 --> N gamma or e- + Cl38: 2 Q = 2.2794 MeV
neutron + Cl37 --> neutron + Cl37: 4 Q = 0.03902 eV
neutron + Fe56 --> neutron + Fe56: 7 Q = 0.054133 eV
neutron + H1 --> N gamma or e- + deuteron: 6440 Q = 2.2257 MeV
neutron + H1 --> neutron + proton: 883295 Q = 0.040764 eV
neutron + H2 --> neutron + deuteron: 11 Q = 0.031576 eV
neutron + K39 --> N gamma or e- + K40: 28 Q = 7.7999 MeV
neutron + K39 --> neutron + K39: 31 Q = 0.039309 eV
neutron + Mg24 --> neutron + Mg24: 11 Q = 0.032293 eV
neutron + N14 --> N gamma or e- + N15: 35 Q = 15.421 MeV
neutron + N14 --> neutron + N14: 7484 Q = 0.03756 eV
neutron + N14 --> proton + C14: 636 Q = 626.34 keV
neutron + N15 --> neutron + N15: 18 Q = 0.030973 eV
neutron + Na23 --> N gamma or e- + Na24: 6 Q = 4.2662 MeV
neutron + Na23 --> neutron + Na23: 58 Q = 0.037226 eV
neutron + O16 --> N gamma or e- + O17: 1 Q = 1.9588 MeV
neutron + O16 --> neutron + O16: 63007 Q = 0.037945 eV
neutron + O17 --> neutron + O17: 23 Q = 0.028674 eV
neutron + O18 --> N gamma or e- + alpha + C15: 5 Q = 1.8139 keV
neutron + O18 --> alpha + C15: 1 Q = -0.078233 eV

neutron + O18 --> neutron + O18: 133 Q = 0.036248 eV
neutron + P31 --> N gamma or e- + P32: 2 Q = 7.9364 MeV
neutron + P31 --> neutron + P31: 73 Q = 0.039881 eV
neutron + S32 --> N gamma or e- + S33: 2 Q = 8.6423 MeV
neutron + S32 --> neutron + S32: 27 Q = 0.030366 eV
neutron + S34 --> neutron + S34: 2 Q = 0.023194 eV

number of gamma or e- (ic): N = 1 --> 6

List of generated particles:
C12: 37764 Emean = 0.048819 eV (1.6371e-05 eV --> 0.39176 eV)
C13: 399 Emean = 45.171 eV (0.00054206 eV --> 3.8557 keV)
C14: 637 Emean = 41.945 keV (2.5717 keV --> 42.141 keV)
C15: 6 Emean = 0.028274 eV (0.013872 eV --> 0.074037 eV)
Ca40: 3 Emean = 0.012711 eV (0.0043656 eV --> 0.025088 eV)
Cl35: 233 Emean = 0.041914 eV (0.0010696 eV --> 0.25381 eV)
Cl36: 255 Emean = 890.52 eV (1.8828 eV --> 4.7424 keV)
Cl37: 4 Emean = 0.043236 eV (0.011016 eV --> 0.078471 eV)
Cl38: 2 Emean = 20.663 eV (7.3586 eV --> 33.967 eV)
Fe56: 7 Emean = 0.050591 eV (0.014254 eV --> 0.13524 eV)
K39: 31 Emean = 0.046102 eV (0.00010914 eV --> 0.13907 eV)
K40: 28 Emean = 217.05 eV (1.7943 eV --> 822.35 eV)
Mg24: 11 Emean = 0.038825 eV (0.0027831 eV --> 0.11121 eV)
N14: 7484 Emean = 0.046662 eV (4.0018e-05 eV --> 0.28464 eV)
N15: 53 Emean = 2.7654 keV (0.0039709 eV --> 13.269 keV)
Na23: 58 Emean = 0.042392 eV (0.0019791 eV --> 0.13338 eV)
Na24: 6 Emean = 229.06 eV (12.482 eV --> 468.99 eV)
O16: 63007 Emean = 0.046254 eV (2.5466e-05 eV --> 0.37126 eV)
O17: 24 Emean = 0.43471 eV (0.00030923 eV --> 9.5488 eV)
O18: 133 Emean = 0.047274 eV (0.0010696 eV --> 0.20865 eV)
P31: 73 Emean = 0.041126 eV (0.0016917 eV --> 0.18633 eV)
P32: 2 Emean = 704.67 eV (339.11 eV --> 1.0702 keV)
S32: 27 Emean = 0.032443 eV (0.001095 eV --> 0.12427 eV)
S33: 2 Emean = 606.22 eV (2.5576 eV --> 1.2099 keV)
S34: 2 Emean = 0.028767 eV (0.0059263 eV --> 0.051608 eV)
S35: 3 Emean = 17.237 keV (17.228 keV --> 17.254 keV)
alpha: 6 Emean = 0.0068364 eV (0.003351 eV --> 0.017827 eV)
deuteron: 6451 Emean = 1.3167 keV (0.0062453 eV --> 1.3515 keV)
gamma: 7434 Emean = 2.4118 MeV (1.3947 keV --> 10.833 MeV)
proton: 883934 Emean = 422.53 eV (3.7517e-06 eV --> 598 keV)

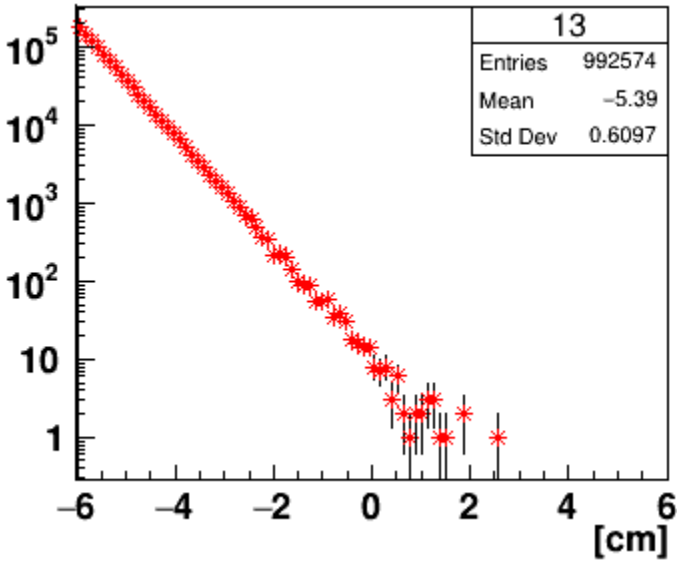

0.1 eV Neutron Penetration into the soft tissue (12 cm thick)

1 eV neutrons

The run is 1000000 neutron of 1 eV through 12 cm of SoftTissue (density: 1 g/cm3)

Process calls frequency:

hadElastic= 997249 nCapture= 2528 neutronInelastic= 223

List of nuclear reactions:

neutron + C12 --> N gamma or e- + C13: 6 Q = 5.7719 MeV
neutron + C12 --> neutron + C12: 38204 Q = 0.037942 eV
neutron + C13 --> neutron + C13: 392 Q = 0.025194 eV
neutron + Ca40 --> neutron + Ca40: 4 Q = 0.036304 eV
neutron + Cl35 --> N gamma or e- + Cl36: 89 Q = 10.306 MeV
neutron + Cl35 --> neutron + Cl35: 235 Q = 0.036961 eV
neutron + Cl35 --> proton + S35: 2 Q = 615.23 keV
neutron + Cl37 --> neutron + Cl37: 6 Q = 0.036374 eV
neutron + Fe56 --> N gamma or e- + Fe57: 1 Q = 12.681 MeV
neutron + Fe56 --> neutron + Fe56: 2 Q = 0.045123 eV
neutron + H1 --> N gamma or e- + deuteron: 2409 Q = 2.2257 MeV
neutron + H1 --> neutron + proton: 887018 Q = 0.038499 eV
neutron + H2 --> neutron + deuteron: 18 Q = 0.042125 eV
neutron + K39 --> N gamma or e- + K40: 8 Q = 7.7998 MeV
neutron + K39 --> neutron + K39: 31 Q = 0.039508 eV
neutron + K41 --> N gamma or e- + K42: 2 Q = 7.5342 MeV
neutron + K41 --> neutron + K41: 6 Q = 0.031881 eV
neutron + Mg24 --> neutron + Mg24: 5 Q = 0.058176 eV
neutron + N14 --> N gamma or e- + N15: 9 Q = 11.262 MeV
neutron + N14 --> neutron + N14: 7262 Q = 0.038376 eV
neutron + N14 --> proton + C14: 218 Q = 626.34 keV
neutron + N15 --> neutron + N15: 6 Q = 0.069767 eV
neutron + Na23 --> N gamma or e- + Na24: 1 Q = 6.1905 MeV
neutron + Na23 --> neutron + Na23: 76 Q = 0.035811 eV
neutron + O16 --> neutron + O16: 63722 Q = 0.038098 eV
neutron + O17 --> neutron + O17: 27 Q = 0.044854 eV
neutron + O18 --> N gamma or e- + alpha + C15: 2 Q = 2.0472 keV
neutron + O18 --> neutron + O18: 115 Q = 0.032513 eV
neutron + P31 --> neutron + P31: 86 Q = 0.033987 eV

```
neutron + S32 --> N gamma or e- + S33:       3   Q =  8.6429 MeV
neutron + S32 --> alpha + Si29:       1   Q =   1.529 MeV
neutron + S32 --> neutron + S32:      31   Q = 0.052178 eV
neutron + S33 --> neutron + S33:       1   Q = 0.043664 eV
neutron + Zn64 --> neutron + Zn64:       1   Q = 0.058431 eV
neutron + Zn66 --> neutron + Zn66:       1   Q = 0.076819 eV

number of gamma or e- (ic): N = 1 --> 6

List of generated particles:
C12:   38204  Emean = 0.17762 eV   ( 0.00012733 eV  --> 0.74069 eV )
C13:     398  Emean =  16.709 eV      ( 0.0016007 eV  --> 1.3456 keV)
C14:     218  Emean =  42.009 keV    ( 41.866 keV --> 42.198 keV)
C15:       2  Emean = 0.063881 eV     ( 0.013792 eV  --> 0.11397 eV )
Ca40:      4  Emean = 0.053798 eV   ( 0.0070359 eV  --> 0.085434 eV )
Cl35:    235  Emean = 0.087531 eV  ( 0.0013097 eV  --> 0.30909 eV )
Cl36:     89  Emean =  854.05 eV      ( 4.101 eV  --> 5.0557 keV)
Cl37:      6  Emean = 0.11469 eV     ( 0.057262 eV  --> 0.24671 eV )
Fe56:      2  Emean =  0.1152 eV      ( 0.088112 eV  --> 0.1423 eV )
Fe57:      1  Emean =   912.5 eV       ( 912.5 eV  --> 912.5 eV )
K39:      31  Emean = 0.094019 eV   ( 0.0093714 eV  --> 0.22999 eV )
K40:       8  Emean =  145.64 eV       ( 2.1723 eV  --> 821.59 eV )
K41:       6  Emean = 0.083055 eV    ( 0.029198 eV  --> 0.15007 eV )
K42:       2  Emean =  359.02 eV       ( 2.2216 eV  --> 715.83 eV )
Mg24:      5  Emean = 0.073682 eV  ( 0.0096115 eV  --> 0.15654 eV )
N14:    7262  Emean = 0.16046 eV   ( 0.00016007 eV  --> 0.71439 eV )
N15:      15  Emean =  1.8713 keV     ( 0.070335 eV  --> 5.2993 keV)
Na23:     76  Emean = 0.11061 eV   ( 0.0059808 eV  --> 0.35958 eV )
Na24:      1  Emean =  807.13 eV      ( 807.13 eV  --> 807.13 eV )
O16:   63722  Emean = 0.14615 eV   ( 0.00015825 eV  --> 0.87866 eV )
O17:      27  Emean =  0.1309 eV      ( 0.014925 eV  --> 0.36564 eV )
O18:     115  Emean = 0.12601 eV    ( 0.008924 eV  --> 0.42151 eV )
P31:      86  Emean =  0.1051 eV      ( 0.0055334 eV  --> 0.39986 eV )
S32:      31  Emean = 0.10315 eV     ( 0.0026521 eV  --> 0.32888 eV )
S33:       4  Emean =  912.44 eV      ( 0.146 eV  --> 1.2259 keV)
S35:       2  Emean =  17.201 keV     ( 17.18 keV --> 17.222 keV)
Si29:      1  Emean =  185.54 keV     ( 185.54 keV --> 185.54 keV)
Zn64:      1  Emean = 0.077271 eV   ( 0.077271 eV  --> 0.077271 eV )
Zn66:      1  Emean = 0.14905 eV     ( 0.14905 eV  --> 0.14905 eV )
alpha:     3  Emean =  447.81 keV    ( 0.003728 eV  --> 1.3434 MeV)
```

```
deuteron:    2427  Emean =  1.3102 keV        ( 0.18357 eV  --> 1.3895 keV)
gamma:    2729  Emean =  2.3943 MeV        ( 2.0203 keV --> 10.833 MeV)
proton:  887238  Emean =  145.44 eV          ( 5.2864e-05 eV  --> 598.05 keV)
```

10 eV neutrons

The run is 1000000 neutron of 10 eV through 12 cm of SoftTissue (density: 1 g/cm3)

Process calls frequency:

hadElastic= 999127 nCapture= 800 neutronInelastic= 73

List of nuclear reactions:

neutron + C12 --> N gamma or e- + C13: 2 Q = 5.5786 MeV
neutron + C12 --> neutron + C12: 38224 Q = 0.038375 eV
neutron + C13 --> neutron + C13: 442 Q = -0.080087 eV
neutron + Ca40 --> neutron + Ca40: 12 Q = 0.043735 eV
neutron + Cl35 --> N gamma or e- + Cl36: 24 Q = 8.0764 MeV
neutron + Cl35 --> neutron + Cl35: 250 Q = 0.034184 eV
neutron + Cl37 --> N gamma or e- + Cl38: 1 Q = 11.046 MeV
neutron + Cl37 --> neutron + Cl37: 4 Q = 0.024212 eV
neutron + Fe56 --> neutron + Fe56: 4 Q = 0.01537 eV
neutron + H1 --> N gamma or e- + deuteron: 765 Q = 2.2257 MeV
neutron + H1 --> neutron + proton: 888697 Q = 0.04071 eV
neutron + H2 --> neutron + deuteron: 21 Q = 0.028886 eV
neutron + K39 --> N gamma or e- + K40: 2 Q = 7.8 MeV
neutron + K39 --> neutron + K39: 47 Q = 0.032249 eV
neutron + K41 --> neutron + K41: 2 Q = 0.02265 eV
neutron + Mg24 --> neutron + Mg24: 7 Q = 0.048291 eV
neutron + N14 --> N gamma or e- + N15: 5 Q = 15.538 MeV
neutron + N14 --> neutron + N14: 7419 Q = 0.038567 eV
neutron + N14 --> proton + C14: 72 Q = 626.34 keV
neutron + N15 --> neutron + N15: 10 Q = 0.045113 eV
neutron + Na23 --> neutron + Na23: 55 Q = 0.040827 eV
neutron + O16 --> neutron + O16: 63661 Q = 0.038278 eV
neutron + O17 --> neutron + O17: 27 Q = 0.036431 eV
neutron + O18 --> N gamma or e- + O19: 1 Q = 3.9557 MeV
neutron + O18 --> neutron + O18: 145 Q = -0.021504 eV
neutron + P31 --> neutron + P31: 70 Q = 0.034405 eV
neutron + S32 --> neutron + S32: 27 Q = 0.030641 eV
neutron + S33 --> alpha + Si30: 1 Q = 3.4965 MeV
neutron + S33 --> neutron + S33: 1 Q = 0.032144 eV
neutron + S34 --> neutron + S34: 2 Q = 0.025148 eV

number of gamma or e- (ic): N = 1 --> 6

List of generated particles:

```
C12:   38224  Emean =  1.4646 eV    ( 0.00023101 eV  --> 3.9717 eV )
C13:     444  Emean =  5.5397 eV    ( 0.0034361 eV  --> 1.0494 keV)
C14:      72  Emean =  42.007 keV   ( 41.683 keV --> 42.369 keV)
Ca40:     12  Emean = 0.34882 eV    ( 0.053726 eV  --> 1.0494 eV )
Cl35:    250  Emean = 0.59621 eV    ( 0.0056789 eV  --> 1.598 eV )
Cl36:     24  Emean =  701.58 eV    ( 53.145 eV  --> 3.1911 keV)
Cl37:      4  Emean = 0.73731 eV    ( 0.61507 eV  --> 1.018 eV )
Cl38:      1  Emean =  817.58 eV    ( 817.58 eV  --> 817.58 eV )
Fe56:      4  Emean = 0.50667 eV    ( 0.34933 eV  --> 0.69591 eV )
K39:      47  Emean = 0.51556 eV    ( 0.019769 eV  --> 1.0679 eV )
K40:       2  Emean =  417.11 eV    ( 3.5429 eV  --> 830.68 eV )
K41:       2  Emean = 0.31797 eV    ( 0.25253 eV  --> 0.38341 eV )
Mg24:      7  Emean = 0.87469 eV    ( 0.33464 eV  --> 1.5869 eV )
N14:    7419  Emean =  1.2851 eV    ( 0.0039418 eV  --> 3.6064 eV )
N15:      15  Emean =  1.1556 keV   ( 0.40869 eV  --> 8.5342 keV)
Na23:     55  Emean = 0.85189 eV    ( 0.046577 eV  --> 2.0184 eV )
O16:   63661  Emean =  1.1519 eV    ( 0.00056207 eV  --> 3.4376 eV )
O17:      27  Emean =   1.128 eV    ( 0.036767 eV  --> 2.5337 eV )
O18:     145  Emean =  1.0009 eV    ( 0.0023247 eV  --> 2.2099 eV )
O19:       1  Emean =  432.48 eV    ( 432.48 eV  --> 432.48 eV )
P31:      70  Emean =  0.6798 eV    ( 0.022334 eV  --> 1.6333 eV )
S32:      27  Emean = 0.78917 eV    ( 0.049069 eV  --> 1.4114 eV )
S33:       1  Emean =   0.248 eV    ( 0.248 eV  --> 0.248 eV )
S34:       2  Emean = 0.15197 eV    ( 0.088399 eV  --> 0.21554 eV )
Si30:      1  Emean =  411.38 keV   ( 411.38 keV --> 411.38 keV)
alpha:     1  Emean =  3.0851 MeV   ( 3.0851 MeV --> 3.0851 MeV)
deuteron:    786  Emean =   1.288 keV      ( 0.11594 eV  --> 1.4917 keV)
gamma:     843  Emean =  2.3901 MeV      ( 517.08 keV --> 10.833 MeV)
proton:  888769  Emean =  52.357 eV      ( 0.00056662 eV  --> 584.66 keV)
```

100 eV neutrons

The run is 1000000 neutron of 100 eV through 12 cm of SoftTissue (density: 1 g/cm3)

Process calls frequency:

hadElastic= 999745 nCapture= 238 neutronInelastic= 17

List of nuclear reactions:

neutron + C12 --> neutron + C12: 37997 Q = 0.043034 eV
neutron + C13 --> neutron + C13: 409 Q = -1.0811 eV
neutron + Ca40 --> neutron + Ca40: 10 Q = 0.050155 eV
neutron + Cl35 --> N gamma or e- + Cl36: 1 Q = 7.4475 MeV
neutron + Cl35 --> neutron + Cl35: 113 Q = 0.037994 eV
neutron + Cl37 --> neutron + Cl37: 3 Q = 0.031427 eV
neutron + Fe56 --> neutron + Fe56: 6 Q = 0.03162 eV
neutron + H1 --> N gamma or e- + deuteron: 237 Q = 2.2257 MeV
neutron + H1 --> neutron + proton: 889505 Q = 0.065199 eV
neutron + H2 --> neutron + deuteron: 18 Q = 0.040971 eV
neutron + K39 --> neutron + K39: 33 Q = 0.050845 eV
neutron + Mg24 --> neutron + Mg24: 4 Q = 0.028266 eV
neutron + Mg26 --> neutron + Mg26: 1 Q = 0.0036431 eV
neutron + N14 --> neutron + N14: 7277 Q = 0.041089 eV
neutron + N14 --> proton + C14: 17 Q = 626.34 keV
neutron + N15 --> neutron + N15: 13 Q = 0.058962 eV
neutron + Na23 --> neutron + Na23: 58 Q = 0.041567 eV
neutron + O16 --> neutron + O16: 64051 Q = 0.041089 eV
neutron + O17 --> neutron + O17: 22 Q = 0.048439 eV
neutron + O18 --> neutron + O18: 118 Q = -0.5606 eV
neutron + P31 --> neutron + P31: 76 Q = 0.038809 eV
neutron + S32 --> neutron + S32: 29 Q = 0.035687 eV
neutron + S33 --> neutron + S33: 1 Q = 0.014565 eV
neutron + S34 --> neutron + S34: 1 Q = 0.014437 eV

number of gamma or e- (ic): N = 1 --> 6

List of generated particles:
C12: 37997 Emean = 14.385 eV (0.0018917 eV --> 31.771 eV)

```
C13:     409  Emean =  13.461 eV      ( 0.092532 eV  --> 28.038 eV )
C14:      17  Emean =  41.723 keV     ( 41.124 keV --> 43.009 keV)
Ca40:     10  Emean =  6.7004 eV      ( 0.22378 eV  --> 10.474 eV )
Cl35:    113  Emean =  5.3551 eV      ( 0.096436 eV  --> 11.235 eV )
Cl36:      1  Emean =  457.46 eV      ( 457.46 eV  --> 457.46 eV )
Cl37:      3  Emean =  6.1571 eV      ( 4.6047 eV  --> 7.2157 eV )
Fe56:      6  Emean =  3.1214 eV      ( 2.0002 eV  --> 4.5312 eV )
K39:      33  Emean =   4.185 eV      ( 0.28496 eV  --> 9.2118 eV )
Mg24:      4  Emean =  9.4783 eV      ( 2.4629 eV  --> 14.077 eV )
Mg26:      1  Emean =  3.8838 eV      ( 3.8838 eV  --> 3.8838 eV )
N14:    7277  Emean =   12.61 eV      ( 0.0018208 eV  --> 27.569 eV )
N15:      13  Emean =  15.722 eV      ( 4.6934 eV  --> 24.449 eV )
Na23:     58  Emean =  8.1343 eV      ( 0.21915 eV  --> 15.382 eV )
O16:   64051  Emean =  11.212 eV      ( 0.00050932 eV  --> 25.57 eV )
O17:      22  Emean =  9.7842 eV      ( 0.10662 eV  --> 19.175 eV )
O18:     118  Emean =  10.205 eV      ( 0.044773 eV  --> 20.165 eV )
P31:      76  Emean =  5.7172 eV      ( 0.11244 eV  --> 12.247 eV )
S32:      29  Emean =  5.6363 eV      ( 0.42286 eV  --> 12.164 eV )
S33:       1  Emean = 0.15914 eV      ( 0.15914 eV  --> 0.15914 eV )
S34:       1  Emean = 0.053871 eV     ( 0.053871 eV  --> 0.053871 eV )
deuteron:     255  Emean =  1.2922 keV        ( 8.8228 eV  --> 1.8836 keV)
gamma:     239  Emean =  2.2369 MeV         ( 2.2243 MeV --> 3.8255 MeV)
proton:  889522  Emean =  61.263 eV          ( 0.0002201 eV  --> 585.31 keV)
```

1 keV neutrons

The run is 1000000 neutron of 1 keV through 12 cm of SoftTissue (density: 1 g/cm3)

Process calls frequency:
hadElastic= 999928 nCapture= 68 neutronInelastic= 4

MeanFreePath: 7.0269 mm +- 7.0127 mm massic: 702.69 mg/cm2
CrossSection: 1.4231 cm^-1 massic: 1.4231 cm2/g

Verification: crossSections from G4HadronicProcessStore:
hadElastic= 1.4242 cm2/g
nCapture= 10.564 um2/mg
neutronInelastic= 1.0215 um2/mg
total= 1.4243 cm2/g

List of nuclear reactions:

neutron + C12 --> N gamma or e- + C13: 1 Q = 4.9469 MeV
neutron + C12 --> neutron + C12: 38297 Q = 0.09 eV
neutron + C13 --> neutron + C13: 442 Q = -10.843 eV
neutron + Ca40 --> neutron + Ca40: 5 Q = 0.057286 eV
neutron + Cl35 --> neutron + Cl35: 34 Q = 0.056579 eV
neutron + Cl37 --> neutron + Cl37: 2 Q = 0.045422 eV
neutron + Fe56 --> neutron + Fe56: 3 Q = 0.045175 eV
neutron + H1 --> N gamma or e- + deuteron: 67 Q = 2.2252 MeV
neutron + H1 --> neutron + proton: 888924 Q = 0.3101 eV
neutron + H2 --> neutron + deuteron: 25 Q = 0.15491 eV
neutron + K39 --> neutron + K39: 22 Q = 0.052374 eV
neutron + K41 --> neutron + K41: 1 Q = 0.03 eV
neutron + Mg24 --> neutron + Mg24: 7 Q = 0.080257 eV
neutron + Mg26 --> neutron + Mg26: 1 Q = 0.099959 eV
neutron + N14 --> neutron + N14: 7226 Q = 0.072061 eV
neutron + N14 --> proton + C14: 4 Q = 626.34 keV
neutron + N15 --> neutron + N15: 11 Q = 0.056484 eV
neutron + Na23 --> neutron + Na23: 78 Q = 0.061952 eV
neutron + O16 --> neutron + O16: 64574 Q = 0.068665 eV

```
neutron + O17 --> neutron + O17:      29   Q = 0.065514 eV
neutron + O18 --> neutron + O18:     135   Q = -5.9505 eV
neutron + P31 --> neutron + P31:      76   Q = 0.049831 eV
neutron + S32 --> neutron + S32:      31   Q = 0.050756 eV
neutron + S34 --> neutron + S34:       5   Q = 0.038544 eV

number of gamma or e- (ic): N = 0 --> 0

List of generated particles:
C12:   38297  Emean =   143.3 eV     ( 0.0085311 eV  --> 295.75 eV )
C13:     443  Emean =  133.88 eV     ( 0.13658 eV  --> 1.5363 keV)
C14:       4  Emean =  43.307 keV    ( 39.606 keV --> 45.372 keV)
Ca40:      5  Emean =  55.382 eV     ( 12.988 eV  --> 78.225 eV )
Cl35:     34  Emean =  47.193 eV     ( 1.2466 eV  --> 106.6 eV )
Cl37:      2  Emean =  82.662 eV     ( 67.684 eV  --> 97.64 eV )
Fe56:      3  Emean =  41.866 eV     ( 19.248 eV  --> 63.416 eV )
K39:      22  Emean =  51.684 eV     ( 6.0786 eV  --> 95.504 eV )
K41:       1  Emean =  63.286 eV     ( 63.286 eV  --> 63.286 eV )
Mg24:      7  Emean =  106.75 eV     ( 43.764 eV  --> 152.36 eV )
Mg26:      1  Emean =  34.581 eV     ( 34.581 eV  --> 34.581 eV )
N14:    7226  Emean =  124.95 eV     ( 0.027825 eV  --> 256.95 eV )
N15:     11  Emean =  131.94 eV      ( 46.076 eV  --> 210.41 eV )
Na23:    78  Emean =  80.484 eV      ( 0.52324 eV  --> 158.85 eV )
O16:   64574  Emean =  111.79 eV     ( 0.018101 eV  --> 230.64 eV )
O17:     29  Emean =  103.86 eV      ( 7.8277 eV  --> 206.09 eV )
O18:    135  Emean =  102.16 eV      ( 2.5392 eV  --> 201.11 eV )
P31:     76  Emean =  58.694 eV      ( 1.9232 eV  --> 120.67 eV )
S32:     31  Emean =  62.431 eV      ( 0.49197 eV  --> 117.4 eV )
S34:      5  Emean =  53.321 eV      ( 7.4903 eV  --> 107.14 eV )
deuteron:     92  Emean =  1.4529 keV        ( 7.1324 eV  --> 3.4315 keV)
gamma:        68  Emean =  2.2644 MeV        ( 2.2244 MeV --> 4.9463 MeV)
proton:  888928  Emean =  502.79 eV          ( 0.0021734 eV  --> 587.73 keV)
```

10 keV neutrons

The run is 1000000 neutron of 10 keV through 12 cm of SoftTissue (density: 1 g/cm3)

Process calls frequency:
hadElastic= 999973 nCapture= 26 neutronInelastic= 1

MeanFreePath: 7.3255 mm +- 7.3105 mm massic: 732.55 mg/cm2
CrossSection: 1.3651 cm^-1 massic: 1.3651 cm2/g

Verification: crossSections from G4HadronicProcessStore:
hadElastic= 1.3656 cm2/g
nCapture= 3.2238 um2/mg
neutronInelastic= 0.32408 um2/mg
total= 1.3657 cm2/g

List of nuclear reactions:

neutron + C12 --> neutron + C12: 40043 Q = 0.55886 eV
neutron + C13 --> neutron + C13: 412 Q = -109.13 eV
neutron + Ca40 --> neutron + Ca40: 8 Q = 0.14874 eV
neutron + Cl35 --> neutron + Cl35: 17 Q = 0.18045 eV
neutron + Cl37 --> neutron + Cl37: 4 Q = 0.21111 eV
neutron + Fe56 --> neutron + Fe56: 3 Q = 0.11672 eV
neutron + Fe57 --> neutron + Fe57: 1 Q = 0.18416 eV
neutron + H1 --> N gamma or e- + deuteron: 26 Q = 2.2197 MeV
neutron + H1 --> neutron + proton: 885257 Q = 2.762 eV
neutron + H2 --> neutron + deuteron: 23 Q = 1.2804 eV
neutron + K39 --> neutron + K39: 54 Q = 0.16936 eV
neutron + K41 --> neutron + K41: 1 Q = 0.1637 eV
neutron + Mg24 --> neutron + Mg24: 6 Q = 0.25274 eV
neutron + Mg26 --> neutron + Mg26: 1 Q = 0.32167 eV
neutron + N14 --> neutron + N14: 6395 Q = 0.37747 eV
neutron + N14 --> proton + C14: 1 Q = 626.34 keV
neutron + N15 --> neutron + N15: 18 Q = 0.27779 eV
neutron + Na23 --> neutron + Na23: 110 Q = 0.24009 eV
neutron + O16 --> neutron + O16: 67325 Q = 0.34593 eV
neutron + O17 --> neutron + O17: 23 Q = 0.29672 eV
neutron + O18 --> neutron + O18: 156 Q = -57.134 eV

```
neutron + P31 --> neutron + P31:      91   Q = 0.17168 eV
neutron + S32 --> neutron + S32:      23   Q = 0.20233 eV
neutron + S33 --> neutron + S33:       1   Q = 0.078685 eV
neutron + S34 --> neutron + S34:       1   Q = 0.25084 eV

number of gamma or e- (ic): N = 0 --> 0

List of generated particles:
C12:   40043  Emean =  1.4251 keV  ( 0.19302 eV  --> 2.8872 keV)
C13:     412  Emean =  1.3115 keV  ( 0.96121 eV  --> 2.6535 keV)
C14:       1  Emean =  52.496 keV  ( 52.496 keV --> 52.496 keV)
Ca40:      8  Emean =   435.8 eV   ( 37.768 eV  --> 888.1 eV )
Cl35:     17  Emean =  537.73 eV   ( 25.127 eV  --> 1.0413 keV)
Cl37:      4  Emean =  586.07 eV   ( 154.74 eV  --> 938.85 eV )
Fe56:      3  Emean =  344.77 eV   ( 1.3455 eV  --> 561.49 eV )
Fe57:      1  Emean =   638.9 eV   ( 638.9 eV  --> 638.9 eV )
K39:      54  Emean =  477.55 eV   ( 3.0928 eV  --> 974.65 eV )
K41:       1  Emean =  376.93 eV   ( 376.93 eV  --> 376.93 eV )
Mg24:      6  Emean =  740.67 eV   ( 135.38 eV  --> 1.3398 keV)
Mg26:      1  Emean =  1.1855 keV  ( 1.1855 keV --> 1.1855 keV)
N14:    6395  Emean =  1.2404 keV  ( 0.31368 eV  --> 2.5296 keV)
N15:      18  Emean =  1.0024 keV  ( 163.25 eV  --> 2.1237 keV)
Na23:    110  Emean =  798.93 eV   ( 14.357 eV  --> 1.5977 keV)
O16:   67325  Emean =  1.1229 keV  ( 0.057205 eV  --> 2.2571 keV)
O17:      23  Emean =  1.0214 keV  ( 57.224 eV  --> 2.0954 keV)
O18:     156  Emean =  976.15 eV   ( 6.9459 eV  --> 1.9956 keV)
P31:      91  Emean =  496.94 eV   ( 32.2 eV  --> 1.2249 keV)
S32:      23  Emean =  619.22 eV   ( 25.963 eV  --> 1.1787 keV)
S33:       1  Emean =   150.1 eV   ( 150.1 eV  --> 150.1 eV )
S34:       1  Emean =   729.2 eV   ( 729.2 eV  --> 729.2 eV )
deuteron:     49  Emean =  4.9661 keV      ( 69.561 eV  --> 10.822 keV)
gamma:        26  Emean =  2.2244 MeV      ( 2.2243 MeV --> 2.2244 MeV)
proton:  885258  Emean =  5.0056 keV      ( 0.011984 eV  --> 583.84 keV)
```

100 keV neutrons

The run is 100000 neutron of 100 keV through 12 cm of SoftTissue (density: 1 g/cm3)

Process calls frequency:
Transportation= 1 hadElastic= 99999

Nb of incident particles surviving after 12 cm of SoftTissue : 1

MeanFreePath: 1.0513 cm +- 1.0479 cm massic: 1.0513 g/cm2
CrossSection: 0.95122 cm^-1 massic: 95.122 mm2/g

Verification: crossSections from G4HadronicProcessStore:
Transportation= 0 um2/mg
hadElastic= 94.672 mm2/g
total= 94.672 mm2/g

List of nuclear reactions:

neutron + C12 --> neutron + C12: 5413 Q = 5.1296 eV
neutron + C13 --> neutron + C13: 54 Q = -1.0988 keV
neutron + Cl35 --> neutron + Cl35: 4 Q = 1.2788 eV
neutron + Cl37 --> neutron + Cl37: 1 Q = 0.21319 eV
neutron + H1 --> neutron + proton: 84524 Q = 27.244 eV
neutron + H2 --> neutron + deuteron: 4 Q = 14.928 eV
neutron + K39 --> neutron + K39: 1 Q = 2.6694 eV
neutron + Mg24 --> neutron + Mg24: 1 Q = 4.1149 eV
neutron + N14 --> neutron + N14: 510 Q = 3.2287 eV
neutron + N15 --> neutron + N15: 5 Q = 3.6828 eV
neutron + Na23 --> neutron + Na23: 11 Q = 2.4027 eV
neutron + O16 --> neutron + O16: 9379 Q = 3.2216 eV
neutron + O17 --> neutron + O17: 4 Q = 2.6311 eV
neutron + O18 --> neutron + O18: 12 Q = -618.1 eV
neutron + P31 --> neutron + P31: 7 Q = 1.4115 eV
neutron + S32 --> neutron + S32: 66 Q = 1.677 eV
neutron + S34 --> neutron + S34: 2 Q = 1.9837 eV
neutron + Zn66 --> neutron + Zn66: 1 Q = 0.9238 eV

List of generated particles:

C12:	5413	Emean = 13.931 keV	(2.1127 eV --> 28.675 keV)
C13:	54	Emean = 13.2 keV	(100.26 eV --> 25.668 keV)
Cl35:	4	Emean = 4.6847 keV	(1.1719 keV --> 9.3592 keV)
Cl37:	1	Emean = 593.79 eV	(593.79 eV --> 593.79 eV)
K39:	1	Emean = 9.54 keV	(9.54 keV --> 9.54 keV)
Mg24:	1	Emean = 14.851 keV	(14.851 keV --> 14.851 keV)
N14:	510	Emean = 11.644 keV	(33.185 eV --> 25.056 keV)
N15:	5	Emean = 15.191 keV	(5.8248 keV --> 20.693 keV)
Na23:	11	Emean = 9.4413 keV	(2.6552 keV --> 15.982 keV)
O16:	9379	Emean = 11.612 keV	(0.44295 eV --> 22.37 keV)
O17:	4	Emean = 10.064 keV	(5.0643 keV --> 20.369 keV)
O18:	12	Emean = 10.554 keV	(341.94 eV --> 18.852 keV)
P31:	7	Emean = 4.9827 keV	(1.5378 keV --> 8.0674 keV)
S32:	66	Emean = 6.0657 keV	(50.3 eV --> 11.459 keV)
S34:	2	Emean = 7.5005 keV	(5.0288 keV --> 9.9721 keV)
Zn66:	1	Emean = 3.4753 keV	(3.4753 keV --> 3.4753 keV)
deuteron:	4	Emean = 54.586 keV	(32.455 keV --> 82.676 keV)
proton:	84524	Emean = 49.987 keV	(0.58323 eV --> 100.05 keV)

1 MeV neutrons

The run is 1000000 neutron of 1 MeV through 12 cm of SoftTissue (density: 1 g/cm3)

Process calls frequency:

Transportation= 2542 hadElastic= 997324 nCapture= 14 neutronInelastic= 120

Nb of incident particles surviving after 12 cm of SoftTissue : 2542

List of nuclear reactions:

neutron + C12 --> neutron + C12: 60372 Q = 49.041 eV

neutron + C13 --> neutron + C13: 648 Q = -10.628 keV

neutron + Ca40 --> neutron + Ca40: 9 Q = 7.477 eV

neutron + Cl35 --> neutron + Cl35: 126 Q = 9.386 eV

neutron + Cl35 --> proton + S35: 1 Q = 615.19 keV

neutron + Cl37 --> neutron + Cl37: 20 Q = 4.9897 eV

neutron + Fe56 --> N gamma or e- + neutron + Fe56: 2 Q = -460.33 eV

neutron + Fe56 --> neutron + Fe56: 3 Q = 7.5371 eV

neutron + H1 --> N gamma or e- + deuteron: 7 Q = 1.7413 MeV

neutron + H1 --> neutron + proton: 537614 Q = 272.72 eV

neutron + H2 --> neutron + deuteron: 45 Q = 133.2 eV

neutron + K39 --> neutron + K39: 157 Q = 10.183 eV

neutron + K41 --> neutron + K41: 13 Q = 9.9547 eV

neutron + Mg24 --> neutron + Mg24: 8 Q = 17.577 eV

neutron + Mg25 --> neutron + Mg25: 2 Q = 7.1642 eV

neutron + Mg26 --> neutron + Mg26: 4 Q = 9.011 eV

neutron + N14 --> alpha + B11: 13 Q = -157.21 keV

neutron + N14 --> neutron + N14: 4988 Q = 33.155 eV

neutron + N14 --> proton + C14: 62 Q = 626.33 keV

neutron + N15 --> neutron + N15: 17 Q = 32.797 eV

neutron + Na23 --> N gamma or e- + neutron + Na23: 22 Q = -191.7 eV

neutron + Na23 --> neutron + Na23: 141 Q = 12.73 eV

neutron + O16 --> N gamma or e- + O17: 7 Q = 3.9153 MeV

neutron + O16 --> neutron + O16: 392704 Q = 30.374 eV

neutron + O17 --> N gamma or e- + neutron + O17: 1 Q = -16.957 eV

neutron + O17 --> alpha + C14: 2 Q = 1.8187 MeV

neutron + O17 --> neutron + O17: 22 Q = 31.497 eV

neutron + O18 --> N gamma or e- + alpha + C15: 15 Q = -944.72 keV

neutron + O18 --> N gamma or e- + neutron + O18: 1 Q = 548.03 eV

neutron + O18 --> neutron + O18: 149 Q = -5.7081 keV

neutron + P31 --> neutron + P31: 150 Q = 11.999 eV

neutron + S32 --> alpha + Si29: 1 Q = 1.5289 MeV

neutron + S32 --> neutron + S32: 120 Q = 11.23 eV

neutron + S33 --> neutron + S33: 1 Q = 4.8423 eV

neutron + S34 --> neutron + S34: 8 Q = 16.951 eV

neutron + Zn66 --> neutron + Zn66: 1 Q = 5.5237 eV

neutron + Zn68 --> neutron + Zn68: 2 Q = 1.0837 eV

number of gamma or e- (ic): N > 0

List of generated particles:

B11:	13	Emean = 250.37 keV	(56.246 keV --> 430.5 keV)
C12:	60372	Emean = 134.1 keV	(12.242 eV --> 286.42 keV)
C13:	648	Emean = 127.68 keV	(523.27 eV --> 264.09 keV)
C14:	64	Emean = 191.8 keV	(13.967 keV --> 966.15 keV)
C15:	15	Emean = 41.926 keV	(41.84 keV --> 42.01 keV)
Ca40:	9	Emean = 27.123 keV	(1.4678 keV --> 72.915 keV)
Cl35:	126	Emean = 35.098 keV	(519.93 eV --> 107.41 keV)
Cl37:	20	Emean = 19.782 keV	(1.1425 keV --> 102.52 keV)
Fe56:	5	Emean = 25.014 keV	(6.5589 keV --> 52.996 keV)
K39:	157	Emean = 36.867 keV	(869.68 eV --> 97.796 keV)
K41:	13	Emean = 38.454 keV	(3.5463 keV --> 87.946 keV)
Mg24:	8	Emean = 63.956 keV	(471.42 eV --> 145.63 keV)
Mg25:	2	Emean = 27.084 keV	(490.59 eV --> 53.678 keV)
Mg26:	4	Emean = 35.294 keV	(60.794 eV --> 59.08 keV)
N14:	4988	Emean = 120.84 keV	(13.503 eV --> 250.87 keV)
N15:	17	Emean = 137 keV	(26.158 keV --> 231.76 keV)
Na23:	163	Emean = 52.345 keV	(685.43 eV --> 158.3 keV)
O16:	392704	Emean = 110.63 keV	(0.32797 eV --> 223.61 keV)
O17:	30	Emean = 104.49 keV	(15.839 keV --> 205.19 keV)
O18:	150	Emean = 97.267 keV	(2.1839 keV --> 199.43 keV)
P31:	150	Emean = 43.378 keV	(196.64 eV --> 122.11 keV)
S32:	120	Emean = 41.381 keV	(1.0273 keV --> 116.46 keV)
S33:	1	Emean = 18.937 keV	(18.937 keV --> 18.937 keV)
S34:	8	Emean = 64.574 keV	(10.622 keV --> 111.22 keV)
S35:	1	Emean = 80.526 keV	(80.526 keV --> 80.526 keV)

```
   Si29:      1  Emean =  481.54 keV      ( 481.54 keV --> 481.54 keV)
   Zn66:      1  Emean =  21.984 keV     ( 21.984 keV --> 21.984 keV)
   Zn68:      2  Emean =  4.4648 keV     ( 2.7653 keV --> 6.1644 keV)
  alpha:     31  Emean =  443.52 keV     ( 11.158 keV --> 2.0474 MeV)
deuteron:    52  Emean =   492.7 keV    ( 5.8872 keV --> 883.92 keV)
  gamma:     92  Emean =   681.8 keV   ( 1.2149 keV --> 4.1431 MeV)
 neutron:    26  Emean =   436.4 keV     ( 59.968 keV --> 553.55 keV)
  proton:  537677  Emean =  501.46 keV( 0.26039 eV  --> 1.6124 MeV)
```

The above provided simulation results can be useful for the future development of:

- Monitoring system for a BNCT
  - Monitoring based on 478keV prompt gammas of the capture…
    - "Here should be a scheme of the head phantom surrounded with high precision gamma detectors, which will detect gammas (478 keV) as result of boron neutron capturing reaction with 478 keV gamma emission …"
    - “Scheme of the reaction and energy, angular distributions”
      - (3 - 4 figures/images)
  - e plus e minus annihilation
    - “Scheme of the reaction and energy, angular distributions”
  - All prompt gammas from H, N
    - “Scheme of the reactions and energy, angular distributions”

Bibliography

S. Abramovich et al., "Nuclear physics constants for thermonuclear fusion", IAEA 1991M. Adrian et al., "Shield Modeling of Boron Neutron Capture Therapy Facility with Kartini Reactor's Thermal Column as Neutron Source using Monte Carlo N Particle Extended Simulator", Indonesian Journal of Physics and Nuclear Applications 1(2016) 44

S. Agostinelli et al., GEANT4 - A Simulation Toolkit, Nucl. Instrum. Meth. A 506(2003) 250.

D. Alberti et. al., "A theranostic approach based on the use of a dual boron/Gd agent to improve the efficacy of Boron Neutron Capture Therapy in the lung cancer treatment", Nanomedicine: Nanotechnology. Biology, and Medicine 11 (2015) 741.

S. Altieri and N. Protti, "A brief review on reactor-based neutron sources for boron neutron capture therapy" , Ther. Radiol. Oncol. 2 (2018) 47.

J. Allison et al., GEANT4 Developments and Applications, IEEE Trans. Nucl. Sc., 53(2006) 270.

J. Allison et al., Recent Developments in GEANT4, Nucl. Instrum. Meth. A 835 (2016) 186-225.

R. Avagyan, R. Avetisyan, V. Ivanyan*, I, Kerobyan: "Calculations of Neutron Yield and Gamma Rays Intensity by GEANT4 ", Armenian Journal of Physics, 9 (2016) 315.

R. Avagyan, R. Avetisyan, V. Ivanyan, I, Kerobyan: "GEANT4 Simulations of a Beam Shaping Assembly Design and Optimization for Thermal/Epithermal Neutrons", Act. Phys. Pol. B, 48 (2017) 1693.

R. Barth et al., Boron neutron capture therapy for cancer, Cancer 70 (1992) 2995.

R. Barth et al.: "Current status of boron neutron capture therapy of high grade gliomas and recurrent head and neck cancer", Radiation Oncology 7 (2012) 146.

R. Barth et al., Cancer Commun. 38, (2018)

G. Battistoni et al., "The FLUKA code: description and benchmarking", AIP Conf. Proc. 896 (2007) 31.

E. Bavarnegin et al. "Neutron beams implemented at nuclear research reactors for BNCT", JINST 12 (2017) P05005.

A. Berlizov, "MCNP-CP: A Correlated Particle Radiation Source Extension of a General Purpose Monte Carlo N-Particle Transport Code", ACS Symposium Series, Vol. 945, Chapter 13pp 183-194, (2006)

T. Bohlen et al., "The FLUKA Code: Developments and Challenges for High Energy and Medical Applications", Nuclear Data Sheets 120 (2014) 211.

R. Brugger, "'Summing up': The physics of NCT", Advances in Neutron Capture Therapy, (SOLOWAY, A.H., BARTH, R.F., CARPENTER, D.E., Eds.), Plenum Press, New York (1993) 775.

J. Chadwick "Possible Existence of a Neutron", Nature volume 129, page 312 (1932).

I. Chatzis & M. Barbarino, "What is Fusion, and Why Is It So Difficult to Achieve?" IAEA bulletin 62 (2021) 2.

C. Cristache et al., "Determination of elemental content in geological samples", Rom. Journ. Phys., 53(2008)7.

N. Dzysiuk, I. Kadenko, A. J. Koning, R. Yermolenko „Cross sections for fast neutron interaction with Lu, Tb and Ta isotopes", Phys. Rev. C 81 (2010) 014610.

N. Dzysiuk et. al., "Cross-section measurement of the ^{159}Tb(n, γ)^{160}Tb nuclear reaction", Nucl. Phys. A 936 (2015) 66.

A. El-Taher et al., "Elemental analysis of limestone by instrumental neutron activation analysis" J Radioanal. Nucl. Chem. 299 (2014) 1949.

C. R. Gibson et al., "Pharmacokinetics of sodium borocaptate: a critical assessment of dosing paradigms for boron neutron capture therapy", Journal of Neuro-Oncology 62 (2003) 157.

T. Goorley, et al., "Initial MCNP6 Release Overview", Nuclear Technology, 180, pp 298-315 (Dec 2012).

M. Ginzberg et al., "On being the right (cell) size", Science , 348 (2015) 6236.

J. Fantidis and A. Antoniadis. "Optimization study for BNCT facility based on a DT neutron generator." Iranian Journal of Radiation Research 13 (2015) 13.

J. Fantidis et al: "Optimized BNCT facility based on a compact DD neutron generator". Int. J. Radiat. Res., 11 (2013) 207.

R. Farias et al.," Exploring Boron Neutron Capture Therapy for non-small cell lung cancer", Phys Med., 30 (2014) 888.

A. Fassò et al., "A comparison of FLUKA simulations with measurements of fluence and dose in calorimeter structures", Nucl. Instr. Meth. in Phys. Res. A332(1993) 59.

H. Fukuda et al.,"Boron neutron capture therapy (BNCT) for malignant melanoma with special reference to absorbed doses to the normal skin and tumor ", Australas Phys Eng Sci Med, 26 (2003) 97.

J. Holmes et al., "Tables of thermonuclear-reaction-rate data for neutron-induced reactions on heavy nuclei", Atomic Data and Nuclear Data Tables, 18 (1976) 305.

W. Huda, "Kerma-Area Product in Diagnostic Radiology", American Journal of Roentgenology, 203 (2014) 565.

M. Hsieh et al "A feasibility study of a deuterium-deuterium neutron generator-based boron neutron capture therapy system for treatment of brain tumors", Med Phys. 44 (2017) 637.

IAEA Reports No1, "Neutron generators for analytical purposes" 2012

IAEA-TECDOC-1153, "Use of accelerator based neutron sources", IAEA, VIENNA, 2000

IAEA-TECDOC-1223, "Current status of neutron capture therapy", IAEA, VIENNA, 2001

V. Ivanyan, "The possibility of an appropriate neutron beam achievement for medical purposes based on GEANT4 calculations", Eur. Phys. J. Plus, 135 (2020) 69.

IBA Brochure, https://www.researchgate.net/publication/338531143_C189_of_IBA

JANIS (Java-based Nuclear Data Information Software); The JEFF-3.1.1 Nuclear Data Library

B. Jones, "Clinical Radiobiology of Fast Neutron Therapy: What Was Learnt?", Front. Oncol. 10 (2020) 1537.

I. Kadenko, "Possible observation of the dineutron in the ^{159}Tb (n, 2n) ^{158g}Tb nuclear reaction", EPL 114 (2016) 42001.

I. M. Kadenko, "New direction in nuclear physics originated from the neutron activation technique application", Acta Phys. Polon. B 48 (2017) 1669.

K. Kanda et al., “Experiences of BNCT Using the KUR”, Advances in Neutron Capture Therapy. Edited by A.H Soloway et ai., Plenum Press, New York, pp. 683-687, 1993

D. Kaniowski et al, “High Boron-loaded DNA-Oligomers as Potential Boron Neutron Capture Therapy and Antisense Oligonucleotide Dual-Action Anticancer Agents” Molecules 2017, 22(9), 1393

N. Kardjilov et al, “Neutron imaging in materials science”, Materials Today, 14 (2011) 248.

Y. Kawabata and Y. Saito, “Current activities of neutron imaging facilities in KUR (Kyoto University research reactor)”, Physics Procedia 43 (2013) 42.

Y. Kasesaz et al, “Optimization of the beam shaping assembly in the D–D neutron generators-based BNCT using the response matrix method”, Appl. Radiat. Isot. 82(2013) 55.

Y. Kiyanagi et al. “Status of accelerator-based BNCT projects worldwide”, AIP Conf. Proc. 2160 (2019) 050012.

R. Kumar, “Evaluation of Prokaryotic and Eukaryotic Cell”, Asian Journal of Pharmaceutical Research, 11 (2021) 202

J. Kunikowska et al, “68Ga–Prostate-Specific Membrane Antigen-11 PET/CT A New Imaging Option for Recurrent Glioblastoma Multiforme?”, Clinical Nuclear Medicine, 45(1), (2020), 11-18.

G.L. Locher, “Biological effects and therapeutic possibilities of neutrons”, Am. J. Roentgenol. Radium. Ther. 36 (1936) 1.

T. Malouff et al., “Boron Neutron Capture Therapy: A Review of Clinical Applications”, Front. Oncol. 11 (2021) 601820.

S. Masoudi et al: “BNCT of skin tumors using the high-energy DT neutrons”, Appl. Radiat. Isot . 122 (2017) 158.

G. McIntyre & P. Holden, “Neutron scattering at the OPAL research reactor”, J. Phys.: Conf. Ser. 746 (2016) 012001.

N. Metropolis: “The beginning of the Monte-Carlo method”, Los Alamos Science Special Issue (1987)

H. Michiue et al., “The acceleration of boron neutron capture therapy using multi-linked mercaptoundecahydrododecaborate (BSH) fused cell-penetrating peptide”, Biomaterials 35 (2014) 3396.

T. Mitsumoto et al., “BNCT system using 30 MeV H^- cyclotron” , 01 Cyclotrons Applications (2010) 430.

S. Mortazavi et al., “Production of a datolite-based heavy concrete for shielding nuclear reactors and megavoltage radiotherapy rooms”, Iran. J. Radiat. Res. 8 (2010) 11.

M. Mu’alim. et al, “Modeling the radiation shielding of boron neutron capture therapy based on 2.4 MeV DD neutron generator facility”, Journal of Nuclear Reactor Technology 20 (1) (2018) 13

P. Moskal, “Nuclear physics in medicine, minefield and kitchen”, Annales Universitatis Mariae Curie-Skłodowska, sectio AAA - Physica V66 71-88 (2011)

H. Nakamaura et al., Boron Compounds: New Candidates for Boron Carriers in BNCT, in: W.A.G. Sauerwein et al. (Eds.), Neutron Capture Therapy: Principles and Applications, Heidelberg: Springer-Verlag, 2012.

K. Nedunchezhian, N. Aswath, M. Thiruppathy, S. Thirugnanamurthy, "Boron Neutron Capture Therapy-A Literature Review", J. Clin. Diagn. Res. 10 (2016) ZE01.

D. Novopashina et al. "Recent Advances in the Synthesis of High Boron-Loaded Nucleic Acids for BNCT", Front. Chem., 2021, Vol. 9, https://doi.org/10.3389/fchem.2021.619052

I.W. Osborne-Lee & C. W. Alexander, "CALIFORNIUM-252: A Remarkably Versatile Radioisotope", Oak Ridge National Laboratory, ORNL/TM-12706, 1995

E. Pozzi et al., "Boron neutron capture therapy (BNCT) for liver metastasis: therapeutic efficacy in an experimental model", Radiat. Environ. Biophys. 51 (2012) 331.

T. Pui Lou, "Compact D-D/D-T Neutron Generators and Their Applications", PhD Thesis, University of California, Berkley, 2014

PSI "What is Neutron Imaging ? | NIAG | Paul Scherrer Institute (PSI)" 2016 https://www.psi.ch/en/niag/what-is-neutron-imaging (linked to the image on February 2022)

F. Rasouli et al. " Design and optimization of a beam shaping assembly for BNCT based on D–T neutron generator and dose evaluation using a simulated head phantom", Appl. Radiat. Isot. 70 (2012) 2755. a)

Sh. Robinson et al., "Production of Cf-252 and other transplutonium isotopes at Oak Ridge National Laboratory", Radiochimica Acta 108 (2020) 737.

Sandia National Laboratory https://newatlas.com/sandia-neutristor-neutron-generator-chip/23856/

W. Sauerwein et al., "Neutron Capture Therapy", ISBN 978-3-642-31334-9, Springer 2012

W. A. G. Sauerwein et al., "Theranostics in Boron Neutron Capture Therapy", Life 11 (2021) 330.

S. Savolinen et al., "Boron neutron capture therapy (BNCT) in Finland: technological and physical prospects after 20 years of experiences", Phys. Med. 29 (2013) 233.

M. Szczepanek, "Application of 3D model of cancer cells in research on the effectiveness of BNCT in the treatment of melanoma", Acta Phys. Polon. B 51(2020) 413.

R. Schwarz et al., "Graphical user input interface for MCNP", American Nuclear Society (ANS) winter meeting; San Francisco, CA (United States); 14-18 Nov 1993; CONF-931160

P. Sibczyński, et al "Monte Carlo N-Particle simulations of an underwater chemical threats detection system using neutron activation analysis", JINST 14 (2019) P09001

M. Silarski "Hazardous Substance Detection in Water Environments using Neutron Beams: the SABAT Project", Problems of Mechatronics. Armament, Aviation, Safety Engineering 10 (2019) 49.

Z. Song et al., "The calibration of DD neutron indium activation diagnostic for Shenguang-III facility", arXiv:1405.2520 [physics.ins-det], e-print 2014

A. Susilowati et al., "Boron Neutron Capture Therapy (BNCT) using Compact Neutron generator", Ind. Jour. of Phys. and Nuc. Appl. 1 (2016) 73.

M. Suzuki et al., " First Attempt of Boron Neutron Capture Therapy (BNCT) for Hepatocellular Carcinoma", Japanese Journal of Clinical Oncology 37 (2007) 376.

S. Taskaev et al., “Neutron Source Based on Vacuum Insulated Tandem Accelerator and Lithium Target”, Biology 10 (2021) 350.

A. Taniguchi et al., “Design for an upgrade of the gas-jet type ISOL at KUR”, Nuclear Instruments and Methods in Physics Research Section B: Beam Interactions with Materials and Atoms 317 (2013) 476.

V. Trivillin et al., “Translational boron neutron capture therapy (BNCT) studies for the treatment of tumors in lung”, Int. J. Radiat. Biol. 95 (2019) 646.

Yu. Toporov, “Production of radionuclide preparations and ionizing sources of medical use”, IAEA-CN-114/33p, 2004

H. Vega-Carrillo & S. Martinez-Ovalle, “Neutron spectra and dosimetric features of Isotopic neutron sources: A review”, Leon, Gto. Mexico, pp. 698-727, 2015

F. J. Wheeler et al., “Physics design for the Brookhaven Medical Research Reactor epithermal neutron source”, Neutron Beam Design, Development, and Performance for Neutron Capture Therapy, (HARLING, O.K., BERNARD, J.A., AND ZAMENHOF, R.G., Ed.), Plenum Press, New York (1990) 83.

E. B. Wilson, “The Cell in Development and Heredity ”, (Macmillan, New York, ed. 3, 1925), p. xxxvii

T. Yuan et al., “Boron neutron capture therapy of cancer: Critical issues and future prospects”, Thorac. Cancer. 10 (2019) 2195.

L. Zaidi et al., "Beam shaping assembly design of ^{7}Li(p,n)^{7}Be neutron source for boron neutron capture therapy of deep-seated tumor”, Appl. Radiat. Isot. 139 (2018) 316.

R. Zamenhof et al,“Boron neutron capture therapy for the treatment of cerebral gliomas, I: Theoretical evaluation of the efficacy of various neutron beams”, Medical Physics 2 (1975) 47.

A. Zonta et al., “Extra-corporeal liver BNCT for the treatment of diffuse metastases: what was learned and what is still to be learned”, Appl. Radiat. Isot., 67 (2009) S67.